

Situation-based Risk Evaluation and Behavior Planning

Vom Fachbereich
Elektrotechnik und Informationstechnik
der Technischen Universität Darmstadt
zur Erlangung des akademischen Grades
eines Doktor-Ingenieurs (Dr.-Ing.)
genehmigte Dissertation

von

Dipl.-Ing. Florian Damerow

geboren am 20. August 1984 in Ludwigshafen am Rhein

Referent: Prof. Dr.-Ing. Jürgen Adamy
Korreferent: Prof. Dr. rer. nat. Bernhard Sendhoff
Tag der Einreichung: 2. Mai 2017
Tag der mündlichen Prüfung: 14. August 2017

D17
Darmstadt 2018

Preface

This dissertation is the result of my work in a cooperation between the Control Methods and Robotics Lab of the Institute of Automatic Control and Mechatronics, TU Darmstadt and the Honda Research Institute Europe GmbH, Offenbach. At first, I want to thank my supervisor Prof. Jürgen Adamy for the opportunity to work on this highly inspiring and trend-setting project. He always achieved a very pleasant working climate in his institute and enabled each employee to act with great freedom and high self-responsibility in all matters. Furthermore, I want to thank Prof. Bernhard Sendhoff for his acceptance to act as a second referee, all his support and the highly motivating working environment at the Honda Research Institute. Very special thanks go to my direct supervisor at the Honda-RI, Dr. Julian Eggert, for the innumerable deep discussions, his straightforward, friendly and motivating character. He had a great impact on the success of the presented PhD project. All my past colleagues at the Honda-RI, I want to thank for the great time and the fruitful discussions, especially my advisor Stephan Hasler who always had an open ear and a helping hand. Further thanks go to my supervisor at the TU Darmstadt, Volker Willert, for all the open and helpful conversations. I am truly grateful for every single colleague and friend I had at the RMR Lab. Andrea Schnall, Andreea Röthig and Stephan Klingelschmitt were the best office mates I could imagine. Special thanks go to Phil Evans, Martin Buczko, Andrea Schnall, Julian Schwehr and Nicolai Schweizer for proofreading the manuscript and Valentina Ansel for fine tuning the layout. Last but not least, there are my parents to be grateful to. They always supported me in all matters. The same holds for Sarah, whom I deeply thank for her extensive, unconditional support and understanding.

Darmstadt, in August 2017

Florian Damerow

Contents

| | |
|--|--------------|
| Abbreviations and Symbols | VIII |
| Abstract | XVI |
| Kurzfassung | XVIII |
| 1 Introduction | 1 |
| 1.1 Contributions | 4 |
| 1.2 Thesis Structure | 5 |
| 2 Related Work | 8 |
| 2.1 Situation Classification and Trajectory Prediction | 9 |
| 2.1.1 Spatio-temporal Trajectory Prediction | 9 |
| 2.1.2 Situation Classification | 11 |
| 2.1.3 Joint Situation Classification and Trajectory Prediction | 13 |
| 2.2 Risk Evaluation | 15 |
| 2.3 Behavior Planning | 17 |
| 2.4 Traffic Models | 19 |
| 3 Basic Concepts | 22 |
| 3.1 Situations and their Modeling | 23 |
| 3.1.1 Situations in Traffic Scenarios | 24 |
| 3.1.2 Interaction-aware Situation Model | 26 |
| 3.1.3 Situation Pre-Selection | 29 |
| 3.2 Risk | 29 |
| 3.2.1 Risk Estimation for Dynamic Scenes | 30 |
| 3.2.2 General Risk Model | 33 |
| 3.2.3 Approximate Risk Model | 40 |
| 3.3 Trajectory Similarity | 53 |
| 3.4 Conclusion | 56 |
| 4 Framework for Risk Evaluation and Behavior Planning | 59 |

| | | |
|----------|---|------------|
| 4.1 | Framework Overview | 60 |
| 5 | The Foresighted Driver Model | 65 |
| 5.1 | The Intelligent Driver Model | 67 |
| 5.2 | The Foresighted Driver Model | 68 |
| 5.3 | Results | 74 |
| 5.3.1 | Curve Driving Scenario | 75 |
| 5.3.2 | Intersection Scenario | 78 |
| 5.3.3 | Highway Accessing Scenario | 81 |
| 5.4 | Conclusion | 84 |
| 6 | Situation Classification and Trajectory Prediction | 86 |
| 6.1 | Prediction-based Situation Classification | 88 |
| 6.2 | Situation Classification based on Trajectory Similarity Evaluation | 90 |
| 6.3 | Situation Classification for Interaction Detection and Lane Assignment | 93 |
| 6.4 | Situation-based Trajectory Prediction | 94 |
| 6.5 | Results: Interaction Detection | 94 |
| 6.5.1 | Evaluation of a Multi-Lane-Intersection Scenario | 95 |
| 6.5.2 | Statistical Evaluation | 96 |
| 6.6 | Conclusion | 100 |
| 7 | Risk Evaluation | 101 |
| 7.1 | Predictive Risk Maps | 101 |
| 7.1.1 | Basic Risk Shapes | 106 |
| 7.2 | Conclusion | 106 |
| 8 | Behavior Planning | 109 |
| 8.1 | Behavior Planning under Consideration of a Single Situation | 110 |
| 8.1.1 | General Cost Function | 111 |
| 8.1.2 | Rapidly-exploring Random Tree (RRT) | 112 |
| 8.1.3 | Asymptotic Optimal Extension RRT* | 113 |
| 8.1.4 | Adaptation of RRT* to Velocity Planning in Traffic Environments | 115 |
| 8.1.5 | Simulation Results | 118 |
| 8.2 | Behavior Planning under Multiple Situations with Uncer- tainty | 124 |
| 8.2.1 | Approach | 124 |
| 8.2.2 | Results | 129 |

| | | |
|----------|--|------------|
| 8.3 | Conclusion | 136 |
| 9 | Summary and Outlook | 140 |
| 9.1 | Summary | 140 |
| 9.2 | Outlook | 144 |
| A | Appendix | 146 |
| A.1 | Approximate Accumulated Curvature Risk Model | 146 |
| A.2 | Paramters | 147 |
| A.3 | Camera to map alignment | 148 |
| | Bibliography | 149 |
| | Curriculum Vitae | 165 |

Abbreviations and Symbols

Abbreviations

| Abbreviation | Description |
|---------------------|--|
| ACC | Adaptive Cruise Control |
| ADAS | Advanced Driver Assistance Systems |
| AV | Autonomous Vehicle |
| DCE | Distance-Of-Closest-Encounter |
| ESP | Electronic Stability Program |
| FDM | Foresighted Driver Model |
| GNSS | Global Navigation Satellite System |
| HMM | Hidden Markov Model |
| HOG | Histogram of Oriented Gradients |
| ICS | Inevitable Collision States |
| IDM | Intelligent Driver Model |
| IEEE | Institute of Electrical and Electronics Engineers |
| ITS | Intelligent Transportation Systems |
| ITSS | Intelligent Transportation Systems Society |
| IVMC | Indicator-Value-Of-Maximal-Curvature |
| IVMR | Indicator-Value-Of-Maximal-Risk |
| LCSS | Longest Common Sub-Sequence |
| MASE | Mean Absolute Scaled Error |
| MOBIL | Minimizing Overall Braking Induced by Lane Changes |
| MPC | Model Predictive Control |
| PCE | Probabilistic Collision States |
| SAE | Society of Automotive Engineers |
| TCE | Time-Of-Closest-Encounter |
| TLC | Time-To-Lane-Crossing |
| TMC | Time-Of-Maximal-Curvature |
| TMR | Time-Of-Maximal-Risk |
| TTC | Time-To-Collision |
| TTR | Time-To-React |
| TTX | Time-To-X |

Notation

| Notation | Description |
|------------------|---|
| x | Scalar |
| \hat{x} | Estimated quantity |
| \dot{x} | Time derivative of x |
| x_t | Current quantity |
| x_{t+s} | Quantity at future time $t + s$ (s into future) |
| $x_{t:t+s}$ | Sequence of quantities with $x_{t:t+s} = \{x_t, x_{t+1}, \dots, x_{t+s}\}$ |
| \mathbf{x} | Column vector |
| $P(x y)$ | Conditional probability of x given y |
| $\ \mathbf{x}\ $ | L_2 -norm of \mathbf{x} |

Important Functions and Transformations

| Function | Description |
|--|---|
| $B(\cdot)$ | Approximate car-to-car collision event probability term for modeling the prediction uncertainty propagation |
| $\hat{c}_{t+s}(e_{t+s}, \mathbf{x}_{t+s})$ | Deterministic damage function |
| $\hat{c}_{co}(\mathbf{e}_{co}, \cdot)$ | Approximate car-to-car collision damage function |
| $\hat{c}_{mr}(\mathbf{e}_{mr}, \cdot)$ | Approximate damage function for a future maximal risk event |
| $\text{Cost}(\cdot)$ | Trajectory cost function |
| $\text{Cost}_{norm}(\cdot)$ | Normalized trajectory cost function |
| $\text{DCE}(\cdot)$ | Distance-Of-Closest-Encounter function |
| $\text{DCost}(\cdot)$ | Differential trajectory cost function |
| $\delta(\cdot)$ | Dirac delta function |
| $\text{FS}(\mathbf{x}_t, h_t)$ | Forward simulation function of sensed scene \mathbf{x}_t for situation h_t |
| $L(s)$ | Trajectory length function |
| $M_{sim,total}(h_t)$ | Situation similarity function |
| $P(c_{t+s} \cdot)$ | Damage probability at future time $t + s$ |
| $P^\infty(\mathbf{e} \cdot)$ | Approximate event probability accumulated over future time interval $[t, \infty]$ |
| $P(e_{t+s} \cdot)$ | Event probability at future time $t + s$ |

| | |
|--|---|
| $\int_0^\infty P(e_{t+s} \cdot)ds$ | Accumulated event probability |
| $\sum_{e_{t+s}} P(e_{t+s} \cdot)$ | Total event probability |
| $\int_0^s \sum_{e_{t+s}} P(e_{t+s} \cdot)ds$ | Accumulated, total event probability |
| $P(\mathbb{H}_t^{\text{inter,inter}} \cdot)$ | Interaction/Non-interaction probability |
| $P(\mathbb{H}_t^\chi \cdot)$ | Probability for another entity choosing path χ |
| $P(h_t \cdot)$ | Situation occurrence probability |
| $P(\mathbf{x}_{t:t+s} \cdot)$ | Prediction probability of future state vector sequence |
| $r_\infty^{co}(\cdot, h_t)$ | Situation-dependent, approximate car-to-car collision risk accumulated over the time interval $[t, \infty]$ |
| $R_{comb}(\cdot)$ | Combined risk map |
| $r_\infty^{co}(\cdot)$ | Total approximate car-to-car collision risk accumulated over the time interval $[t, \infty]$ |
| $r_\infty^{cv}(\cdot)$ | Total approximate curve driving risk accumulated over the time interval $[t, \infty]$ |
| $r_\infty(\cdot, h_t)$ | Situation-dependent, approximate risk accumulated over the time interval $[t, \infty]$ |
| $R(\cdot, \hat{l}_{t+s}^0, h_t)$ | Predictive risk map, represented in terms of future driven longitudinal distance |
| $R^{tmp}(\cdot, t + s, h_t)$ | Predictive risk map, temporal representation |
| $r(t + s, \cdot)$ | Risk function at future time $t + s$ |
| $r(\cdot, h_t)$ | Situation-dependent risk function |
| $S(\cdot)$ | Survival function |
| $\tau_b^{-1}(\cdot)$ | Event rate for losing control due to heavy braking |
| $\tau_c^{-1}(\cdot)$ | Curvature event rate |
| $\tau_d^{-1}(\cdot)$ | Car-to-car collision event rate |
| $\tau_{e_{t+s}}^{-1}(\cdot)$ | Event rate |
| $\tau^{-1}(\cdot)$ | Total event rate |
| $TC(\cdot)$ | Travel cost function accounting for utility considerations |
| $TCE_{max}(\text{DCE})$ | Time-Of-Closest-Encounter of maximal risk as function of Distance-Of-Closest-Encounter |
| $TCE(\cdot)$ | Time-Of-Closest-Encounter function |
| $TMR(\cdot)$ | Time-Of-Maximal-Risk function |
| $IVMR(\cdot)$ | Indicator-Value-Of-Maximal-Risk function |
| $\beta_{d/c/b}(s)$ | Time-dependent uncertainty event rate term |
| $\Delta_{lat/lon}(s)$ | Lateral/longitudinal distance function |

| | |
|-------------------------------------|---|
| $M_{\Delta_{lat/lon}}(\cdot)$ | Trajectory similarity assignment functions for spatial similarity |
| $M_{\dot{\Delta}_{lat/lon}}(\cdot)$ | Trajectory similarity assignment functions for derivative of spatial similarity |
| $M_{lat/lon}(\cdot)$ | Mean lateral/longitudinal similarity based on spatial distance |
| $\dot{M}_{lat/lon}(\cdot)$ | Mean lateral/longitudinal similarity based on derivative of spatial distance |
| $M_{sim}(\cdot)$ | Similarity of two spatio-temporal trajectories, comprising lateral, longitudinal similarity |

Symbols

Latin Capital Letters

| Symbol | Description |
|-----------------------------------|--|
| A | Interaction matrix |
| F_{co} | Approximate car-to-car collision event probability weighting factor |
| F_{mr} | Approximate event probability weighting factor |
| $\mathbb{H}_{r_{low}}$ | Set of situations of low risk |
| \mathbb{H} | Set of situations |
| \mathbb{H}_t^{inter} | Set of situations assuming that another involved entity does consider the ego entity for interaction |
| $\mathbb{H}_t^{\overline{inter}}$ | Set of situations assuming that another involved entity does not consider the ego entity for interaction |
| \mathbb{H}_t^χ | Set of situation assuming the other entity choosing the spatial path χ |
| l_{t+s} | Predicted longitudinal distance driven at future time $t + s$ |
| N | Number of scene entities |
| $N_{\mathbb{H}}$ | Number of situations |
| N_q^i | Number of lon. behavior alternatives per entity |
| N_χ^i | Number of possible drivable paths per entity |
| P_{FDM} | FDM model parameter set |
| R | Curve radius |
| $S_{1,2,3}^{co}$ | FDM model parameter accounting for situation occurrence probabilities |

| | |
|----------------|---|
| $S_{h_t}^{co}$ | FDM model parameter accounting for situation occurrence probabilities |
| TC_0 | Travel cost function parameters |

Latin Lowercase Letters

| Symbol | Description |
|------------------------------------|---|
| a | FDM model parameters, accounting for the maximal acceleration/deceleration to reach the desired velocity v_0 |
| $a_{c,max}$ | Maximal allowed centrifugal acceleration in a curve segment |
| $a_{max,comfort}$ | Maximal acceleration/deceleration value for the behavior planner in the comfort region |
| $a_{max,total}$ | Maximal acceleration/deceleration value for the planner outside the comfort region |
| $a^{u,w}$ | Interaction value between entity u and w |
| $b_{b,max}$ | Maximal allowed deceleration |
| b_{risk} | Risk threshold defining when a situation is considered as being of low risk |
| $\hat{b}_{t+s}(\mathbf{x}_t, h_t)$ | Predicted deceleration at time $t + s$ |
| c_{t+s} | Future damage at time $t + s$ |
| d_{min} | Minimal allowed distance |
| $\hat{d}_{t+s}(\mathbf{x}_t, h_t)$ | Predicted distance between two entities at time $t + s$ |
| e_{t+s} | Critical event happening at future time $t + s$ |
| \mathbf{e} | Critical event happening in the entire future time interval $[t, \infty]$ |
| h | Situation |
| i | Scene entity |
| m | Travel cost function parameters |
| m_0 | Ego entity mass |
| m_i | Other entity mass |
| $\mathbf{p}^{1/2}(s)$ | Trajectory of entity i comprising purely spatio-temporal information in the time interval $[a, b]$, explicitly represented as a function of predicted time s |
| $\mathbf{p}^{1 \rightarrow 2}(s)$ | Projected position of trajectory 1 onto trajectory 2 |

| | |
|--|--|
| p_{t+s}^i | Predicted spatial position at time $t + s$ of entity i |
| q | Variation parameter |
| $r_b(h)$ | Maximal possible risk the ego entity can encounter in situation h |
| $s_{b,0}$ | Modeling parameter for time-dependent uncertainty in event rate for control loss due to heavy braking |
| $s_{c,0}$ | Modeling parameter for time-dependent uncertainty in curvature event rate |
| $s_{d,0}$ | Modeling parameter for time-dependent uncertainty in car-to-car collision event rate |
| v | Longitudinal velocity |
| $v_{c,max}$ | Maximal allowed longitudinal velocity in a curve segment |
| Δv | Velocity difference between two cars driving along the same spatial path |
| $\frac{dv}{dt}^{\text{free}}$ | Free-driving velocity adaptation |
| $\frac{dv}{dt}^{\text{risk}}$ | Risk-aversive velocity adaptation |
| $\hat{v}_{t+s}(\mathbf{x}_t, h_t)$ | Predicted longitudinal velocity at time $t + s$ |
| x | Longitudinal path position |
| $\hat{\mathbf{x}}_{t:t+s}^0(\mathbf{x}_t, h_t, q)$ | Variation of ego trajectories, using variation parameter q |
| $\mathbf{x}_{a:b}^i$ | Trajectory of entity i comprising at least spatio-temporal information in the time interval $[a, b]$ |
| \mathbf{x}_t | Currently sensed scene state vector |
| \mathbf{x}_t^i | Currently sensed vehicle state vector |
| $\mathbf{x}_{t:t+s}$ | Future scene state vector sequence |
| $\mathbf{x}_{t:t+s}^0$ | Future state vector sequence of vehicle I |
| $\hat{\mathbf{x}}_{t:t+s}$ | Prototypically predicted scene state vector sequence |

Greek Letters

| Symbol | Description |
|------------------------|---|
| α | Approximate car-to-car collision event probability parameter accounting for the uncertainty propagation in the prediction process |
| β | FDM model parameter, accounting for the maximal acceleration/deceleration to the desired velocity v_0 |
| $\beta_{b,0}$ | Parameter for modeling time-dependency in event rate for control loss due to heavy braking |
| $\beta_{c,0}$ | Parameter for modeling time-dependency in curvature event rate |
| $\beta_{d,0}$ | Parameter for modeling time-dependency in car-to-car collision event rate |
| β_b^{const} | Time-independent uncertainty parameter in control loss due to heavy braking event rate |
| β_c^{const} | Time-independent uncertainty parameter in curvature event rate |
| β_d^{const} | Time-independent uncertainty parameter in car-to-car collision event rate |
| $\Delta_{lat/lon,max}$ | Similarity assignment function parameters |
| η | Gradient-descent parameter |
| γ | Approximate car-to-car collision event probability parameter accounting for the uncertainty propagation in the prediction process |
| σ_{co} | Approximate car-to-car collision event probability parameter accounting for temporal uncertainties |
| $\sigma_{co,1}$ | Approximate car-to-car collision event probability parameter accounting for temporal uncertainties |
| $\sigma_{co,2,3}$ | Approximate car-to-car collision event probability parameter accounting for temporal uncertainties |
| σ_{cv} | Approximate curvature event probability parameter accounting for temporal uncertainties |

| | |
|---------------------|---|
| σ_d | Approximate car-to-car collision event probability parameter accounting for spatial uncertainties |
| σ_{tmr} | Approximate event probability parameter accounting for temporal uncertainties |
| σ_{ivmr} | Approximate event probability parameter accounting for indicator value uncertainties |
| τ_0^{-1} | Constant event escape rate |
| $\tau_{d/c/b}^{-1}$ | Maximal event rate value |
| Ξ | Set of spatial paths |
| χ | Spatial path |

Abstract

The presented dissertation addresses the problem of risk evaluation and behavior planning for future intelligent Advanced Driver Assistance Systems (ADAS). For this purpose, a novel framework for situation-based risk evaluation and behavior planning, targeting highly automated driving, is presented.

After properly sensing the current scene, including the current road topology and other traffic participants, the proposed framework first estimates and predicts the future behavior of all involved entities comprising a situation classification and trajectory prediction step. This is then followed by the generation of the own future behavior in a behavior planning step which is based on an evaluation of possible ego behavior alternatives in terms of risk and utility considerations. The future behavior is planned in a way to find a tradeoff between the expected future risk and utility.

Inner-city traffic scenarios in particular are usually complex and of high uncertainty, considering measurements as well as behavioral decisions. To reduce the complexity, similar behavior alternatives are clustered and represented by prototypical behavior patterns using so-called situations. A novel situation classification approach is proposed to estimate how good a situation matches with the actual behaviors. This approach is based on a comparison of the prototypically predicted trajectories of the considered situations with the actual measured trajectories. For this purpose a novel measure for spatio-temporal trajectory similarity, based on the evaluation of longitudinal and lateral spatio-temporal distance, is derived. The situation classification system is used to detect incorrect and critical traffic behaviors, especially in scenarios with a disregard of right-of-way. Evaluating the system using real-world crash cases reveals that it is able to warn the driver reliably of an upcoming crash, with sufficient time to initiate a suitable evasive behavior.

For the prediction of situation-dependent prototypical scene evolution patterns, the interaction-aware *Foresighted Driver Model* (FDM) is applied in a forward simulation of a sensed scene under different situation-dependent behavioral assumptions. The proposed FDM is a novel, time continuous driver model for the simulation and prediction of freeway and

urban traffic. Based on the general risk evaluation and behavior planning framework developed in this thesis, the driver model equations are introduced from the assumption that a driver tries to balance predictive risk (e.g. due to possible collisions along its route) with utility (e.g. the time required to travel, smoothness of ride, etc.). For this purpose, a computationally inexpensive, approximate risk model targeting only risk maxima and a gradient descent-based behavior generation is applied. It is shown, how such a model can be used to simulate and predict driving behavior with a similar performance compared to full behavior planning models. The FDM is applicable to a wide range of different scenarios, e.g. intersection or highway-accessing scenarios, with the consideration of an arbitrary number of traffic entities. Thus, the FDM generalizes and reaches beyond state-of-the-art driver models.

Complex traffic situations require the estimation of future behavior alternatives in terms of predictive risks. Risk assessment has to be driven from the knowledge that the acting scene entity requires to evaluate the own future behavior. Based on the predicted future dynamics of traffic scene entities, an approach is presented, where a continuous, probabilistic model for future risk is used to build so-called *predictive risk maps*. These maps indicate how risky a certain ego behavior will be at different future times, so that they can be used to directly plan the best possible future behavior.

The behavior in complex scenarios differs strongly, depending on the actually occurring situation. However, sensory measurements of the ego and other involved entities' states as well as the prediction of possible future states are generally of high uncertainty. As a consequence, the current driving situation can only be approximated. Additionally, a situation can change very quickly, e.g. if a traffic participant suddenly changes its behavior. In this thesis an approach is proposed, how to plan a safe, but still efficient future behavior under consideration of multiple possible situations with different occurrence probabilities. In several traffic scenarios comprising simulated as well as recorded real-world data, it is shown that the approach generates an efficient behavior for situations which are likely to occur, while generating a *plan B* to safely deal with improbable but risky situations.

Kurzfassung

Diese Dissertation behandelt das Problem der Verhaltensevaluierung und -planung für zukünftige, intelligente Fahrerassistenzsysteme (FAS). Hierzu wird ein neues Framework für die situationsbezogene Risikobewertung und Verhaltensplanung im Bereich des hochautomatisierten Fahrens vorgestellt.

Nach der sensorischen Erfassung der aktuellen Szene, einschließlich der Straßentopologie sowie weiterer Verkehrsteilnehmer, schätzt das vorgestellte Framework zunächst das zukünftige Verhalten aller involvierten Teilnehmer in einem Situationsklassifikations- und Trajektorienprädiktionsschritt. Basierend darauf wird eine Risikoauswertung von möglichen Verhaltensalternativen des Ego-Fahrzeugs durchgeführt, um dann durch eine Verhaltensanpassung einen Kompromiss aus Risiko und Nutzen zu finden.

Vor allem innerstädtische Verkehrsszenarien sind in der Regel komplex und mit hoher Unsicherheit behaftet. Zur Reduzierung der Komplexität werden ähnliche Verhaltensweisen zusammengefasst und durch prototypische Verhaltensmuster in so genannten Situationen dargestellt. Um abzuschätzen, wie gut eine Situation dem tatsächlichen Verhalten entspricht, werden prototypische Verhaltensprädiktionen der berücksichtigten Situationen mit dem tatsächlich gemessenen Verhalten verglichen. Hierbei wird ein neu entwickeltes Ähnlichkeitsmaß für raumzeitliche Trajektorien angewandt, das auf der getrennten Auswertung des lateralen und longitudinalen raumzeitlichen Abstands basiert. Unter Verwendung des neuartigen Systems zur Situationsklassifikation werden riskante Situationen zuverlässig erkannt, welche sich durch “fehlende Interaktion” zwischen Verkehrsteilnehmern auszeichnen.

Für die prototypische Vorhersage situationsbezogener Trajektorien wird das interaktionsbewusste Fahrermodell *Foresighted Driver Model* (FDM) in einer Vorwärtssimulation der sensorisch erfassten Szene unter situationsbezogenen Verhaltensannahmen angewandt. Das in dieser Arbeit vorgeschlagene Fahrermodell FDM ist ein neuartiges, zeitkontinuierliches Fahrermodell für die Simulation und Vorhersage von Autobahn- und innerstädtischen Verkehrssituationen. Hierbei wird davon ausgegangen, dass ein Fahrer durch sein Verhalten versucht, einen Kompromiss zwischen

zukünftigem Risiko (auf Grund möglicher Kollisionen entlang eines Pfades) und Effizienz (bezüglich Reisezeit und Komfort) zu finden. Basierend auf dem allgemeinen Framework zur Verhaltensplanung und einem angenäherten Risikomodell, werden die Fahrermodellgleichungen durch die Annahme begründet, dass ein Fahrer in erster Linie versucht, Risikomaxima sowohl räumlich als auch zeitlich zu vermeiden. In dieser Arbeit konnte gezeigt werden, dass ein solches Fahrermodell in Simulations- und Prädiktionsanwendungen eine Leistung ähnlich der einer vollen Verhaltensplanung erreicht. Das FDM ist auf ein breites Spektrum an unterschiedlichen Szenarien, wie z.B. Kreuzungs- oder Autobahnszenarien, unter Berücksichtigung beliebig vieler Verkehrsteilnehmer anwendbar. Daher werden die dem Stand der Technik entsprechenden Fahrermodelle durch das FDM verallgemeinert und eine Anwendung auf weiterführenden Szenarien wird ermöglicht.

Komplexe Verkehrssituationen erfordern die Auswertung von Verhaltensmöglichkeiten hinsichtlich des zukünftigen Risikos. Die Risikobewertung des eigenen zukünftigen Verhaltens ist getrieben von verhaltensbezogenen Bedürfnissen des agierenden Verkehrsteilnehmers. Im vorgeschlagenen Ansatz wird basierend auf der vorhergesagten Dynamik der Verkehrsteilnehmer ein zeitlich kontinuierliches Wahrscheinlichkeitsmodell für künftige Risiken verwendet, um sogenannte *prädiktive Risikokarten* zu erzeugen. Diese Risikokarten beschreiben, wie riskant ein bestimmtes Ego-Verhalten zu verschiedenen zukünftigen Zeitpunkten sein wird. Somit können sie direkt dazu verwendet werden, das bestmögliche zukünftige Verhalten zu planen.

Verhalten in komplexen Szenarien unterscheiden sich stark in Abhängigkeit der tatsächlich auftretenden Situationen. Im Allgemeinen kann die aktuelle Situation oft nur mit hoher Unsicherheit anhand gegenwärtiger und vergangener sensorischer Messungen des Ego-Fahrzeugs und anderer beteiligter Fahrzeuge bestimmt werden. Zusätzlich kann sich eine vorherrschende Verkehrssituation schnell ändern, z.B. wenn ein Verkehrsteilnehmer sein Verhalten plötzlich ändert. In dieser Arbeit wird daher ein Ansatz vorgestellt, der es ermöglicht das zukünftige Verhalten unter Berücksichtigung von mehreren möglichen Situationen mit unterschiedlichen Eintrittswahrscheinlichkeiten sicher und trotzdem effektiv zu planen. Dieser Ansatz generiert speziell für Situationen mit hoher Wahrscheinlichkeit sehr effizientes Verhalten. Für unwahrscheinliche, aber riskante Situationen wird ein *Plan B* bereit gestellt, der lediglich auf die Minimierung des Risikos abzielt, falls eine dieser Situationen unerwartet eintritt.

1 Introduction

Road traffic accidents are one of the biggest problems in public health. The World Health Organization (WHO) recorded 1.24 million deaths and over 50 million injured humans related to car accidents in 2010, which accounts for 2.1 % of the global mortality [141].

Several studies analyzing the cause of traffic accidents have determined human error as the main accident reason. For example in [60] 2258 accidents were observed, of which 93 % can be explained by human misbehavior. In [44] the authors analyzed accidents registered by the German Federal Statistical Office. Here, 84 % of the accidents were caused by the human driver.

The prognosis given in [100] from the year 2004 expected an increase of personal damage by 65 % in the time span from 2000 until 2020 due to an increase of traffic volume. This prognosis was made under the assumption that no further safety system would be developed. However, the analysis in [125] could determine a steady decrease of deaths (by ~ 80 %) and injured persons (by ~ 30 %) in German road traffic between 1970 and 2014. This decrease is even more valuable, if the increase in traffic volume by 270 % in this period is considered. The early decrease in the number of deaths and injuries, until approximately the year 2000, can mainly be explained by the development of passive safety systems, such as seat belts, airbags, the enhancement of the physical vehicle structure, and traffic safety regulations. Regulations which have had a great influence on traffic safety are e.g. the introduction of a speed limit at 100 km/h for rural roads and the reduction of the legal blood alcohol level to 0.5 ‰. For the later decrease of personal damage after the year 2000, mainly the increasing number of active safety functions such as the electronic stability program (ESP) is responsible.

In 2012, only 0.9 % of the accidents could be identified as caused by technical breakdowns or lack of maintenance [44]. Therefore, it can be concluded that the potential for safety improvement in the area of structural reliability is largely saturated. On the other side, it can be seen that systems incorporating environmental knowledge to assist or actively protect a driver promise high development potential. To date, there is already

a wide range of such so-called advanced driver assistance systems (ADAS) available to support the driver by perceiving the environment using a wide range of sensors such as radar, LIDAR¹, or cameras.

Currently available ADAS, such as lane-keeping, park assistance and adaptive cruise control (ACC), generally try to achieve an individual target and operate mostly independent of each other. An increasing number of ADAS also intensifies the problem of conflicting targets and, as a result, requires an integrated evaluation to allow joint solutions, optimizing the integrity of parallel acting ADAS. This work originates from the need of such an integrated evaluation method for ADAS to achieve an optimal behavior, considering multiple different and possibly competing targets.

In general, the target of ADAS is to relief the strain on the driver by taking over more and more responsibility, starting from any kind of warning system up to partially or fully automated driving. This evokes the development of a suitable, integrated system framework and behavior evaluation method, as one of the main challenges. Especially in road traffic environments the estimation and evaluation of possible future hazards is crucial.

The main questions addressed in this thesis are the following:

1. How can an entity's own behavior be generated in general traffic environments, minimizing risk and maximizing utility?

Generating the own behavior relies on an evaluation of possible future behavior alternatives, which raises the question:

2. How can an entity's possible future behavior be evaluated in an integrated way in terms of behavioral risk and utility?

The evaluation of possible upcoming hazards expressed by an integrated risk estimation method requires a prediction of possible state evolutions of the current scene into the future. In general, there are unlimited possibilities how a scene can evolve. As a consequence, the behavior evaluation becomes computationally infeasible, which causes the question:

3. How can the complexity in the evaluation of future behavior alternatives be reduced to allow a computationally efficient evaluation of behavioral risk and utility?

¹Light detection and ranging (LIDAR) is an optical method for distance and velocity measurement, similar to radar. For the measurement, the run time of laser beams is used, instead of radio waves, as applied in radar.

Many previous works have addressed problems which target parts of the raised questions, as it will be discussed in detail in Chapter 2. However, current approaches are mostly designed to work under narrowly defined conditions, e.g. limited to certain types of traffic scenarios such as highway driving, or target only sub-problems of the those questions, e.g. the classification of possible future traffic maneuvers. A general framework, comprising approaches to the raised questions in an integrated way and not restricted to certain traffic scenarios, is still missing, which is the overall target of the presented thesis.

Approaching the three questions raised above, especially the task of behavior generation in traffic environments, leads to the field of automated driving. The different approaches towards driving automation are categorized by six different levels, ranging from 0 to 5, defined as follows by the Society of Automotive Engineers (SAE) in the standard J3016 [110]:

- **Level 0 - No Automation** describes an automation level in which the human driver has to handle all aspects of driving.
- **Level 1 - Driver Assistance** describes systems, where an assistance function takes over either steering or acceleration/deceleration for a well-defined purpose.
- **Level 2 - Partial Automation** describes systems, where both, steering and acceleration/deceleration is performed by one or more assistance functions in a well-defined driving mode.
- **Level 3 - Conditional Automation** describes systems, where the entire dynamic driving task is performed by an automated driving system. Here the human driver only has to intervene when requested by the system.
- **Level 4 - High Automation** describes systems, where the entire dynamic driving task is performed by an automated driving system. In case the human driver does not respond to a take-over request the system has to be able to reach a safe state.
- **Level 5 - Full Automation** describes systems, where the entire dynamic driving task in any kind of traffic environment is fully performed by an automated driving system, without the need of a human driver.

Parts of the presented thesis are applicable to any of the SAE-levels. However, in particular the presented framework for *situation-based risk eval-*

uation and behavior planning targets SAE-level 4 and 5. The following section summarizes the main contributions of this thesis, approaching the questions raised above.

1.1 Contributions

The contributions of this thesis can be summarized as follows:

- Novel situation representation, clustering similar behavior alternatives for each involved traffic scene entity and represent each cluster by one prototypical behavior per entity [30, 31, 39].
- Novel probabilistic risk model, expressing the expectation value of the damage related to critical future events, targeted for situation-dependent, prototypically predicted, future behavior patterns [27, 30, 39].
- Novel similarity metric for spatio-temporal trajectories², targeted at road traffic scenarios [31].
- Novel integrated framework for situation-based risk evaluation and behavior planning [30, 39].
- Novel microscopic driver model, called the *Foresighted Driver Model* (FDM), based on a simplification of the framework for *situation-based risk evaluation and behavior planning* [33, 37, 38].
- Novel method for situation classification, based on a similarity evaluation between several situation-dependent expected behavior alternatives and the actually sensed behavior [31].
- Novel method for detecting the *lack of interaction* between traffic participants, when the entities should interact to avoid upcoming risks [31].
- Novel model-based method for trajectory prediction, utilizing the Foresighted Driver Model in a multi-agent forward simulation, considering situation-dependent behavior assumptions [30, 31].

²A spatio-temporal trajectory describes a temporal sequence of state-vectors, e.g. of a vehicle, such that a state comprises spatial (e.g. two-dimensional) information, dedicated to its temporal appearance.

- Novel method for the evaluation of risk by building so-called *predictive risk maps*. Such a predictive risk map represents how risky a certain behavior under consideration of a certain situation will be in the future. The risk map is generated by building a set of different ego behavior alternatives and evaluating the future risk for each [26, 27, 30, 39].
- Novel sampling-based, globally optimal method for behavior planning, minimizing risk and maximizing utility, while considering multiple situations with uncertainty [27, 30, 39].

All contributions are integrated in a system for *situation-based risk evaluation and behavior planning*, to generate a risk-averse future behavior in an efficient way. The system has mainly been analyzed in a simulation environment. Nevertheless, parts of the system, such as the situation classification and trajectory prediction, have been applied to real-world data to show their feasibility.

The contributions have been published to the Intelligent Transportation Systems (ITS) community in [22, 26, 27, 30, 31, 33, 37–39]. Furthermore, important aspects have been patented in [28, 29, 32].

1.2 Thesis Structure

The thesis is structured as shown in Figure 1.1. After the introduction, Chapter 2 gives an overview of research related to the presented work and its comprising approaches. Chapter 3 introduces novel basic concepts, e.g. the concept of risk and situations, which build the basis of the following chapters. Those concepts are covered separately, as they are applicable to tasks beyond the scope of this thesis. Section 3.1 introduces the basic concept of situations, which combine similar and separate generally different behavior possibilities of involved entities. A situation defines a prototypical behavior of a small number of traffic scene entities. Section 3.2 proposes a time-continuous, probabilistic model for future risk. Risk is considered as the expectation value of the costs related to critical future events. The risk model naturally allows the integrated consideration of different risk sources, such as several traffic participants or road structure elements, as well as different risk types, such as the car-to-car collision risk, the risk of skidding off the road while driving too fast on curves, and the risk of losing control due to heavy braking. Furthermore, from the general risk measure, this chapter derives a simplified model

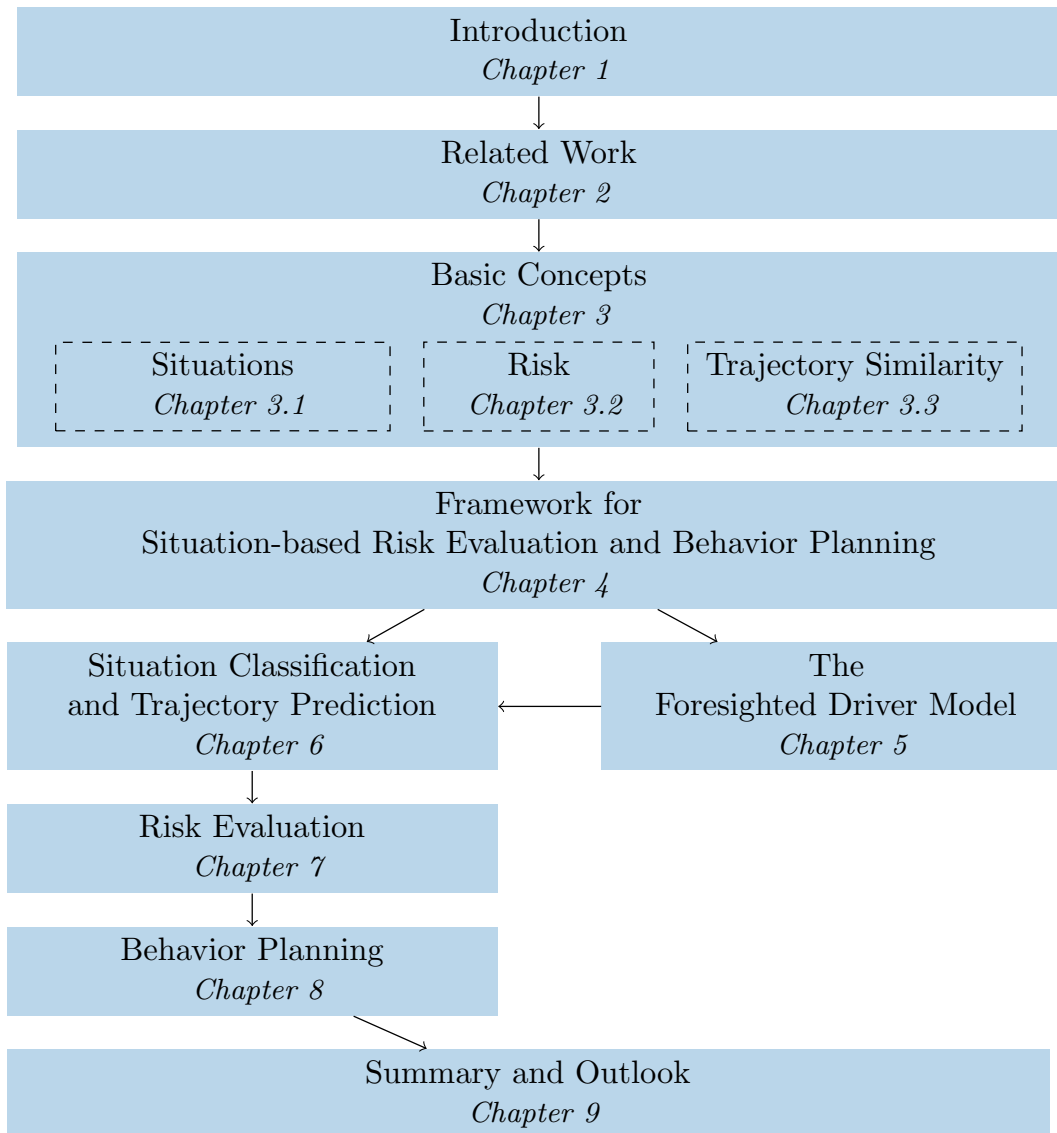


Figure 1.1: Thesis overview.

for the risk accumulated over future time based on risk indicators, which are directly extractable from predicted, spatio-temporal trajectories, such as the time-of-closest-encounter (TCE) and distance-of-closest-encounter (DCE).

Chapter 4 presents the framework for *situation-based risk evaluation and behavior planning*, which mainly consists of the six steps: 1) scene observation, 2) situation classification, 3) trajectory prediction, 4) risk evaluation, 5) behavior planning, and 6) behavior execution.

Based on this framework, Chapter 5 proposes a novel, microscopic driver model, the *Foresighted Driver Model* (FDM), which integrates those steps in a simplified, computationally inexpensive way. The FDM is applicable

to a wide range of different scenarios, such as intersections and highway traffic and, as a consequence, allows the application to simulation as well as prediction tasks comprising several traffic participants.

The following Chapters 6 - 8 introduce explicit realizations for the main steps of the framework. The different approaches are designed to collaborate naturally with each other. Nevertheless, each step can be considered separately and allows the application to individual tasks, such as driver information or warning systems.

Chapter 6 proposes an approach to classify and select those situations, which are relevant for an entity's own future behavior. The presented approach is based on similarity calculations between situation-dependent predicted and actually sensed behaviors of all involved entities. Furthermore, as a prerequisite, this chapter introduces an approach for trajectory prediction, by applying the Foresighted Driver Model in a situation-dependent multi-agent forward simulation of a sensed scene.

The following Chapter 7 introduces an approach for risk evaluation by building so-called situation-dependent *predictive risk maps* which indicate how risky a certain behavior will be at a certain point in the future.

Chapter 8 introduces a globally optimizing, sampling-based approach for behavior planning. The presented approach minimizes risk and maximizes utility, while considering multiple situations with uncertainty. The approach relies on the risk evaluation step, providing situation-dependent predictive risk maps, as well as on the situation classification step, providing an estimate, how likely it is that a situation will occur. The behavior is planned with a focus on the most likely situations. However, for unlikely but risky situations, a "plan B", which purely targets safety considerations, is provided to keep the overall behavior safe in case one of those situations suddenly occurs.

Finally, Chapter 9 summarizes the results and suggests possible subsequent work.

2 Related Work

This chapter gives an overview of relevant work in the field of situation-based risk evaluation and behavior planning and puts the approach presented in this thesis into context. Close thematic relations between discussed work and novel approaches presented in this thesis are highlighted.

The main steps of the presented system for *situation-based risk evaluation and behavior planning* (see Figure 2.1), which build upon one another, are

1. situation classification and trajectory prediction
2. risk evaluation
3. behavior planning

As a consequence, the related work discussed in this chapter is structured accordingly. Situation classification describes the joint estimation of one or several drivers' intended future behaviors on an abstract level. Trajectory prediction is the subsequent estimation of a future behavior on a physical level resulting in spatio-temporal trajectories. Furthermore, risk evaluation is used to assess the criticality (the expected damage) of a possible future behavior and is applied in the behavior planning step to plan an ego entity's future behavior. Such a behavior is generally represented by spatio-temporal trajectories.

In addition to future behavior planning, work related to the novel microscopic driver model, introduced in this thesis and applied to the prediction step of the system, is applicable to tasks beyond trajectory prediction (e.g. traffic simulation) and therefore covered in a separate section.

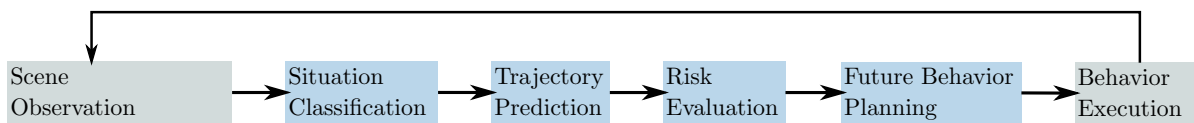


Figure 2.1: Framework for *situation-based risk evaluation and behavior planning*.

2.1 Situation Classification and Trajectory Prediction

To enable a system to act safely in traffic environments, it is crucial to predict how the traffic participants that appear in the current scene will behave in the future. For traffic environments, this implies in particular the prediction of spatio-temporal trajectories.

On the one hand, approaches have been developed which directly predict spatio-temporal trajectories. This can range from prediction methods considering purely physical vehicle states, up to methods taking additional environmental knowledge and an estimation of the driver's intention into account. Even the interaction between traffic participants is considered in some prediction approaches.

On the other hand, there is the large area of situation classification methods, for which each driver's intent is inferred on an abstract level (e.g. "turning left"). More advanced methods combine both, first estimating each driver's intent, followed by a detailed prediction of spatio-temporal trajectories. Furthermore, in each area, there are approaches applying machine learning methods to tackle the prediction problem.

The following gives an overview on current methods for spatio-temporal trajectory prediction, followed by an outline on situation classification/recognition techniques and finally approaches considering the joint problem of situation-dependent trajectory prediction.

2.1.1 Spatio-temporal Trajectory Prediction

This section concentrates first on methods taking purely the vehicle's physical states into consideration to predict its future spatio-temporal trajectory, the so-called short-term prediction models. Then, with increasing complexity, methods promising a longer prediction horizon, are discussed.

For methods with a prediction horizon less than one second, the vehicle dynamics are generally considered as dominant [116, 117]. Furthermore, changes of the vehicle control inputs as well as external influences on the vehicle's motion model are assumed to be neglectable. In this area of prediction methods, it is common to apply tracking filters, e.g. the Kalman filter [63], with an underlying model of the vehicle's system dynamics, to enable a probabilistic treatment of trajectory prediction. Frequently used models are based on the assumption of constant-velocity, constant-acceleration, or constant-turn-rate, as applied in [10, 11, 23, 91, 107, 118].

Especially, when using probabilistic filters¹, more complex models such as single- or two-track models [115], which model the physical vehicle dynamics in more detail (e.g. by considering the tire forces), are often avoided due to their increasing computational complexity.

In most cases the prediction of a single vehicle's future behavior is not sufficient. Moreover, systems strive for a prediction of the entire future evolution of a sensed scene, including the ego- and several other traffic participants. For prediction horizons below one second, each traffic participant can be assumed as independent from others and as a result each entity can be considered separately. As knowledge on the ego vehicle's states is often of greater detail, more complex physical models (e.g. single- or two-track models) can be applied to predict the ego entity's future spatio-temporal trajectory.

Learning-based prediction methods for spatio-temporal trajectories with short prediction horizons are possible, but due to the increase in complexity and, compared to model-based approaches, the low gain in prediction accuracy not widely spread. In [143] a neural network (NN) is applied to learn the vehicle's dynamics from training data, where only the vehicle's current steering angle and velocity are used to recursively predict the future states of the system.

The advantage of prediction models which purely rely on physical vehicle states is the low computational complexity and the little required knowledge on vehicle states. On the contrary the prediction can only be considered as valid for a prediction horizon up to approximately one second [84].

In order to reach methods that provide a longer prediction horizon, further knowledge besides the own vehicle's state has to be taken into account. A first step in this direction is the consideration of road geometry in the prediction task, as it is done e.g. in [90, 102, 107]. In such approaches, short-term prediction models, e.g. constant velocity models, are applied longitudinally on a reference path, e.g. the current lane's centerline, which is derived from the current road geometry. As a consequence, those methods allow a longer prediction horizon and represent an intermediate stage between short- and long-term prediction, while keeping the computational effort low.

Likewise, road geometry information plays a major role in the novel trajectory prediction approach introduced in Chapter 6 of this thesis, where reachable lane centerlines are used as prediction reference paths.

¹Here probabilistic filtering mainly refers to recursive Bayesian estimation (Bayes filter) [24].

To allow even longer prediction horizons, methods have been proposed which integrate an estimate of the driver’s intent into the prediction process. Knowledge about a driver’s intent naturally enables an estimation of the driver’s preferred actions (to reach the intent) and leads to a finer prediction of the resulting spatio-temporal trajectories. Prediction methods which enhance physical prediction models with intent and environment knowledge are [6, 20, 40, 45, 46, 80, 112, 117, 123].

Predefined high-level actions or maneuvers such as lane-changing, lane-keeping or turning at intersections can represent a driver’s intent and can be employed to increase the prediction performance. As an example see [117]. A target position the driver tries to reach (e.g. a final parking position) can also represent a driver’s intent. For this purpose, path planning algorithms have been employed in the trajectory prediction to achieve possible reference paths as done in [6, 20, 40].

Furthermore, the road geometry can be considered to assess possible driver intents. In general, the road environment is laterally strongly constrained which justifies the simplifying assumption that traffic participants purely act longitudinally along the lane centerlines of the considered road network [6, 45]. This assumption drastically reduces the computational effort and allows more complex prediction models. In [45], all possible connecting lanes are considered equally at an intersection for trajectory prediction. This results in a low prediction accuracy for scenarios, where a predicted future trajectory depends on a discrete decision on the chosen path or maneuver.

As a consequence, estimating the likelihood of a driver’s future maneuver or intent can further increase the prediction horizon and accuracy. Methods targeting at the estimation of a driver’s future maneuver or intent, belong to the area of maneuver or situation classification.

2.1.2 Situation Classification

Maneuver or situation classification tries to infer one or several drivers’ intents on an abstract level. Instead of estimating a driver’s future behavior in terms of predicted spatio-temporal trajectories, those methods assess the likelihood of a high-level maneuver or situation such as “turning right”, “stopping at stop line” or “vehicle A giving way to vehicle B”. Maneuver classification is generally applied to tasks, where the future maneuver of a single entity is assessed. To the contrary, situation classification applies to tasks assessing the joint maneuver constellation of multiple traffic

participants in a scene. Numerous approaches tackle the problem of maneuver or situation classification with a wide range of different methods. Rule-based representatives for maneuver and situation classification are provided in [58, 98, 113, 114, 124]. Those methods generally incorporate a large and usually deeply nested rule-based assessment of the different aspects of a maneuver or situation. Advantages of rule based methods are the low computational effort and the human comprehensibility. On the other side, those methods are often complex to set up and do not scale well with the complexity of situations.

Methods for situation classification which treat the problem in a more probabilistic way are e.g. approaches utilizing the Dempster-Shafer theory of evidence [120]. These approaches combine beliefs of individually modeled situations or maneuvers to assess the currently executed maneuver [101, 134].

Another large field of probabilistic situation classification comprises methods based on Bayesian networks. In this area, task-specific Bayesian networks are modeled graphically to represent the relevant dependencies between measurable features and the considered maneuver or situation. The network is then applied to infer if a certain situation holds for the currently sensed scene. Representatives of this field are [1, 12, 15, 25, 46, 72, 75, 78, 82, 93, 104–106, 114, 116, 119, 137]. In general, Bayesian filters such as Kalman or Particle filters can be represented as Bayesian networks. This allows the realization of sequential Bayesian inference, as it is done in [46, 47, 83, 145]. Those methods can be summarized under the term Dynamic Bayesian Networks.

When considering interaction between traffic participants, which is especially relevant for the prediction of inner-city scenes, Bayesian models become relatively complex due to the conditional dependencies [47]. Some approaches tackle this problem by extending the basic Bayesian Network with so-called relations and object orientation [57, 75, 111]. In [75] an object-oriented, probabilistic approach for estimating traffic participants' future routes is proposed. In this approach the Bayesian inference of the interaction between traffic participants is carried out in an intermediate step. At an intersection scenario this approach justified that the incorporation of interaction can reduce the route prediction uncertainty.

Another approach that explicitly takes interaction into account is [8]. In this approach the interaction-aware intention of each driver is estimated by performing a multi-agent simulation. This estimate is then used in subsequent steps to perform lateral and longitudinal motion predictions. For the lateral motion a Bayesian Network classifier is applied, while the longitu-

dinal motion prediction utilizes the acceleration/deceleration results from the multi-agent simulation. However, the approach targets only highway environments and is not directly applicable to inner-city scenarios.

In the situation classification and trajectory prediction approach presented in this thesis (see Chapter 6), interaction is taken into account similarly to [8], by applying interaction-aware microscopic² prediction models in situation-dependent multi-agent forward simulations. The situation representation explicitly separates interacting and non-interacting behaviors, targeting especially, but not only, inner-city scenarios such as intersections. Interaction is relevant to detect critical situations, as many accidents are caused by a lack of interaction between traffic participants.

Methods from the field of machine learning are commonly applied to maneuver or situation classification. In general, in a first step, a classifier is trained based on labeled training data, which is then used to classify the currently sensed situation, as it is done in [72, 104]. The training as well as the actual classification step usually rely on extracted features, specifically chosen to separate the considered situations. Machine learning-based approaches generally perform well, if enough training data is available. However, especially for critical traffic situations this is often not the case.

The situation classification and trajectory prediction approach proposed in Chapter 6 targets especially at detecting and predicting dangerous traffic situations. Hence, a model-based approach is preferred.

2.1.3 Joint Situation Classification and Trajectory Prediction

Methods targeting a long prediction horizon couple the tasks of situation classification and trajectory prediction.

Approaches combining risk-aware trajectory prediction methods with a high-level interaction-aware situation classification that detects if and how traffic participants interact, push the prediction horizon even further. This is because the scene understanding reaches a level, where the predicted spatio-temporal trajectories are substantiated by the detected cause (situation) for this specific behavior.

²Microscopic driver or traffic models describe general traffic characteristics, such as density and flow, by modeling each driver individually.

In [61] the assumption that drivers generally act in a risk-averse fashion, meaning that each driver usually tries to avoid collisions with other entities, is explicitly taken into account to enhance the prediction accuracy as well as the prediction horizon. Such approaches incorporate an estimation of the risk or collision probability inside the actual prediction process. Approaches for risk estimation are discussed separately in Section 2.2. The advantage of those methods is a high accuracy in complex scenarios, where the future behavior significantly depends on the interaction between multiple traffic participants. Disadvantages are the relatively high computational costs as the risk assessment itself is usually a computational expensive task. Furthermore, the assumption that drivers always act in a risk-averse fashion makes the prediction and detection of unlikely but risky situations difficult.

Further approaches utilize microscopic driver models to determine the actual driving behavior. Those approaches also belong to the category of interaction-aware, risk-averse situation classification and trajectory prediction, as microscopic driver models generally model interaction between different traffic participants and generate the behavior in a way to avoid collisions. Exemplarily, car-following driver models capture the longitudinal behavior of each entity in relation to a leading vehicle and adapt the velocity in a collision-avoiding way. In those approaches future maneuvers of the involved entities are estimated in a forward simulation using microscopic driver models under different maneuver-dependent assumptions. By comparing the actually sensed behavior of each entity with the situation- or maneuver-dependent predicted behaviors, the current high-level driving situation can be estimated. This estimation can be used to enhance the lower-level prediction of spatio-temporal trajectories. In [87] a driver model based on the Intelligent Driver Model (IDM) [133] is used to determine the actual driving behavior at intersections by comparing the actual driving behavior with trajectory predictions for different possible maneuvers.

In this thesis a joint situation classification and trajectory prediction approach is presented in Chapter 6. For each relevant situation in the current scene, spatio-temporal trajectories are predicted, which are then compared to the actually driven trajectories of the involved entities. The similarity between the predicted trajectories and the driven trajectory is then applied to estimate each driver's intent. For the trajectory prediction the novel, interaction-aware Foresighted Driver Model is applied.

The FDM is able to generate a risk-averse behavior. Hence, the presented system can distinguish between interacting, risk-averse and non-interacting, risky behavior.

The machine learning-based approach presented in [97] studies the effectiveness of convolutional recurrent neural networks to predict spatio-temporal trajectories of vehicles by using raw image-like tensors as input. The deeper layers of the neural network learn an abstract representation of the current situation. Consequently, those methods can also be considered as a combined situation classification and trajectory prediction approach.

Recapitulating, situation classification and trajectory prediction is generally substantiated by the overlying goal of a safely acting system. Before generating a safe behavior some definition how to quantify a *safe behavior*, or vice versa a *risky behavior*, has to be provided.

2.2 Risk Evaluation

In Chapter 6 a novel approach for situation classification and trajectory prediction is proposed. The situation classification system, acting on an abstract level to infer the involved traffic participants' intents, represented by situations, has been coupled with a prediction of spatio-temporal trajectories on a physical level. In Section 2.1, a variety of methods has been discussed, relating this approach to the current state-of-the-art.

Relying on such methods for situation classification and trajectory prediction, different kind of approaches have been proposed assessing an entity's future risk. Risk is generally understood as the expected damage related to critical future events. For traffic environments, this implies an understanding of expected damage in terms of collision prediction [84].

The majority of approaches for risk assessment performs first a prediction of possible future trajectories for all entities involved in a current scene, followed by a collision detection to achieve at a likelihood estimation of future collisions. The collision estimation can be combined with an evaluation of the severity in case the collision occurs.

The detection of collision of two predicted spatio-temporal trajectories is often carried out by checking for spatial overlap using the predicted vehicle states at the same moment in future time [96]. Therefore, in many methods a vehicle's shape is represented by a surrounding polygon [19, 20, 40, 62, 129]. However, when examining a large number of trajectories, the overlap detection can be computationally expensive. As a consequence,

approximate methods have been proposed [7, 13]. For this purpose, purely distance-based methods, or methods approximating the vehicle shape by a set of circles [7], can be employed. The overlap verification of circles is a computational inexpensive distance calculation.

The prediction of spatio-temporal trajectories as well as the subsequent risk assessment is usually uncertain. Consequently, probabilistic methods for the assessment of risk have been proposed, taking the uncertainties, e.g. in the prediction process into account.

In Section 2.1, state-of-the-art trajectory prediction approaches have been discussed which use sampling-based methods, based on e.g. Monte-Carlo simulations or Kalman filters, to achieve a probabilistic distribution of possible trajectories. By integrating over the collision inspection of the entire sampled trajectory distribution the likelihood of collision can be estimated, as it is e.g. carried out in [80, 116, 129].

Other approaches leading to a probabilistic collision assessment utilize prediction methods providing a stochastic reachable set for each entity's trajectory. This set of reachable states can be employed to check for spatial overlap, while the amount of overlap is assumed to be proportional to the collision probability [5, 6, 49].

A similar approach is followed in [3], where inevitable collision states (ICS) are used as a risk measure. A movement for an entity is determined in order to avoid those ICS. For a large number of scene entities the set of ICS becomes unacceptably large and no safe movement can be determined anymore. As a consequence, the idea of ICS has been extended to probabilistic collision states (PCS), allowing a certain collision probability of the entity movements.

The estimation of collision probability alone is not always sufficient to generate the best possible behavior. As an example consider [18], where in the case of inevitable car-to-pedestrian collisions a risk function in terms of pedestrian injury is used in pedestrian protection scenarios. The injury risk function is based on the collision velocity. Another approach considering the expected damage is [109], where a risk measure is introduced, that is based on a reachable space evaluation, taking the expected collision damage in terms of an impact factor into account.

This thesis follows a similar approach. The risk estimation in Chapter 3.2, which is applied to evaluate possible ego behavior alternatives in Chapter 7, always combines a calculation of an event/collision probability along with an estimation of the damage for the predicted critical events.

Risk assessment methods relying on a large sampled distribution of future trajectories combined with a subsequent collision examination, generally have a high computational effort. To reduce the complexity, those approaches often use relatively simple prediction models, such as constant-velocity, as well as a simplified binary collision checking procedure, neglecting the severity of a collision.

Another group of widely used approaches does not try to estimate the collision probability, but quantifies the future risk in terms of time measures. Especially the time-to-X (TTX) indicators are very popular, to which also the well-known time-to-collision (TTC) belongs. The TTC represents the expected time left until a collision occurs. Representative risk evaluation approaches, which are based on the TTC measure are [7, 17, 19, 40, 54, 77, 85, 96, 126]. In [96] the TTC is employed to select a future behavior or trajectory of lowest risk (largest TTC) from a set of possible behaviors. Another TTX measure is the time-to-react (TTR) which quantifies the time left for the driver to react, before a collision occurs [54, 81]. This measure is derived by estimating the last moment in predicted time at which a performed action of the driver could avoid a collision. Further similar measures are the headway time [108] and the required deceleration to avoid an incident [66]. The great benefit of these approaches is their simplicity and the low computational effort. However, they are generally restricted to well-defined scenarios such as car-following or longitudinal collisions and not applicable in a straightforward way to other scenarios.

A further class of risk estimating methods relies on the assumption that unexpected behavior which deviates from the normal behavior in traffic scenarios, is generally assumed to be critical. In [83] a particle filter is applied to estimate how good a driver's intention (what a driver actually intends to do) fits to the expected behavior. The larger the discrepancy, the larger the assumed risk for colliding with other entities. Those measures generally need a good estimation of what is considered as *normal* or *expected* behavior. Each behavior that is not considered could result in a false assessment of high risk.

2.3 Behavior Planning

To achieve a system that is able to act safely in traffic environments, a behavior planning step, subsequent to the situation classification, trajectory

prediction and risk evaluation steps, is necessary.

One group of behavior generating approaches utilizes deterministic graph search algorithms, focusing on the calculation of collision-free spatial paths. For this purpose, Hybrid A* algorithms are applied in [35, 43], while [88, 103] use state grid search approaches. In [76] a sampling-based approach is utilized to gather a collision-free drivable path. The advantage of those algorithms is the ability to find globally optimal paths which prevents the algorithms from getting stuck in local minima. Furthermore, the approaches are suitable for spatially very complex environments, such as parking. However, mostly static environments are targeted, without the consideration of other dynamic entities. Alternatively, dynamic entities are considered as static between two consecutive planning steps. Furthermore, those approaches are generally only applicable to low-velocity scenarios, where the system dynamics are neglectable, as they are generally not considered.

Having a deeper look at road traffic environments, it can be noticed that the environment is highly structured and laterally constrained, e.g. by lanes and road boundaries. Additionally, for urban and highway scenarios many dynamic objects have to be dealt with. As a consequence, in traffic environments, the longitudinal behavior, e.g. velocity adaptation, is often more important than the lateral component. Therefore purely spatial path planning methods are not sufficient for the behavior generation in on-road scenarios. To approach on-road scenarios, methods which consider both, path planning and the vehicle's dynamics, have been developed. Many approaches apply model-predictive motion planning algorithms that consider longitudinal and lateral motion [131, 135, 139]. Also sampling-based motion planners are commonly used for the joint consideration of spatial paths and dynamics. In [92] a large set of possible spatio-temporal trajectories is generated to select one for execution [135]. Considering the entire state space in terms of spatio-temporal motions as a search space is computationally very demanding. To retain the advantages of a full spatio-temporal motion planner but reduce the computational effort, hierarchical methods have been proposed [50–52, 136].

The consideration of prediction, interaction, and decision uncertainty is missing in many motion planning methods. However, it is a very important aspect to act safely and efficiently in highly dynamic environments such as road traffic [86]. In [142] uncertainties of the ego and other vehicles' predictions are assessed by applying Gaussian filters. In [4, 6] the risk of a planned path is evaluated, while stochastically considering the uncertainties in measurement and behavior.

In [86] a hierarchical framework for trajectory planning is proposed. The high-level planner is responsible for decision making on the maneuver level, such as overtaking or lane-following. The actual collision-free trajectory is then tracked by a low-level controller.

In the situation classification and trajectory prediction approach introduced in Chapter 6 as well as the behavior planning approach introduced in Chapter 8, the lane centerlines, which are derived by a navigational planner using map data, are utilized as reference paths for prediction and planning.

Another hierarchical approach is presented in [136]. The approach basically consists of three layers. The highest, so-called mission-planning layer derives possible routes on the lane-level from a starting- to a target location. The underlying reference planner then calculates desired spatio-temporal trajectories along the given route, considering vehicle dynamics, but neglecting dynamically changing obstacles, such as other traffic participants. On the lowest layer, the behavioral planning layer, the focus lies on the adaptation of the reference trajectory to incorporate dynamic entities. This layer includes a prediction of other entities' trajectories, including an estimation of their intentions and an evaluation of previously generated possible behavior alternatives in terms of a cost function which considers safety as well a comfort aspects.

The framework for situation-based risk evaluation and behavior planning, presented in this thesis would align to the behavioral planning layer, assuming that a desired reference trajectory to follow is given by a higher level instance.

Further hierarchical frameworks for behavior planning are [52, 95, 122]. In [128] a wide range of existing frameworks and architectures for automated driving are analyzed. According to the authors a more unified treatment of the different collaborating steps is necessary. This also includes an integrated approach to evaluate future risk.

2.4 Traffic Models

In Chapter 5 a novel microscopic driver model is introduced, which is based on a simplified system for *situation-based risk evaluation and behavior planning*. This includes the consideration of multiple driving situations with a prediction of spatio-temporal trajectories, a simplified risk assess-

ment part and a behavior generation step performing a gradient descent on a cost function including risk and utility considerations. This *Foresighted Driver Model* is applied as a prediction model to the situation classification and trajectory prediction step in Chapter 6.

There are in general two major categories of traffic models. Macroscopic traffic models simulate the traffic flow by modeling its stream characteristics, such as flow and density, without considering each vehicle individually [16, 74, 121], whereas microscopic traffic or driver models describe the dynamics of each vehicle individually in relation to surrounding traffic. As a consequence, microscopic traffic models are preferable for the prediction of the future behavior of individual traffic participants, especially on the level of spatio-temporal trajectories, as done in Chapter 6.

Many microscopic approaches model the longitudinal behavior, the behavior along a given path or lane, separately from the lateral behavior [14, 16]. One group of such models are the so-called car-following models. The underlying assumption of car-following models is that the longitudinal behavior of a vehicle is mainly defined by a leading vehicle on the same lane.

When modeling the lateral behavior³, the focus lies on lane changing maneuvers. Lane change is usually modeled as a discrete decision. The approaches in [2, 56, 127, 138] use a decision tree to model gap acceptance and lane change.

Focusing on the longitudinal behavior⁴, microscopic traffic models for driving dynamics can be further differentiated. On the one hand, there are complex models which target at an accurate reproduction of a diversity of driving situations. Usually, these models enable a fine tuning by an extensive number of parameters and are based on a detailed case differentiation using a complex decision logic. Representatives are e.g. the models used in the traffic simulators MITSIM and VISSIM, based on variants of [140]. On the other hand, there are simplified models that allow the analysis of collective traffic dynamics [9]. Between the two categories, new models have been proposed like the Gipps-model [48],[73] and particularly the *Intelligent Driver Model* (IDM) [133], which combines simplicity with good modeling accuracy for car-following behavior, and which has become a standard reference in latest publications because it is easy to use but

³Lateral behavior describes the driving behavior laterally to the driving direction and/or path the entity follows, e.g. the road centerline. This mainly involves steering commands which depart from the original path.

⁴Longitudinal behavior describes the vehicle behavior longitudinally along a spatial path which mainly comprises velocity changes without leaving the original path.

still captures several aspects of microscopic and collective driving to a good extent. The IDM forms an important foundation of the novel Foresighted Driver Model, introduced in Chapter 5 and is therefore separately discussed in detail in Chapter 5.

Most car-following models are purely defined longitudinally with a leading vehicle and well-defined distance between the leading and the following vehicle. Applying the car-following driver models to arbitrary road networks, which also include intersections, rises the problem that no leading vehicle is defined for crossing paths. Therefore, intersection control models have been developed, which control the traffic flow at intersections. In [14] a method is proposed, where a right-of-way matrix determines for each approaching vehicle, if it has to brake or can drive on. As this is a quite conservative way of modeling intersection behavior an extension is proposed in [42], where the expected intersection point as well as the expected time left until a vehicle reaches the intersection point, are considered. Still, only decelerating behavior is presumed. However, in some real-world scenarios, accelerating to clear the intersection would be the favorable action of a human driver.

Furthermore, by treating longitudinal and lateral behavior separately certain behavioral effects are lost, as some require a joint consideration. This is e.g. the case when performing a lane change onto a lane with traffic of significantly higher velocity. In this case only adapting the longitudinal behavior before changing lane, namely accelerating, allows a safe lane change. In [132] a driver model is discussed, that combines acceleration (for car-following), lane-changing and standard car-following behavior, to allow a more accurate modeling for such scenarios.

In Chapter 5 a novel microscopic driver model, the *Foresighted Driver Model*, is presented. The main component in the driver model is a highly general evaluation of future risk according to Chapter 3.2.3. The longitudinal behavior is derived by performing a gradient descent on a cost function combining risk with utility considerations. As a consequence, the driver model is applicable to a wide range of scenarios, such as highway or intersections. A distinction between car-following and intersection behavior is not necessary. Additionally in [33, 37] the author of this thesis presents an extension to naturally incorporate lateral driving behaviors, such as lane-changing, into the model.

3 Basic Concepts

This chapter proposes several novel basic concepts, which are applied to the framework for *situation-based risk evaluation and behavior planning*. Furthermore, these concepts are applicable to tasks beyond the scope of this thesis, as they constitute independent evaluation methods.

First in Section 3.1, the general idea of situations is introduced. Situations are defined to cluster the infinite amount of different behavior possibilities in a traffic scenario into groups of similar behaviors and represent them by prototypical behavior patterns. Situations can be employed to reduce the complexity of traffic scene analysis, prediction and the subsequent task of behavior planning by targeting only a limited number of prototypical behavior patterns, instead of the unfeasible processing of all possible behaviors. Furthermore, information on how those situations and especially the behavior patterns can be generated for traffic scene analysis are briefly described. Here, the focus lies on distinguishing interacting and non-interacting behavior when interaction between traffic participants is necessary for a safe future evolution of a scene.

Second, Section 3.2 proposes a novel, highly general, probabilistic model for future risk as a continuous function over time, indicating the criticality of a certain future behavior. Starting from the common understanding of risk as the expectation value of the cost related to critical future events, a situation-dependent risk expression, incorporating the advantages of behavior clustering, is derived. By assuming that critical events, such as collisions, are sparse, 1) the probability that an event occurs and 2) the expected cost/damage in case such an event occurs, are the main parts which have to be considered in the evaluation of risk. Starting from the Poisson process [69] as a statistical process to model rare events, an explicit model for the event probability can be achieved. Here, 1) the probability that an entity “survives” until a certain event might occur, represented by a so called *survival function* and 2) the probability, that the event occurs in case the entity survives until then, represented by an instantaneous event probability, is taken into account. Besides considering car-to-car collision risks, additional types of risk, such as the risk of skidding off the road in curves or losing control due to high decelerations, are introduced. All

those different types of risk are naturally integrated in the risk model and easily extendable to further types of risk.

For traffic scenarios the risk measure can be used to quantify the expected costs of possible future behaviors, such that the future behavior can be planned in a risk-averse way. In addition, an approximate model for future risk, targeting only the expected risk maxima, using easy-to-extract risk indicators, is derived. Such an approximate risk model can then be employed in time-critical applications.

Finally in Section 3.3, a measure to quantify the similarity of two spatio-temporal trajectories is derived. Traffic environments are in general spatially limited. Especially, behavior lateral to the driving direction is highly constrained by lanes and road boundaries. Therefore, it is explicitly differentiated between longitudinal and lateral trajectory similarities. Such a measure can then be employed to cluster similar spatio-temporal trajectories. In Chapter 6 this similarity measure is applied to compare an actual sensed spatio-temporal trajectory with prototypically predicted trajectories, derived from different situations, in order to obtain an estimate of the current driving situation.

3.1 Situations and their Modeling

The target of the framework for *situation-based risk evaluation and behavior planning* (see Chapter 4) is the generation of a safe and efficient future behavior. This involves the evaluation of possible behaviors in terms of risk. Section 3.2 introduces the concept of risk, which can be understood as the expectation value of the cost or benefit related to a critical future event, e.g. a collision, and which depends heavily on the possible behavior alternatives of all involved entities. In complex traffic scenarios, it is unfeasible to evaluate all possible state evolutions of the involved traffic participants. A way to reduce the complexity is, on the one hand, to group similar behavior alternatives of acting entities by using situations which represent prototypical behavior patterns, and on the other hand, to restrict the behavior alternatives to those which are relevant for the ego entity's behavior.

A situation describes a prototypical behavior of a subset of involved scene entities, comprising the states of the ego car and optionally other traffic participants' parameters, the road structure and their relations. Different behavior alternatives of the involved entities lead to different situations, resulting in a separate risk evaluation and corresponding con-

sequences for the ego vehicle's future behavior¹.

Sampling-based approaches for trajectory generation (see e.g. [117]), use dynamic models of traffic participants and randomly sample over the parameter space to provide a large amount of possible trajectories, as shown in Figure 3.1(a). As a result, the likelihood evaluation of trajectory constellations of a certain traffic scenario ends up in a highly combinatorial problem. Thus, similar trajectories are clustered to reduce the complexity of the problem. Each cluster is then represented by prototypical trajectories, in this case one for each traffic participant. A subset of possible situations is shown in Figure 3.1(b).

3.1.1 Situations in Traffic Scenarios

The general traffic environment is spatially, especially laterally to the driving direction, highly constrained. As a consequence, trajectories of different spatial appearance and trajectories of different longitudinal behavior should be treated separately.

On the one hand, behavior alternatives of involved traffic participants are separated by the given *road structure*, e.g. the type of intersection providing possible spatial paths. On the other hand different *longitudinal behaviors* along a given spatial path such as stopping at stop line or slowing down in curvy road segments can be distinguished. So far, a situation h is defined by a specific combination of entity² behaviors with one specific prototypical behavior per involved entity, which results in one prototypical spatial path χ and one prototypical longitudinal behavior q along this path for each entity.

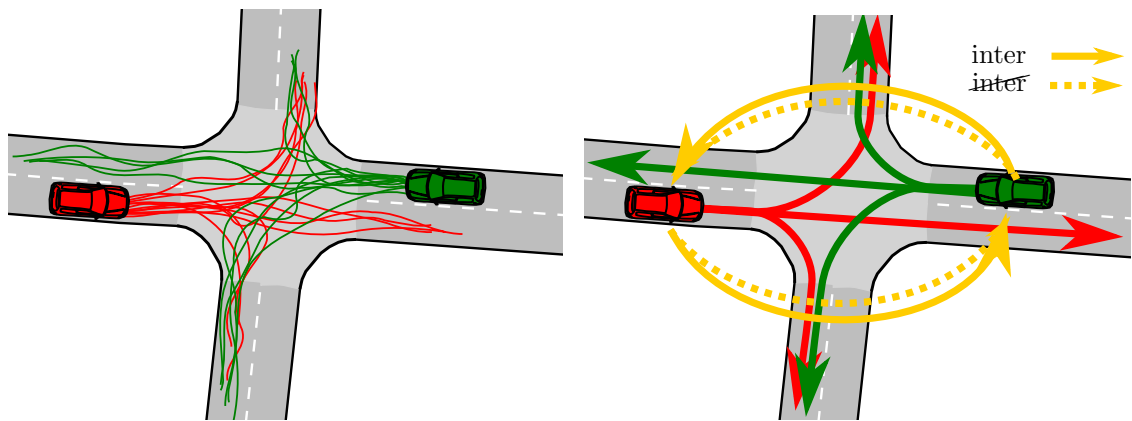
Considering N entities i , where each entity has N_χ^i possible spatial paths and N_q^i possible longitudinal behavior options, the entire set of situations \mathbb{H} in a current scene is obtained by determining all variations of the combinatorial set, resulting in $N_{\mathbb{H}}$ possible situations with

$$N_{\mathbb{H}} = N_\chi^0 \cdot N_q^0 \cdot \dots \cdot N_\chi^N \cdot N_q^N.$$

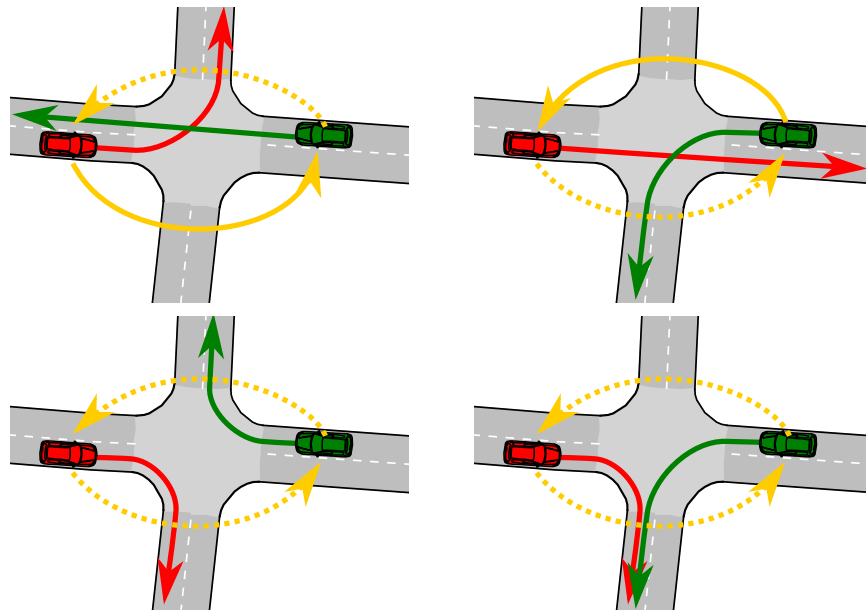
The process of randomly sampling a large amount of possible behaviors or trajectories and afterward clustering them in order to reduce the complexity of the scenario is a computationally demanding task. However, it

¹The main contributions of this section have been published by the author of this thesis to the IEEE Intelligent Transportation System Society (ITSS) in [30, 31, 39].

²A traffic entity can be any dynamic or static object involved in a traffic scenario such as other cars, parking cars, pedestrians or cyclists.



(a) Left: Possible future behaviors/trajectories of the ego car (green) and another car (red). Right: Grouping of behaviors into prototypical behaviors defined by prototypical spatial paths and prototypical longitudinal behavior options (here interacting (*inter*) and non-interacting (*inter*)).



(b) Subset of possible situations. Each situation is defined by one prototypical spatial path for each entity (green and red path) and one prototypical longitudinal behavior (influenced by yellow arrow indicating interaction). The longitudinal behavior is determined here by the interaction pattern, meaning that in the interaction-aware case the risk of the other traffic participant will be explicitly considered for the own driving behavior. The bottom-right situation represents an incorrect risky behavior, as the green ego car is assumed to not yield right-of-way, whereas the other three example situations represent a correct driving behavior.

Figure 3.1: Similar behavior alternatives are clustered and represented by prototypical behavior patterns. A situation is a joint prototypical behavior pattern, comprising one behavior alternative per involved entity.

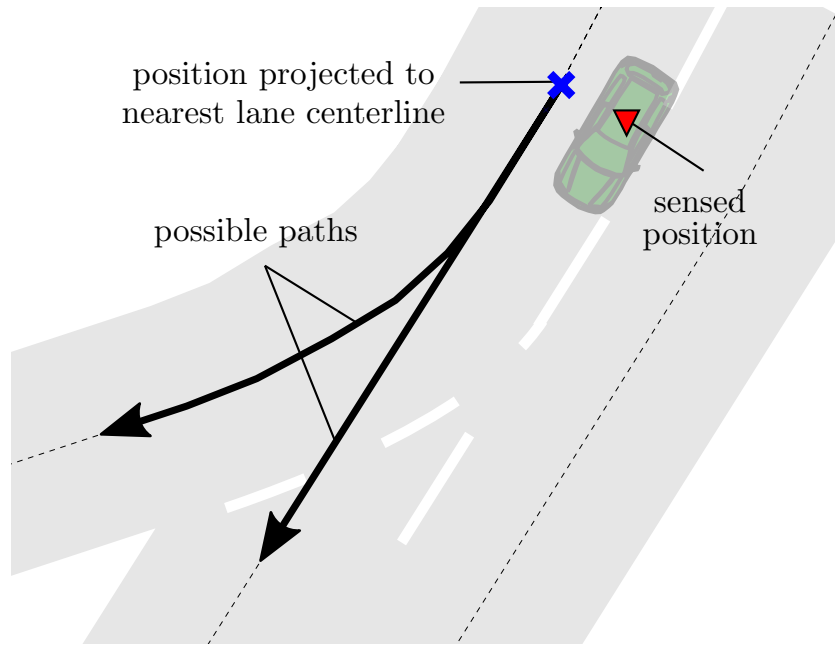


Figure 3.2: Map-based estimation of possible spatial paths. After projecting the measured vehicle position (red triangle) onto the centerlines of the surrounding reachable lanes (blue cross), map information can be employed to derive possible drivable paths of the vehicle (black paths).

is possible to directly predict or generate the prototypical trajectories for each cluster instead of performing an extensive sampling and clustering process.

The possible prototypical spatial paths can be determined in a straightforward way by the given road structure. For this purpose, as shown in Figure 3.2, the current position of the entity is mapped to the center line of the road structure element (e.g. lane or lane junction) to determine possible future paths from the given road geometry.

For road scenarios which are spatially not as structured as intersections, such as highway overtaking or lane-change scenarios, possible drivable path can be determined likewise by assuming a discrete set of drivable paths, e.g. *stay on current lane*, *perform an immediate lane change* or *perform a delayed lane change*.

For the prototypical longitudinal behavior options different longitudinal behavior generating models are necessary.

3.1.2 Interaction-aware Situation Model

It is common to use simple interaction-unaware models, such as constant velocity, constant acceleration or similar [26, 94, 116], for the generation

of different longitudinal behaviors. However, interaction plays a central role in behavior prediction. The behavior of an entity is mainly influenced by the interaction with other traffic participants and structural elements, such as curves or traffic lights. Additionally, the breakdown of interaction between traffic participants, e.g. caused by inattentiveness or observation errors, are identified to be a major reason for collisions, see e.g. [130]. Thus, the detection that a traffic participant does not interact when it indeed should interact due to criticality reasons is a substantial problem, which is targeted in Chapter 6. Therefore, an interaction-aware prediction model is necessary to gather meaningful prototypical behavior options. A suitable model is e.g. the Foresighted Driver Model explained in detail in Chapter 5.

A prerequisite is a situation model that allows to model different assumptions on how/if entities interact with each other and with the road topology. A situation is modeled such that a representing situation parameter h contains a set of spatial paths Ξ (one path χ^i for each entity), an interaction matrix A , indicating which entity considers which other entity for interaction and a set of static model parameters P_{FDM} ,

$$h = (\Xi, A, P_{FDM}),$$

with

$$\Xi = [\chi^0, \dots, \chi^N],$$

$$A = \begin{bmatrix} a^{0,0} & \dots & a^{0,N} \\ \dots & \dots & \dots \\ a^{N,0} & \dots & a^{N,N} \end{bmatrix}.$$

Here, $a^{u,w} = 1$ indicates that entity u considers entity w for interaction, whereas $a^{u,w} = 0$ indicates no interaction. The parameter set P_{FDM} allows different assumptions on how the entities act and interact, e.g. the aggressiveness of a driver, which is further explained in Chapter 6.4. As a result, a situation provides the subsequent *trajectory prediction* step with all information needed to generate a prototypically predicted trajectory for each involved entity, which incorporates different types of interactions of the involved entities.

In Chapter 6.4, the FDM is applied to the trajectory prediction step. It is a highly general, interaction-aware driver model, suitable to predict realistic, long-term stable, spatio-temporal trajectories in a wide range of traffic scenarios, such as intersections with several acting entities, highway

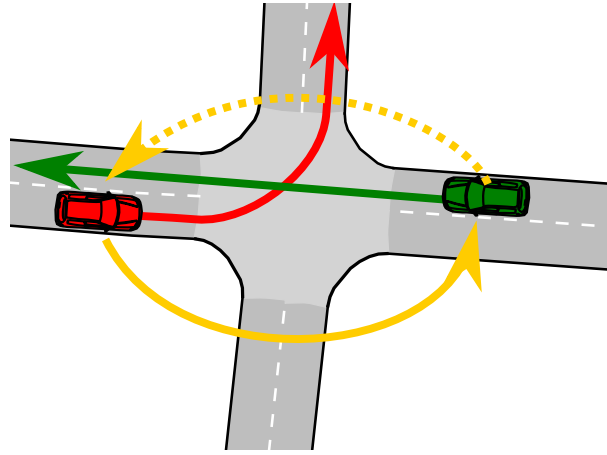


Figure 3.3: Example situation where the other car (red) considers the ego car (green) for interaction and yields right-of-way when turning left, while the ego car drives through without considering the other car.

driving, car following and curve driving. The entities' prototypical spatio-temporal trajectories are then generated by performing a multi-agent forward simulation of the current scene, where each entity is modeled as an FDM using the situation-dependent spatial paths, the entities considered for interaction (defined by the interaction matrix A) and the predefined model parameters.

In Figure 3.1(b) a subset of possible situations is illustrated exemplarily. For the situation in Figure 3.3, Ξ_1 and A_1 have the form

$$\Xi_1 = [\chi_s^0, \chi_l^1],$$

$$A_1 = \begin{bmatrix} 0 & 0 \\ 1 & 0 \end{bmatrix},$$

where χ_s^0 is the “going straight path” of the ego car (0) and χ_l^1 the “turning left path” of the other car (1). A_1 indicates that the other entity (red) considers the ego entity (green) for interaction, while the ego entity does not consider the other entity.

Section 6 utilizes the situation models, which explicitly take different assumptions on interaction into account, to gather prototypical future trajectories. Furthermore, a recognition or classification of the current driving situations as well as of potentially dangerous situations by detecting the *lack of interaction* is performed. For this purpose the actually sensed behavior is compared with “how the driver is expected to behave” for each considered situation.

3.1.3 Situation Pre-Selection

Since the number of situations can become quite large, a simple rule-based filter is defined, which reduces the entire set of situations to a subset that is important for the ego car's behavior. As stated in [70], a proper situation selection approach takes the situation occurrence probability as well as the potentially upcoming risk into account. Thus, the total set of situations is reduced based on a worst case risk estimation. Assuming a distance-based risk measure, as discussed in Section 3.2, the highest possible risk along two trajectories is, where the entities get closest. Additionally taking the vehicle dynamics, especially the maximal deceleration/acceleration, into account, an upper bound r_b for risk can be estimated, representing the maximal possible risk the ego entity can encounter if both (ego- and other car) act in the worst possible way, meaning that the entities get closest possible under consideration of their vehicle dynamics. Thus, the subset of situations of generally low car-to-car collision risk is built as

$$\mathbb{H}^{r_{low}} = \{h \in \mathbb{H} | r_b(h) \leq b_{risk}\},$$

where b_{risk} is a risk threshold, defining when a situation is considered as being “of low risk”.

In situations of low risk, the predicted behavior of the entity with and without the consideration of interaction would be similar, as there is no need for a driver to intervene. Consequently, interaction in situations of low risk plays a minor role and those situations \mathbb{H}^{inter} are removed from the set of considered situations

$$\mathbb{H}^{cons} = \{h \in \mathbb{H} | h \notin \mathbb{H}^{r_{low}} \vee h \in \mathbb{H}^{inter}\}.$$

The result is a set of situations, which are important to understand a scene and important for the own future behavior.

3.2 Risk

A central aspect of advanced driver assistance systems and their underlying traffic scene analysis is the evaluation of future behavior in terms of risk. According to [36], risk is the “probability of something happening multiplied by the resulting cost or benefit if it does”. Such a consideration of risk implies the prediction of future events in a probabilistic fashion, including the estimation of the expected costs in case a critical event occurs.

As a result, risk can be applied to evaluate and plan risk-averse future behavior.

There are many different approaches targeting different aspects of risk, such as the risk resulting from static obstacles (e.g. road boundaries), the probability of colliding with dynamic traffic participants, the risk caused by loss of control due to destabilizing behavior, e.g. full braking, or the probability of reacting to a future critical event in the remaining time. In Chapter 2.2 those approaches were covered in more detail. Despite the extensive research in the area of risk modeling, an approach to model risk in a general way, including all its different aspects in a time-continuous fashion, is missing. This section derives such a general model as a continuous future risk function over time. It can be applied directly to risk estimation, behavior evaluation and behavior planning³.

3.2.1 Risk Estimation for Dynamic Scenes

Chapter 4 introduces a framework for *situation-based risk evaluation and behavior planning* with its different components. The knowledge \mathbf{x}_t about the scene at time t , acquired by sensor measurements in a scene observation step, constitutes an entry point to risk estimation. Since the scene may be composed of several entities (e.g. different traffic participants, infrastructure elements, etc.) with state vectors \mathbf{x}_t^i (ego car state \mathbf{x}_t^0), we write $\mathbf{x}_t := \{\mathbf{x}_t^0, \mathbf{x}_t^1, \dots, \mathbf{x}_t^n\}$. Using discrete time step indices $t, t+1, \dots, t+s$ (time step size Δt), state vector sequences are additionally introduced as

$$\mathbf{x}_{t:t+s} := \{\mathbf{x}_t, \dots, \mathbf{x}_{t+s}\}, \quad (3.1)$$

which describe the states of the scene from t (now) until a time $t+s$ (s into the future).

The overall target of a system based on the framework from Chapter 4, is to compute a behavior in form of a trajectory over the ego-car states $\mathbf{x}_{t:t+s}^0$, minimizing the expected/predicted risk. Since risk is the probability that a disruptive event (e.g. an accident) happens multiplied by the cost/damage if it does, future risk⁴ is defined at $t+s$ as the cost expectation value

$$r(t+s, \mathbf{x}_t) = \int c_{t+s} P(c_{t+s} | \mathbf{x}_t) dc_{t+s}, \quad (3.2)$$

where $P(c_{t+s} | \mathbf{x}_t)$ is the probability of a damage c_{t+s} , happening at future

³The main contributions of this section have been published by the author of this thesis to the IEEE ITS Society in [26, 27, 39].

⁴To be precise, this is the risk *density* over time.

time $t + s$, for the known states \mathbf{x}_t of the current scene.

An all-situation risk prediction is computationally infeasible. Therefore, the prediction space is partitioned into different prototypical situation classes (see Section 3.1). A situation combines a small subset of acting and interacting entities (usually car-car or car-infrastructure pairs) with a prototypical spatio-temporal behavior pattern, like “car A braking to give right-of-way to car B at an intersection”. This results in situation-specific state vector sequences, which depend on a current situation hypotheses h_t , such that the damage probability is

$$P(c_{t+s}|\mathbf{x}_t) = \sum_{h_t} P(c_{t+s}|\mathbf{x}_t, h_t) P(h_t|\mathbf{x}_t). \quad (3.3)$$

The situation occurrence probabilities $P(h_t|\mathbf{x}_t)$ are calculated at t from the evidence \mathbf{x}_t and are valid during the prediction interval $[t, t + s]$, until their calculation is renewed. Section 3.1 provides a more detailed definition of situations and a description of how they can be generated. Furthermore, a prediction-based situation classification approach, providing estimations of situation occurrence probabilities, is introduced in Chapter 6.

The situation-dependent damage probability from (3.3) can be expanded to

$$P(c_{t+s}|\mathbf{x}_t, h_t) := \int_{\mathbf{x}_{t+s}} \cdots \int_{\mathbf{x}_{t+1}} \sum_{e_{t+s}} P(c_{t+s}|e_{t+s}, \mathbf{x}_{t+s}) \quad (3.4)$$

$$\cdot P(e_{t+s}|\mathbf{x}_{t:t+s}) P(\mathbf{x}_{t:t+s}|\mathbf{x}_t, h_t) d\mathbf{x}_{t+s} \cdots d\mathbf{x}_{t+1},$$

i.e., a combination of

1. a damage probability $P(c_{t+s}|\dots)$ given that an event e_{t+s} happens at $t + s$ and the states at the event time are known,
2. a future event triggering probability $P(e_{t+s}|\dots)$, which depends on the future state vector sequence $\mathbf{x}_{t:t+s}$ and
3. a prediction probability $P(\mathbf{x}_{t:t+s}|\dots)$ of the state vector sequences $\mathbf{x}_{t:t+s}$ for each situation hypothesis h_t , starting with the states \mathbf{x}_t .

The discrete variable e_{t+s} describes a certain event at future time $t + s$, such as car-to-car, car-to-pedestrian or car-to-infrastructure collisions or control loss at drivability limits. For each of them, a specific damage probability $P(c_{t+s}|e_{t+s}, \mathbf{x}_{t+s})$ is used. E.g. car-to-car accidents are modeled using an inelastic collision approach. In addition, $e_{t+s} = 0$ indicates

no event, in this case the costs are given by efficiency, utility and comfort considerations.

The event triggering probability $P(e_{t+s}|\mathbf{x}_{t:t+s})$ can be calculated using a so-called *survival function*, as will be presented in Section 3.2.2. What remains to be calculated is the situation-dependent state prediction $P(\mathbf{x}_{t:t+s}|\mathbf{x}_t, h_t)$. A standard way is to use (expensive) stochastic sampling methods in combination with appropriate propagation probabilities $P(\mathbf{x}_{t+s'+1}|\mathbf{x}_{t+s'}, h_t)$ from one time step to the next. However, to reduce the complexity of the integrals in (3.4), yet appropriately capturing the growing prediction uncertainty over time, the probabilistic state vector sequence is approximated by its situation-specific prototypical state vector sequence⁵ $\hat{\mathbf{x}}_{t:t+s}$ (with $\hat{\mathbf{x}}_t = \mathbf{x}_t$)

$$P(\mathbf{x}_{t:t+s}|\mathbf{x}_t, h_t) \sim \delta(\mathbf{x}_{t:t+s} - \hat{\mathbf{x}}_{t:t+s}(\mathbf{x}_t, h_t)), \quad (3.5)$$

where $\delta(\dots)$ is a Dirac delta function. The growing uncertainty is modeled in the event triggering probability by incorporating explicitly the prediction time s to get $P(e_{t+s}|\mathbf{x}_{t:t+s}, s)$.

As a second approximation⁶, a deterministic damage calculation $\hat{c}_{t+s}(e_{t+s}, \mathbf{x}_{t+s})$ for fixed known states \mathbf{x}_{t+s} is introduced, resulting in the probability of damage

$$P(c_{t+s}|e_{t+s}, \mathbf{x}_{t+s}) \sim \delta(c_{t+s} - \hat{c}_{t+s}(e_{t+s}, \mathbf{x}_{t+s})) \quad (3.6)$$

Taking (3.2), (3.3) and (3.4) and inserting (3.5) and (3.6), results in the final risk estimation formula,

$$r(t+s, \mathbf{x}_t) = \sum_{h_t} r(t+s, \mathbf{x}_t, h_t) P(h_t|\mathbf{x}_t) \quad (3.7)$$

with the situation-dependent risk,

$$r(t+s, \mathbf{x}_t, h_t) \sim \sum_{e_{t+s}} \hat{c}_{t+s}(e_{t+s}, \hat{\mathbf{x}}_{t:t+s}(\mathbf{x}_t, h_t)) \cdot P(e_{t+s}|\hat{\mathbf{x}}_{t:t+s}(\mathbf{x}_t, h_t), s). \quad (3.8)$$

⁵A prototypical state vector sequence describes the predicted state of the considered scene at every future time step. This includes states of the ego- as well as other traffic participants, such as position and velocity.

⁶This is however not necessary so that a full probabilistic treatment of the damage can be easily incorporated back again.

The risk calculation therefore contains a damage cost calculation according to $\hat{c}_{t+s}(\dots)$ for critical events, a future event triggering probability $P(e_{t+s}|\dots)$, which depends on the predicted prototypical state sequence $\hat{\mathbf{x}}_{t:t+s}(\mathbf{x}_t, h_t)$, and a situation occurrence probability $P(h_t|\mathbf{x}_t)$.

The situation-dependent prototypical prediction of future states $\hat{\mathbf{x}}_{t:t+s}(\mathbf{x}_t, h_t)$ is achieved by a prediction step, performing a multi-agent forward simulation of the current scene (see Chapter 6.4) using deterministic interaction-aware agent models (see Chapter 5). However, other arbitrary models with a sufficient behavior complexity can be applied.

In Chapter 7, a risk calculation is performed according to (3.8) for different ego car behavior options, resulting in so-called *predictive risk maps*. In Chapter 8, behaviors are planned by searching for the best trajectories in terms of overall cost, combining risk and utility considerations.

3.2.2 General Risk Model

Recapitulating Section 3.2.1, risk is in general defined as the expectation value of the cost or benefit related to future critical events [89] and can be expressed in a probabilistic way as (3.2)

$$r(t + s, \mathbf{x}_t) = \int c_{t+s} P(c_{t+s}|\mathbf{x}_t) dc_{t+s}.$$

By partitioning the prediction space into situation classes h_t (3.3), expanding the situation-dependent damage probability (3.4) and incorporating approximations on the probabilistic state vector sequence by a situation-specific prototypical state vector sequence $\hat{\mathbf{x}}_{t:t+s}(\dots)$ and a deterministic damage calculation $\hat{c}_{t+s}(\dots)$, the general expression for situation-dependent future risk is proposed as (3.8).

In order to advance from the general definition of situation-dependent risk to an actual risk measure for a given prototypically predicted state vector sequence, 1) the deterministic damage calculation using a damage approximation model and 2) the probability of the future event happening at time $t + s$, have to be modeled.

Event Probability

Starting with the event probability, critical events in traffic scenarios, such as car-to-car collisions, are generally rare. Such rare events are commonly modeled as a so-called Poisson process [69], which is a statistical process characterized by the meantime τ between the occurrences of events.

Assuming an event rate $\tau_{e_{t+s}}^{-1}(\hat{\mathbf{x}}_{t+s})$ depending on the predicted future state vector $\hat{\mathbf{x}}_{t+s}$ of the scene at future time $t+s$, an instantaneous event probability for small time intervals $[t+s, t+s+\delta t]$ can be derived as,

$$P(e_{t+s}|\hat{\mathbf{x}}_{t+s}(\mathbf{x}_t, h_t)) = \tau_{e_{t+s}}^{-1}(\hat{\mathbf{x}}_{t+s})\delta t.$$

The instantaneous event probability does not consider the entire course of the predicted state sequence of the scene. As a consequence, it does not consider the case, that the observed entity has possibly already been involved in another critical event, e.g. a collision, before it could actually be involved in the considered event.

This issue can be described by a so-called inhomogeneous survival function [36], taking the entire course of the predicted state vector sequence $\hat{\mathbf{x}}_{t:t+s}(\mathbf{x}_t, h_t)$ into account,

$$\begin{aligned} S(\hat{\mathbf{x}}_{t:t+s}(\mathbf{x}_t, h_t), s) \\ = \exp\left\{-\int_0^s \tau^{-1}(\hat{\mathbf{x}}_{t+s'}(\mathbf{x}_t, h_t), s') ds'\right\}, \end{aligned} \quad (3.9)$$

with a total event rate, combining all possible event probabilities

$$\tau^{-1}(\hat{\mathbf{x}}_{t+s}(\mathbf{x}_t, h_t), s) = \sum_{e_{t+s}} \tau_{e_{t+s}}^{-1}(\hat{\mathbf{x}}_{t+s}(\mathbf{x}_t, h_t), s). \quad (3.10)$$

The survival function decreases monotonically from 1 to 0 with the predicted time s . The higher the total event rate, the faster the survival function decreases. This is due to the fact, that the likelihood of the entity being engaged in an event increases for a higher event rate and as a consequence the likelihood that the entity ‘‘survives’’ decreases.

The survival function represents the probability that the entity is not engaged in any event in the time interval $[t, t+s]$. Conversely, the probability that the entity is involved in any event, namely the accumulated total event probability is

$$\int_0^s \sum_{e_{t+s}} P(e_{t+s}|\hat{\mathbf{x}}_{t:t+s}(\mathbf{x}_t, h_t), s) ds = 1 - S(\hat{\mathbf{x}}_{t:t+s}(\mathbf{x}_t, h_t), s).$$

The total event probability for small time intervals $[t + s, t + s + \delta t]$ is

$$\begin{aligned} \sum_{e_{t+s}} P(e_{t+s} | \hat{\mathbf{x}}_{t:t+s}(\mathbf{x}_t, h_t), s) &= -\frac{d}{ds} S(\hat{\mathbf{x}}_{t:t+s}(\mathbf{x}_t, h_t), s) \delta t \quad (3.11) \\ &= \tau^{-1}(\hat{\mathbf{x}}_{t+s}(\mathbf{x}_t, h_t), s) S(\hat{\mathbf{x}}_{t:t+s}(\mathbf{x}_t, h_t), s) \delta t. \end{aligned}$$

Finally, the event probability $P(e_{t+s} | \dots)$ of a single event e_{t+s} can be expressed as the combination of the instantaneous event rate (assuming that the entity survives until predicted time s) and the probability that the entity actually survives

$$\begin{aligned} P(e_{t+s} | \hat{\mathbf{x}}_{t:t+s}(\mathbf{x}_t, h_t), s) \quad (3.12) \\ = \tau_{e_{t+s}}^{-1}(\hat{\mathbf{x}}_{t+s}(\mathbf{x}_t, h_t), s) S(\hat{\mathbf{x}}_{t:t+s}(\mathbf{x}_t, h_t), s) \delta t \end{aligned}$$

with survival function $S(\dots)$ (3.9), comprising a total event rate $\tau^{-1}(\dots)$ (3.10), and a single event rate $\tau_{e_{t+s}}^{-1}(\dots)$. Every single event rate $\tau_{e_{t+s}}^{-1}(\dots)$ can be modeled using appropriate risk indicators, shown in the following for car-to-car collision risks, the risk for skidding off the road in a curve and the risk of losing control due to strong braking.

But regardless whichever explicit risk indicators and event types are used, there are further reasons why the probability of an entity getting engaged in a future event decreases with predicted time. This is e.g. the increasing probability that a driver acts in an event-/collision-avoidant way or any other uncontrolled world state change. Furthermore the prediction accuracy generally decreases with time. In order to model this issue, a constant ‘‘event escape’’-rate τ_0^{-1} is introduced, leading to the survival function

$$\begin{aligned} S(\hat{\mathbf{x}}_{t:t+s}(\mathbf{x}_t, h_t), s) \quad (3.13) \\ = \exp\left\{-\int_0^s \tau_0^{-1} + \tau^{-1}(\hat{\mathbf{x}}_{t+s'}(\mathbf{x}_t, h_t), s') ds'\right\}. \end{aligned}$$

Assuming that critical events are usually triggered by a single cause (e.g. a car either collides *or* drifts out of the curve), different risk sources are superposed in the total event rate (3.10). Three different event rates are exemplarily modeled as follows.

First, for car-to-car collision risks, an appropriate model for the instantaneous event rate depends on the distance between two traffic participants,

such that the instantaneous event rate is large for small distances and decreases with an increase in predicted distance

$$\begin{aligned} & \tau_d^{-1}(\hat{\mathbf{x}}_{t+s}(\mathbf{x}_t, h_t), s) \\ & = \tau_{d,0}^{-1} \exp\{-\beta_d(s) \cdot \max(\hat{d}_{t+s}(\mathbf{x}_t, h_t) - d_{min}, 0)\}, \end{aligned} \quad (3.14)$$

where $\hat{d}_{t+s}(\mathbf{x}_t, h_t)$ is the predicted distance between the ego car and another traffic participant. The parameter d_{min} is the minimally allowed distance corresponding to a physical overlap.

Second, for risks caused by accidenting in a curve the instantaneous event rate can be modeled as

$$\begin{aligned} & \tau_c^{-1}(\hat{\mathbf{x}}_{t+s}(\mathbf{x}_t, h_t), s) \\ & = \tau_{c,0}^{-1} \exp\{-\beta_c(s) \cdot \max(v_{c,max} - \hat{v}_{t+s}(\mathbf{x}_t, h_t), 0)\}, \end{aligned} \quad (3.15)$$

where $\hat{v}_{t+s}(\mathbf{x}_t, h_t)$ is the predicted longitudinal velocity while driving on the curve, $v_{c,max} = \sqrt{a_{c,max} R}$ the maximal longitudinal velocity with the maximal centrifugal acceleration $a_{c,max}$, and R the curve radius at the driving point⁷. The instantaneous event rate is maximal for velocities larger than the maximally allowed (or physically possible) velocity $v_{c,max}$ and decreases for lower velocities.

Third, the instantaneous event rate for risks caused by losing control due to heavy braking can be modeled as

$$\begin{aligned} & \tau_b^{-1}(\hat{\mathbf{x}}_{t+s}(\mathbf{x}_t, h_t), s) \\ & = \tau_{b,0}^{-1} \exp\{-\beta_b(s) \cdot \max(b_{b,max} - \hat{b}_{t+s}(\mathbf{x}_t, h_t), 0)\}, \end{aligned} \quad (3.16)$$

where $\hat{b}_{t+s}(\mathbf{x}_t, h_t)$ is the predicted deceleration and $b_{b,max}$ the maximally allowed deceleration. Similar to the previous case, the instantaneous event rate is maximal for decelerations larger than the maximal allowed deceleration and decreases for smaller decelerations.

The values $\hat{d}_{t+s}(\mathbf{x}_t, h_t)$, $\hat{v}_{t+s}(\mathbf{x}_t, h_t)$ and $\hat{b}_{t+s}(\mathbf{x}_t, h_t)$ can directly be extracted from the situation-dependent, predicted state vector $\hat{\mathbf{x}}_{t+s}(\mathbf{x}_t, h_t)$. The parameters $\tau_{d,0}^{-1}$, $\tau_{c,0}^{-1}$ and $\tau_{b,0}^{-1}$ define the event rate at minimal dis-

⁷To be more precise, $v_{c,max}$ depends on the situation-dependent prototypically predicted trajectory and the predicted time, such that $\hat{v}_{c,max,t+s}(\hat{\mathbf{x}}_{t+s}(\mathbf{x}_t, h_t)) = \sqrt{a_{c,max} \hat{R}_{t+s}(\mathbf{x}_t, h_t)}$

tance, at maximal longitudinal velocity in a curve, and at maximal deceleration. $\beta_d(s)$, $\beta_c(s)$ and $\beta_b(s)$ define the steepness of the event rates and can be used to model state uncertainties, directly in the event rate term. Choosing $\beta_{d/c/b}(s) = \beta_{d/c/b}^{const}$, describes constant, time independent state uncertainties. Together, (3.14), (3.15) and (3.16) describe a continuous, instantaneous event rate for three different types of risk, whose parameters (especially the steepness parameters) are used to describe uncertainties in the involved context variables d , v , R and b . Further risk sources can be modeled in a similar way and superposed in the total event rate (3.10).

Prediction Uncertainty

So far, a known prototypical future state sequence has been assumed, where only constant, time independent state uncertainties have been considered in (3.14), (3.15), and (3.16), by applying time-independent, instantaneous event rates. This uncertainty assumption is mainly characterized by $\beta_{d/c/b}^{const}$, as schematically illustrated in Figure 3.4. In this way, state measurement uncertainties can be incorporated. However, the increasing uncertainty of the state prediction in future time is not considered. The forward propagation of uncertainty during the state prediction process leads to a time-dependent spatial broadening of predicted states, as schematically illustrated in Figure 3.5.

Expressing this uncertainty propagation explicitly would require to excessively solve the integrals in (3.4), which is a computationally very demanding task, as it requires an explicit propagation of the uncertainties in the prediction process, e.g. by applying a sampling-based procedure as used in [116]. Therefore, it is not suitable for a risk model targeting sparse, prototypical trajectories, as it is the scope of the approach presented in this chapter.

As a result, a model for time-dependent state prediction uncertainty is incorporated directly in the event rate. Here, an explicit time dependency

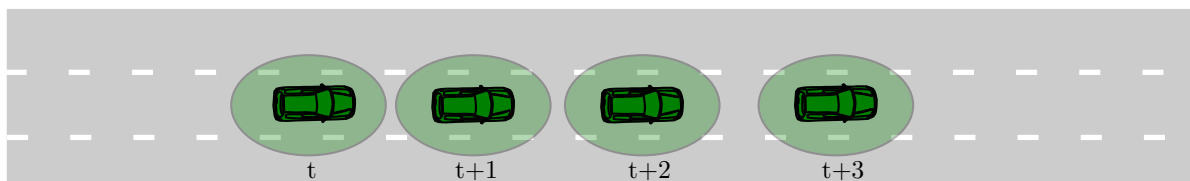


Figure 3.4: Schematic illustration of state or measurement uncertainty (indicated by green circles), assumed to be constant for different prediction times.

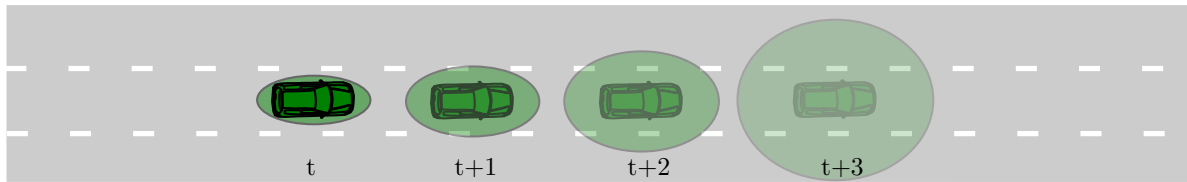


Figure 3.5: Schematic illustration of the state uncertainty (green circles), considering measurement uncertainty as well as the uncertainty propagation in the prediction process for different prediction times.

of the instantaneous event rate $\tau_{(\cdot)}^{-1}(\hat{\mathbf{x}}_{t+s}(\mathbf{x}_t, h_t), s)$ is proposed⁸, such that the event probability is wider distributed for moments further in predicted time and more localized for moments closer in time. For each instantaneous event rate according to (3.14), (3.15) and (3.16), this can be achieved by,

$$\tau_{(\cdot)}^{-1}(\hat{\mathbf{x}}_{t+s}(\mathbf{x}_t, h_t), s) = \tau_{(\cdot),0}^{-1} \beta_{(\cdot)}(s) \exp\{-\beta_{(\cdot)}^{const} \beta_{(\cdot)}(s)(\dots)\}, \quad (3.17)$$

with

$$\beta_{(\cdot)}(s) = \frac{\beta_{(\cdot),0}}{s + s_{(\cdot),0}},$$

as a simple model for the uncertainty propagation in state predictions with the weighting factor $\beta_{(\cdot),0}$. $s_{(\cdot),0}$ defines the state measurement uncertainties of the different considered instantaneous event probabilities. Setting $s_{(\cdot),0} = 0$, would result in the assumption of no uncertainty in state measurements, as $\lim_{s \rightarrow 0} \beta_{(\cdot)}(s) = \infty$. For car-to-car collision events with a distance-based instantaneous event rate, this specifies to

$$\tau_d^{-1}(\hat{\mathbf{x}}_{t+s}(\mathbf{x}_t, h_t), s) = \tau_{d,0}^{-1} \beta_d(s) \exp\{-\beta_d^{const} \beta_d(s)(\hat{d}_{t+s}(\mathbf{x}_t, h_t) - d_{min})\},$$

with

$$\beta_d(s) = \frac{\beta_{d,0}}{s + s_{d,0}}.$$

Deterministic Event Costs

In (3.8), the expected cost/damage is modeled deterministically for the different types of events. For the car-to-car collision risk, an appropri-

⁸(.) denotes the different instantaneous event rate types for different considered types of risk, namely (d/c/b) for distance based collision, curvature and deceleration risk.

ate approximation of the damage in case a collision occurs is the energy transfer between the colliding entities. As a result, a 2D inelastic collision model is considered (more accurate damage models can be applied in similar ways), so that

$$\begin{aligned} \hat{c}_{t+s}(e_{t+s}, \hat{\mathbf{x}}_{t+s}(\mathbf{x}_t, h_t)) & \quad (3.18) \\ & \sim w_c \cdot \frac{1}{2} \frac{m_0 m_i}{m_0 + m_i} \|\hat{v}_{t+s}^0(\mathbf{x}_t, h_t) - \hat{v}_{t+s}^i(\mathbf{x}_t, h_t)\|^2, \end{aligned}$$

where m_0 , m_i are the masses and $v_{t+s}^0(\mathbf{x}_t, h_t)$, $v_{t+s}^i(\mathbf{x}_t, h_t)$ the vectorial velocity components of the ego- and another entity involved in the collision risk estimation and w_c is a weighting factor. The velocity components can be derived from the prototypically predicted state vector $\hat{\mathbf{x}}_{t+s}(\mathbf{x}_t, h_t)$, which rely on the considered situation h_t and the current states of the scene \mathbf{x}_t .

For the risk of skidding in curvy road segments and the risk of losing control due to heavy deceleration, the cost/damage is modeled based on the energy transfer between the considered entity and a static road structure element, such as a road barrier. Therefore, from (3.18) $\hat{v}_{t+s}^i(\mathbf{x}_t, h_t) = 0$ and $m_i \rightarrow \infty$ is assumed, leading to

$$\hat{c}_{t+s}(e_{t+s}, \hat{\mathbf{x}}_{t+s}(\mathbf{x}_t, h_t)) \sim w_c \cdot \frac{1}{2} m_0 \|\hat{v}_{t+s}^0(\mathbf{x}_t, h_t)\|^2. \quad (3.19)$$

Conclusion

In this section, a novel, time-continuous model for future risk has been derived. Risk is considered as the expectation value of the costs (damage) related to critical future events.

The risk model (3.7) is based on a set of situation-dependent state vector sequences (3.1), which are generally expressed by situation-dependent, prototypical spatio-temporal trajectories of each involved entity. Risk is modeled by a situation-dependent risk term and a situation occurrence probability term.

Considering sparse critical future events, (3.8) describes the situation-dependent risk by summing over all possible events at future times $t + s$ and calculating the risk for each event. The event risk can then be modeled by a combination of the expected damage in case the event actually occurs and the event probability.

The situation-dependent probability (3.12) that a considered event hap-

pens in a small time interval $[t+s, t+s+\delta t]$, is modeled by an instantaneous event rate and a survival function. The total event probability, namely the situation-dependent probability that any event happens in $[t+s, t+s+\delta t]$, is modeled in (3.11). The survival function (3.9) describes the likelihood that an entity survives until a certain time in the future without being involved in any earlier event, which is described by the total event rate (3.10). The survival function has been extended in (3.13) by a so-called event escape rate. The event escape rate covers all implicit causes, which do not relate to an entity being involved in an earlier event, but which reduce the probability of an entity being involved in a considered future event, such as a risk-averse behavior of a driver.

In (3.14), (3.15), and (3.16) single event rates for car-to-car collision events, the risk of skidding off the road in a curvy segment, and the risk of losing control due to heavy braking, have been modeled explicitly. To consider the uncertainty propagation in the prediction process, the single event rates have been extended to be time-dependent in (3.17).

Finally, in (3.18) and (3.19) deterministic damage models, based on the resulting energy transfer, when colliding with another dynamic entity or a static road structure element, have been derived for the different event types.

3.2.3 Approximate Risk Model

In the previous subsections, a time-continuous, probabilistic model for future risk, based on prototypically predicted, spatio-temporal trajectories, has been derived. The risk model (3.7) can be applied to evaluate possible behavior alternatives and select or plan a risk-minimizing future behavior.

The computational complexity of the derived risk model gets too high for certain applications, such as prediction tasks of complex traffic situations or traffic simulations with a large number of traffic participants. Therefore, this section strives for an approximate model for situation-dependent future risk, which can be applied to evaluate behavior/trajectory alternatives with reduced computational effort.

Concentrating on the car-to-car collision risk, two scenarios of different structure and different trajectory constellations are analyzed in the following. The accumulated event probability over future time is evaluated in order to determine suitable indicators for a risk approximation, which are directly extractable with low computational effort from the evaluated trajectories. As a result, we get that for the car-to-car collision risk the time when the entities get closest, the time-of-closest-encounter (TCE),

and the minimal distance of the entities, the distance-of-closest-encounter (DCE) mainly characterize the risk of a certain trajectory pair.

Therefore, these risk indicators are utilized to derive a computationally inexpensive, approximate model for the accumulated situation-dependent future risk, which retains the main characteristics of the full risk model.

Discussion of Collision Probability

The target of this section is to derive and justify suitable indicators for risk or event probability maxima, which can be extracted with low computational effort from the predicted trajectories, such that they can serve for an approximate risk model. For this purpose, the two most common dangerous traffic scenarios, namely intersections and parallel driving with different trajectory constellations of the ego- and another entity are analyzed, to discuss the characteristics of the introduced event probability model for car-to-car collision events. The two scenarios are shown in Figures 3.6 and 3.7. For simplicity, constant velocity trajectories with different spatial paths are evaluated⁹. For the intersection scenario the initial position of both entities, before arriving at the intersection, is varied. For the parallel driving scenario the other entity's trajectory is kept constant, while the lateral as well as longitudinal initial position of the ego entity is varied. This way, a wide range of trajectory constellations, with different approaching setups can be modeled.

First, the event probability time course according to (3.12) of three different trajectory pairs dedicated to the intersection scenario are analyzed, as shown in Figure 3.8. A collision event probability peak with its maximum close to the time when the considered cars are predicted to be closest, called the time-of-closest-encounter (TCE), can be observed. This event probability peak decreases for an increasing minimal distance, the distance-of-closest-encounter (DCE). If the expected event probability maximum is located further in the future, the probability that the entity survives, until the considered event occurs, is lower¹⁰. As a result, the probability that the entity gets involved in the event is reduced as well, as shown in Figure 3.8. This consideration motivates the evaluation of the different trajectory constellations' event probabilities in terms of the ego entity's TCE and DCE, because the event probability characteristics can

⁹Neither the assumption of only one other entity nor the constant velocity is not a constraint of the used model for event probability.

¹⁰This considers, that the entity is possibly involved in another, earlier event, or that the entity might act in an event-averse way.

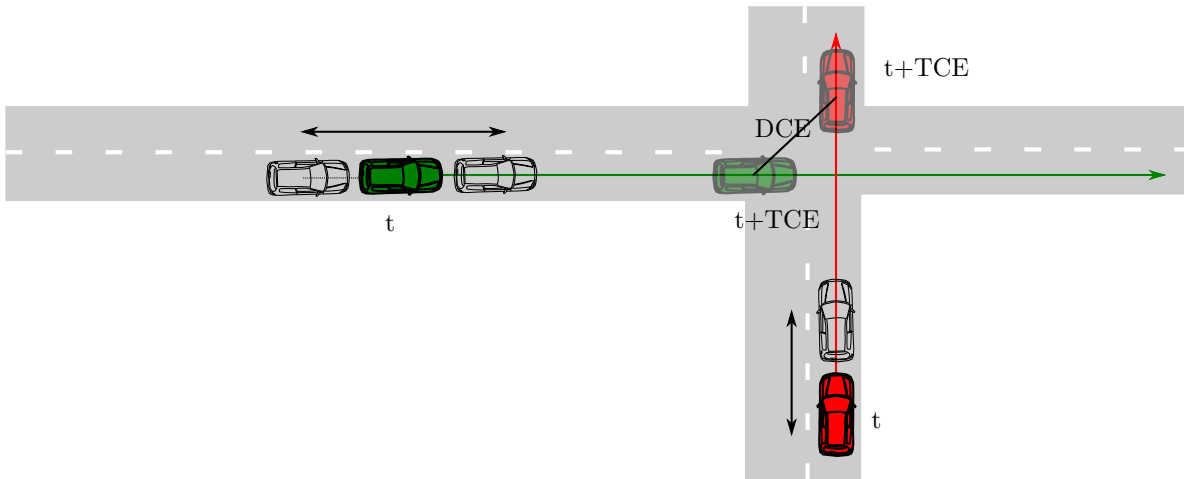


Figure 3.6: Intersection scenario. Both, the ego entity's (green) and other entity's (red) initial position on a fixed spatial path are varied (wire frame vehicles). Constant velocity is assumed to generate a set of spatio-temporal trajectories, for which the future risk is evaluated. The predicted point-of-closest-encounter, expressed by the time-of-closest-encounter (TCE) and distance-of-closest-encounter (DCE) is illustrated by the faded vehicles.

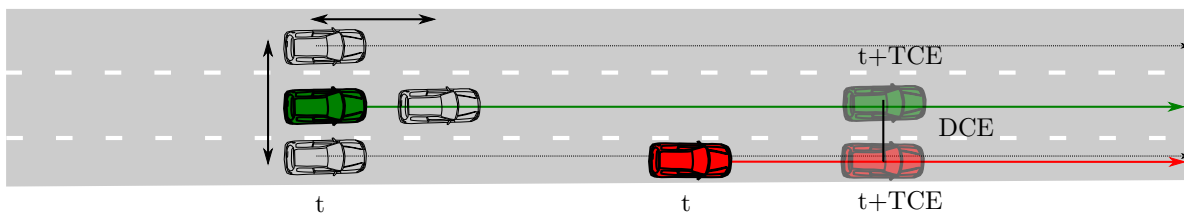


Figure 3.7: Parallel driving scenario. The ego entity's (green) initial position is varied in the longitudinal as well as lateral driving direction (wire frame vehicles). The other entity's trajectory is kept fixed. Constant velocity is assumed to generate a set of spatio-temporal trajectories, for which the future risk is evaluated. The predicted point-of-closest-encounter, expressed by the TCE and the DCE is illustrated by the faded vehicles.

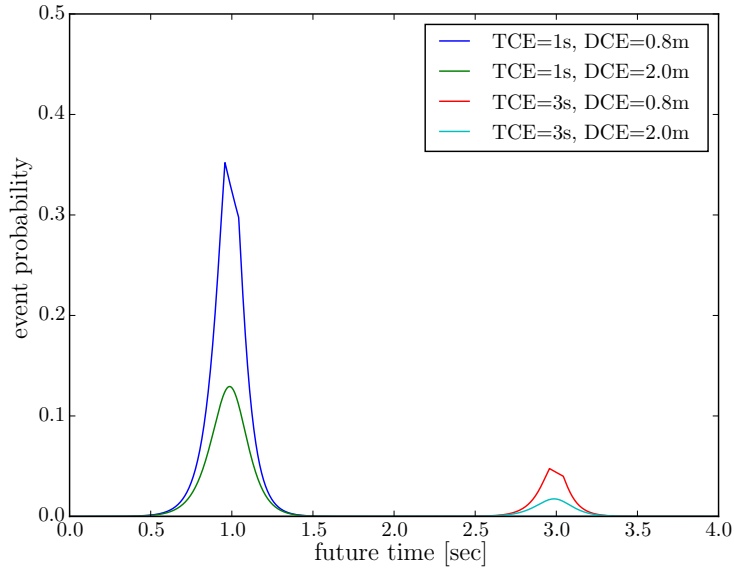


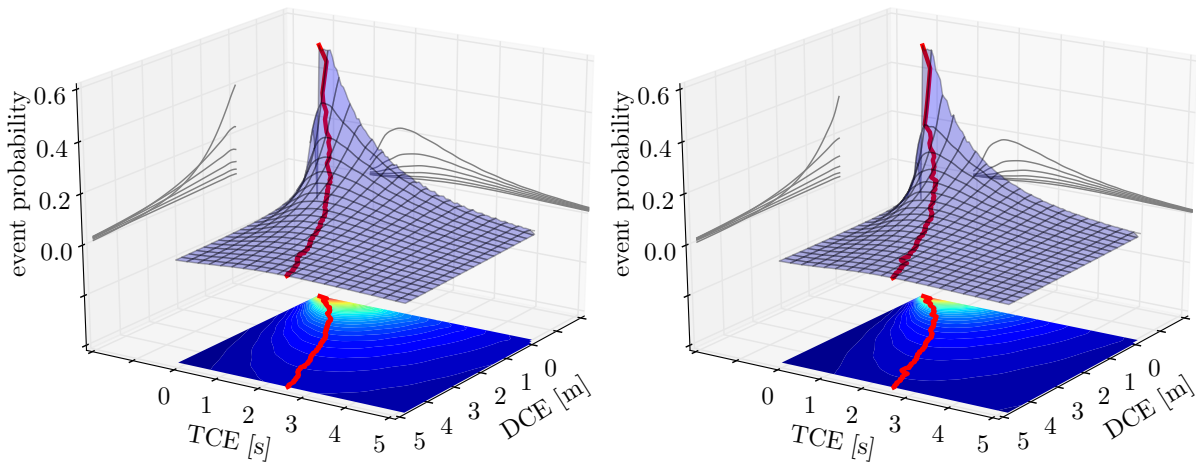
Figure 3.8: Evaluated event probability of the intersection scenario (see Figure 3.6) for trajectory constellations with different TCE and DCE. An event probability peak is located near the TCE. For increasing TCE the event probability decreases due to the decreasing likelihood that the entities survive (as predicted) until the event occurs. Likewise, with an increasing DCE the event probability decreases due to the decrease of the distance-dependent instantaneous event rate.

be mainly approximated by those two values.

To compare the different trajectory constellations, the event probability, according to (3.12), accumulated over the entire future time interval $[t, \infty]$, is evaluated as

$$\begin{aligned}
 P_{e, \text{accu}} &= \int_0^{\infty} P(e_{t+s} | \hat{\mathbf{x}}_{t:t+s}(\mathbf{x}_t, h_t), s) ds \\
 &= \int_0^{\infty} \tau_{e_{t+s}}^{-1}(\hat{\mathbf{x}}_{t:t+s}(\mathbf{x}_t, h_t), s) S(\hat{\mathbf{x}}_{t:t+s}(\mathbf{x}_t, h_t), s) ds.
 \end{aligned} \tag{3.20}$$

Figure 3.9 (a) and (b) show the accumulated event probability of different constellations, depending on the ego entity's TCE and DCE, for the two considered scenarios (intersection and parallel driving). Generally, a combination of low TCE and low DCE values result in a high accumulated event probability. This is the case, when the vehicles are expected



(a) Accumulated event probability (3.20) of intersection scenario.

(b) Accumulated event probability (3.20) of parallel driving scenario.

Figure 3.9: Comparison of the accumulated event probability landscape, for different scenario structures, (a) intersection and (b) parallel driving, evaluated for different trajectory constellations expressed by the corresponding TCE and DCE. The landscape shows a maximum for TCE and DCE close to zero. By comparing the landscapes of the structurally very different scenarios structure, it can be concluded that the influence of the road structure is neglectable and the event probability landscape is mainly defined by TCE and DCE. The ground plane projection of event probability for the two different scenario structures, reveals a shift of the probability maxima (red curve) for increasing DCEs towards slightly larger TCEs. The plane projections intend to increase the visibility of the plots.

to be close and insufficient time is left to react. With an increasing TCE and an increasing DCE the accumulated event probability decreases. The influence of the geometric variability in the evaluated scenario, e.g. the type of road structure, is low, as it can be seen by comparing the probability landscape of the parallel driving and the intersection scenario. This justifies the utilization of the TCE and DCE as suitable indicators for an approximate, accumulated event probability model.

The ground plane projection of the accumulated event probability landscape in Figure 3.9(a) and (b) shows a shift of the maxima (red curve) for increasing DCEs towards slightly larger TCEs. This can be explained by the consideration of uncertainty propagation in the trajectory prediction. For small TCEs, the uncertainty in the predicted states is small. This means that for an expected $DCE > 0$ the maximal probability that the entity gets involved in a collision event is not located at $TCE = 0$, but moved towards larger TCEs.

This effect is schematically shown in Figure 3.10, where the prediction uncertainty is illustrated by the broadening area in front of the vehicles. The collision event probability, illustrated by the yellow, overlapping area, is largest, before the entities are closest ($TCE > 0$). If the entities are closest and did not yet collide ($DCE > 0$) the probability that they will collide relies only on the measurement uncertainty, and is thus relatively small.

Concluding, the discussion shows that the main characteristics of the accumulated collision event probability can approximately be described in terms of the time until the entities are expected to be closest (TCE) and the expected minimal distance (DCE). Generally, for an increasing TCE, the accumulated event probability decreases. Likewise, for an increasing DCE, the accumulated event probability decreases as well. However, taking the uncertainty propagation in the prediction process into account requires a consideration of a more complex coupling of TCE and DCE, to explain the shift of the event probability maxima towards larger TCEs for DCEs > 0 .

Approximation of the Accumulated Collision Event Probability

The probability that the ego entity is involved in a future collision event e_{t+s} in the time interval $[t, \infty]$ is defined in (3.20).

The main characteristics of the accumulated collision event probability can be described by indicators, which are extractable directly from the prototypically predicted trajectories of the involved entities. For car-to-car collision events, those indicators are the time-of-closest-encounter (TCE) and the distance-of-closest-encounter (DCE).

As a consequence, an approximate model for the accumulated event probability, relying purely on those indicators, is proposed as

$$P^\infty(\mathbf{e}_{co}^i | DCE^i(\mathbf{x}_t, h_t), TCE^i(\mathbf{x}_t, h_t)) \quad (3.21)$$

$$\sim \int_0^\infty P(e_{t+s} | \hat{\mathbf{x}}_{t:t+s}(\mathbf{x}_t, h_t), s) ds.$$

Here, only one future collision event per involved other entity i in a certain situation h_t is assumed¹¹. However, several collision events for another entity i , related to different situations, are still considered. \mathbf{e}_{co}^i describes a collision event between the ego- and another vehicle i happening in the entire future time interval $[0, \infty]$. As a consequence, $P^\infty(\mathbf{e}_{co}^i | \dots)$ expresses

¹¹This is not a strict requirement, but reasonable for simplification.

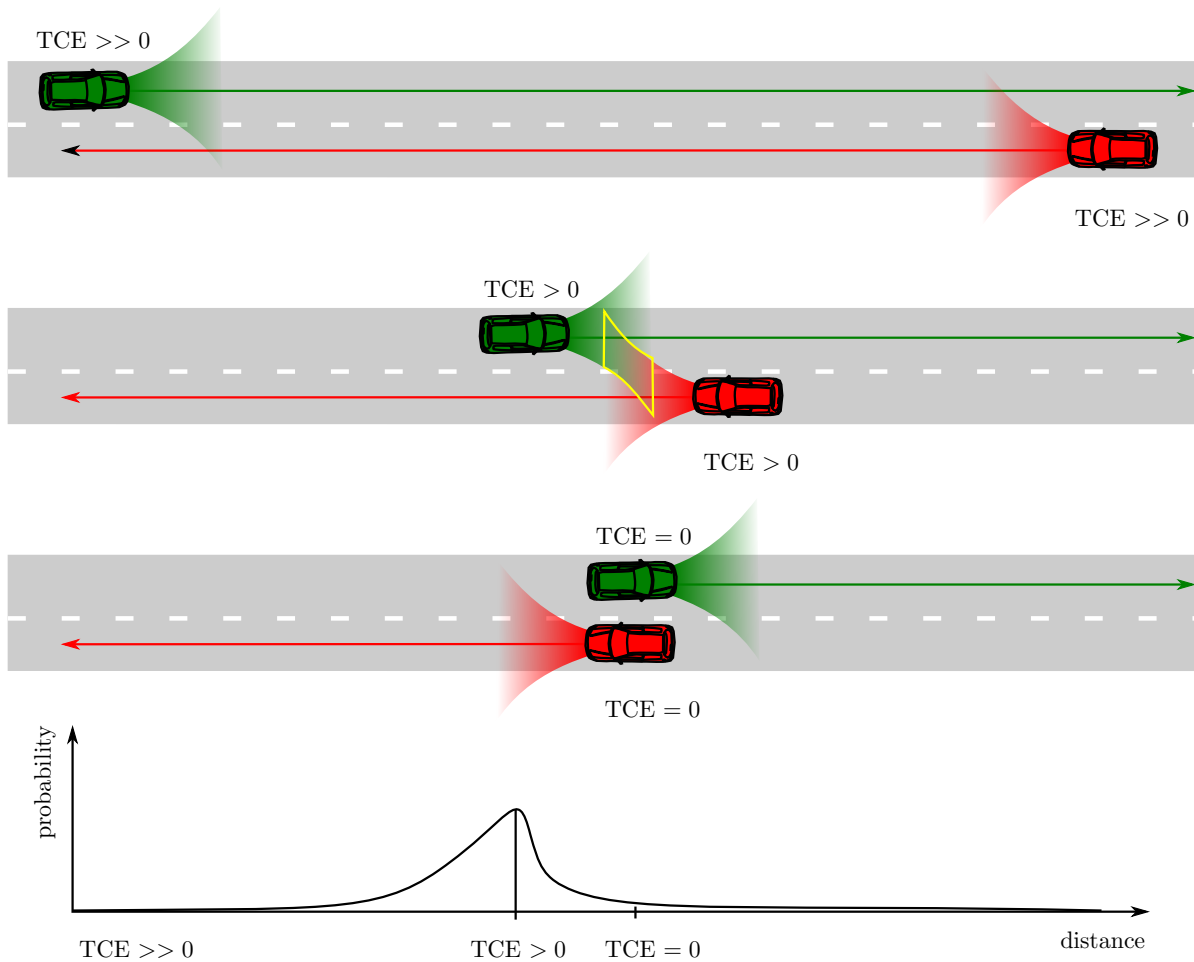


Figure 3.10: Schematic illustration of the event probability over time to explain the shift of the probability maxima for DCEs > 0 towards TCEs > 0 . Starting with a very large $TCE \gg 0$ (top) the accumulated event probability increases, when the cars are getting closer (the TCE decreases). Due to the propagation of uncertainty in the prediction process (green/red widening areas), the event probability maximum is at a TCE slightly larger than zero (middle). At $TCE = 0$ the uncertainty propagation is very low (bottom) and only measurement uncertainties have an influence.

the approximate accumulated probability for a future collision event with another vehicle i . $DCE^i(\mathbf{x}_t, h_t)$ and $TCE^i(\mathbf{x}_t, h_t)$ are abbreviations for $DCE^i(\hat{\mathbf{x}}_{t:t+s}(\mathbf{x}_t, h_t))$ and $TCE^i(\hat{\mathbf{x}}_{t:t+s}(\mathbf{x}_t, h_t))$.

Such an approximate model is computationally significantly cheaper, compared to the full model (3.12). An investigation of the entire spatio-temporal course of the trajectories is no longer required. This model can be applied to systems, where precision is less crucial than computation time and a rough approximation of the accumulated event probability is sufficient.

In Chapter 5 a microscopic driver model, called The Foresighted Driver Model (FDM), is introduced, which performs a gradient descent on the approximate, accumulated risk to achieve a risk-averse behavior in a computationally efficient way. The FDM is then used in Chapter 6 as a model to predict the future evolution of a traffic scene, while considering interactions between the involved traffic participants.

The collision event indicators are defined pairwise as the distance-of-closest-encounter (DCE) of the prototypical future trajectories of the ego entity 0 and another entity i ,

$$DCE^i(\hat{\mathbf{x}}_{t:t+s}(\mathbf{x}_t, h_t)) = \min_{s'} \|\hat{p}_{t+s'}^0(\mathbf{x}_t, h_t) - \hat{p}_{t+s'}^i(\mathbf{x}_t, h_t)\|.$$

Likewise, the time-of-closest-encounter (TCE) is defined as

$$TCE^i(\hat{\mathbf{x}}_{t:t+s}(\mathbf{x}_t, h_t)) = \operatorname{argmin}_{s'} \|\hat{p}_{t+s'}^0(\mathbf{x}_t, h_t) - \hat{p}_{t+s'}^i(\mathbf{x}_t, h_t)\|,$$

where $\hat{p}_{t+s'}^0(\mathbf{x}_t, h_t)$ and $\hat{p}_{t+s'}^i(\mathbf{x}_t, h_t)$ are the predicted spatial positions of the ego (index 0) and another (index i) entity at future time $t+s'$, extracted from the situation-dependent predicted scene state vector $\hat{\mathbf{x}}_{t+s'}(\mathbf{x}_t, h_t)$.

Using those indicators, the accumulated car-to-car collision event probability can be approximated by

$$\begin{aligned} P^\infty(\mathbf{e}_{co}^i | DCE^i(\mathbf{x}_t, h_t), TCE^i(\mathbf{x}_t, h_t)) & \quad (3.22) \\ & = F_{co} \cdot e^{-\frac{\max(DCE^i(\mathbf{x}_t, h_t) - d_0, 0)}{\sigma_d}} \cdot e^{-\frac{TCE^i(\mathbf{x}_t, h_t)}{\sigma_{co}}}, \end{aligned}$$

where σ_d and σ_{co} account for spatial and temporal uncertainties for car-to-car collision events and with F_{co} being a weighting factor¹².

In Section 3.2.2 the event probability model has been extended by a

¹²Here, we assume a maximum of the collision event probability, where the distance between the vehicles and the time left until the ego vehicle reaches this point are both minimal. The uncertainties are assumed to decrease exponentially.

time-dependent event rate (3.17) to consider the uncertainty propagation in the prediction process. As discussed, this consideration causes a shift of the event probability maximum for increasing minimal distances ($DCE > 0$) away from $TCE = 0$ towards slightly larger TCEs. The red curves in Figure 3.9 represent the TCE at which the event probability is maximal (TCE_{max}) for different DCEs. The dependency between DCE and TCE_{max} can be approximated as

$$TCE_{max}^i(DCE^i(\mathbf{x}_t, h_t)) = \alpha \cdot \ln(DCE^i(\mathbf{x}_t, h_t) + \gamma), \quad (3.23)$$

where α and γ are chosen to fit the maximum course of the full event probability model from Section 3.2.2.

The TCE-dependency of the accumulated event probability, as seen in the equi-TCE plane-projections in Figure 3.9, can be expressed in terms of a normalized alpha-function¹³ with its maximum at TCE_{max} . As a consequence, the effect of a DCE-dependent shift of the event probability maximum towards larger TCEs can be modeled by extending (3.22) with an additional term $B(\dots)$,

$$\begin{aligned} P^\infty(\mathbf{e}_{co}^i | DCE^i(\mathbf{x}_t, h_t), TCE^i(\mathbf{x}_t, h_t)) & \quad (3.24) \\ &= F_{co} \cdot e^{-\frac{\max(DCE^i(\mathbf{x}_t, h_t) - d_0, 0)}{\sigma_d}} \cdot e^{-\frac{TCE^i(\mathbf{x}_t, h_t)}{\sigma_{co}}} \\ & \quad \cdot B(TCE^i(\mathbf{x}_t, h_t), DCE^i(\mathbf{x}_t, h_t)) \end{aligned}$$

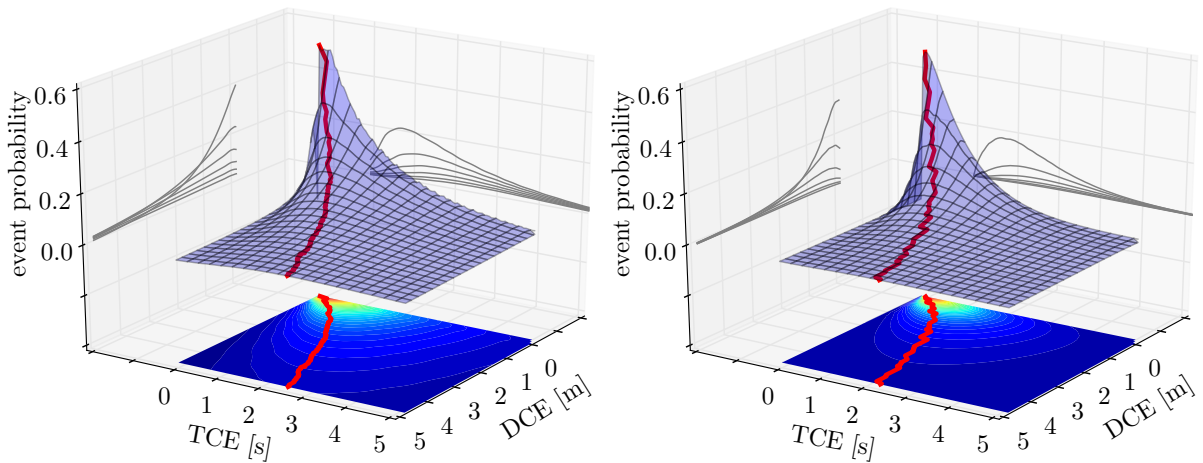
with

$$B(TCE^i(\mathbf{x}_t, h_t), DCE^i(\mathbf{x}_t, h_t)) = \frac{TCE^i(\mathbf{x}_t, h_t)^{TCE_{max}^i(\mathbf{x}_t, h_t)}}{TCE_{max}^i(\mathbf{x}_t, h_t)^{TCE_{max}^i(\mathbf{x}_t, h_t)}},$$

where $TCE_{max}^i(\mathbf{x}_t, h_t)$ is short for $TCE_{max}^i(DCE^i(\mathbf{x}_t, h_t))$.

In Figure 3.11, the approximate accumulated event probability (3.21) for the intersection scenario is evaluated and compared to the full evaluation of the accumulated event probability (3.20). It can be seen that the approximate model nicely retains the general characteristics of the accumulated event probability. Furthermore, the course of the maximum shift for larger DCEs towards higher TCEs of the approximate model, caused by the consideration of the uncertainty propagation, resembles the one of the full accumulated event probability model.

¹³Here, the used alpha function has the form $f(x) = x^{\acute{x}}/\acute{x}^{\acute{x}} \cdot e^{-x}$ with a maximum at \acute{x}



(a) Full accumulated event probability according to (3.20). (b) Approximate, accumulated event probability according to (3.21).

Figure 3.11: The comparison of (a) the accumulated event probability according to the full model (3.20) and (b) the accumulated event probability according to the approximate model (3.21), which targets only the event probability maxima by using the indicators TCE and DCE, shows that the main characteristics can nicely be retained by the approximate model. The event probability maxima for different DCEs are indicated by the red curve. Especially the projection onto the ground plane shows that the effect of shifted maxima for larger DCEs towards higher TCEs is reproduced by the approximate model.

Approximate, Accumulated Event Probability for Different Event Types

For further risk/event types, such as the risk of skidding in a curvy road segment or the risk of losing control due to heavy braking, as introduced in Section 3.2.2, the accumulated event probability in a future time interval $[t, \infty]$ can be approximated similarly to the collision case. A more general form of the approximated, accumulated event probability is

$$\begin{aligned}
 & P^\infty(\mathbf{e}_{mr} | \text{IVMR}(\mathbf{x}_t, h_t), \text{TMR}(\mathbf{x}_t, h_t)) \\
 &= F_{mr} \cdot e^{-\frac{\text{IVMR}(\mathbf{x}_t, h_t)}{\sigma_{ivmr}}} \cdot e^{-\frac{\text{TMR}(\mathbf{x}_t, h_t)}{\sigma_{tmr}}} \\
 &\quad \cdot B(\text{TMR}(\mathbf{x}_t, h_t), \text{IVMR}(\mathbf{x}_t, h_t)).
 \end{aligned} \tag{3.25}$$

\mathbf{e}_{mr} describes any “maximal risk” event happening in the entire future time interval $[t, \infty]$. $P^\infty(\mathbf{e}_{mr} | \dots)$ expresses the approximate accumulated probability of a future “maximal risk” event (mr). $\text{IVMR}(\dots)$ and $\text{TMR}(\dots)$

are indicator-value-of-maximum-risk (an indicator value that is zero at maximal risk and monotonically increasing with a decreasing risk value) and time-of-maximum-risk, similar to DCE and TCE, which should be extractable directly from the predicted trajectories of the involved entities. Again, the parameters σ_{tmr} and σ_{ivmr} account for temporal and value-dependent uncertainties. F_{mr} is a weighting factor. The propagation of uncertainty in the prediction process can be considered similarly to (3.23) and (3.24) by substituting TCE:=TMR and DCE:=IVMR.

The approximate, total event probability, accumulated over $[t, \infty]$, describes the probability of any critical event happening in the future. It can be achieved by summing over all considered events according to (3.11), including all different event types (e.g. car-to-car collision, losing control due to heavy braking) and event sources (e.g. several traffic participants):

$$\begin{aligned}
 P_{\text{total}}^{\infty} &\sim \int_0^{\infty} \sum_{e_{t+s}} P(e_{t+s} | \hat{\mathbf{x}}_{t:t+s}(\mathbf{x}_t, h_t), s) ds \\
 P_{\text{total}}^{\infty} &= \sum_{\mathbf{e}_{mr}} P^{\infty}(\mathbf{e}_{mr} | \text{IVMR}(\mathbf{x}_t, h_t), \text{TMR}(\mathbf{x}_t, h_t)) \\
 &= \sum_{\mathbf{e}_{mr}} F_{mr} \cdot e^{-\frac{1/\text{IVMR}(\mathbf{x}_t, h_t)}{\sigma_{ivmr}}} \cdot e^{-\frac{\text{TMR}(\mathbf{x}_t, h_t)}{\sigma_{tmr}}} \\
 &\quad \cdot B(\text{TMR}(\mathbf{x}_t, h_t), \text{IVMR}(\mathbf{x}_t, h_t)).
 \end{aligned}$$

For collision events, the indicator-value-of-maximum-risk (IVMR) resembles the distance-of-closest-encounter. Likewise, the time-of-maximum-risk (TMR) is equal to the time-of-closest-encounter. Without going into detail, for the risk of skidding in curvy road segments the IVMR can be chosen inversely proportional to the expected maximal lateral acceleration, while the TMR is the time when the maximal lateral acceleration is reached. For the risk of losing control due to strong braking, the IVMR can be chosen inversely proportional to the maximal expected deceleration and the TMR as the time when the maximal deceleration occurs. All those indicators are computationally cheap to extract from the predicted spatio-temporal trajectories.

Approximate Risk Model

So far, an approximate model for the total event probability, accumulated over future time $[t, \infty]$, has been derived. This model resembles the

general characteristics of the full event probability model, introduced in Section 3.2.2 and can be extended to other types of risk, such as the risk of losing control due to heavy braking. To achieve an approximate risk model, the event probability model has to be combined with an expectation of the damage or cost in case a critical event actually occurs. In Section 3.2.2, the expected costs have been modeled deterministically, using a 2D-inelastic collision model for the car-to-car collision risk (3.18), assuming the event happening at future time $t + s$.

For the approximate risk model, the most obvious way of modeling the expected damage would be assuming that the event occurs when the event probability is maximal. For car-to-car collisions according to (3.24), this is the case at future time $t + \text{TCE} - \text{TCE}_{max}^i$, taking the event probability maxima shift (TCE_{max}^i) which is caused by the consideration of the prediction uncertainty propagation into account. This would result in a collision damage model according to (3.18) as

$$\hat{c}_{co}^i(\mathbf{e}_{co}^i, \hat{\mathbf{x}}_{t+\text{TCE}^i - \text{TCE}_{max}^i}(\mathbf{x}_t, h_t)).$$

However, in order to decrease the computational effort for the approximate risk model, the temporal course of the trajectories is not considered. Only the expected risk maxima are targeted, which can be approximated by risk indicators such as TCE and DCE for the car-to-car collision case, or generally TMR and IVMR for any kind of risk. Consequently, to achieve an approximate risk model that purely depends on the predicted states at TCE (or TMR for the general case) the predicted state at the TCE is assumed to be similar to the predicted state at the time when the event probability is maximal,

$$\mathbf{x}_{t+\text{TCE}^i}(\mathbf{x}_t, h_t) \approx \mathbf{x}_{t+\text{TCE}^i - \text{TCE}_{max}^i}(\mathbf{x}_t, h_t).$$

This leads to the expected damage in case a “maximal risk” event (mr) occurs, which is derived in the following explicitly for car-to-car collision events (co), according to (3.18).

$$\begin{aligned} & \hat{c}_{co}^i(\mathbf{e}_{co}^i, \hat{\mathbf{x}}_{t+\text{TCE}^i}(\mathbf{x}_t, h_t)) \\ & \sim \frac{1}{2} \frac{m_0 m_i}{m_0 + m_i} \|\hat{v}_{t+\text{TCE}^i}^0(\mathbf{x}_t, h_t) - \hat{v}_{t+\text{TCE}^i}^i(\mathbf{x}_t, h_t)\|^2, \end{aligned} \quad (3.26)$$

where $\hat{\mathbf{x}}_{t+\text{TCE}^i}(\mathbf{x}_t, h_t)$ is the predicted state vector at the TCE.

For any other event types, such as *skidding off the road in curvy segments* and *losing control due to heavy braking* the expected damage at the risk

maxima can be derived likewise according to (3.19) with the corresponding risk indicators.

The general model for the accumulated future risk in $[t, \infty]$, according to (3.8) is

$$\int_0^{\infty} r(t+s, \mathbf{x}_t, h_t) ds$$

$$\sim \int_0^{\infty} \sum_{e_{t+s}} \hat{c}_{t+s}(e_{t+s}, \hat{\mathbf{x}}_{t+s}(\mathbf{x}_t, h_t)) P(e_{t+s} | \hat{\mathbf{x}}_{t:t+s}(\mathbf{x}_t, h_t), s) ds.$$

Incorporating the approximate event probability (3.25) (for collision events (3.24)) and the approximated expected damage (3.26) in case the event occurs, leads to the approximate model for future risk

$$r^{\infty}(\mathbf{x}_t, h_t) \sim \int_0^{\infty} r(t+s, \mathbf{x}_t, h_t) ds \quad (3.27)$$

$$r^{\infty}(\mathbf{x}_t, h_t) = \sum_{\mathbf{e}_{mr}} \hat{c}_{mr}(\mathbf{e}_{mr}, \hat{\mathbf{x}}_{t+TMR}(\mathbf{x}_t, h_t)) \cdot P^{\infty}(\mathbf{e}_{mr} | \text{IVMR}(\mathbf{x}_t, h_t), \text{TMR}(\mathbf{x}_t, h_t)).$$

The derived approximate model for the accumulated future risk is due to its low computational effort well suited for complex multi-agent simulations, which are used in the predictions of situation-dependent future scene evolutions in Chapter 6.

Conclusion

After extracting indicators for risk maxima, considering different types of events, like the time-of-closest-encounter and the distance-of-closest-encounter for car-to-car collision events, the evaluation of future risk using the approximate risk model is computationally significantly cheaper than the more accurate risk model from Section 3.2.2. While the accurate risk model from Section 3.2.2 performs an evaluation of risk, considering the full temporal course of the predicted spatio-temporal trajectories, the approximate model targets purely the risk maxima to approximate the accumulated future risk.

The reduction of necessary computational effort makes the approximate risk model applicable to tasks, where a low computational time is important. Such applications are e.g. microscopic traffic simulators with a large number of traffic entities or risk-averse driver models used in prediction tasks to predict the future evolution of traffic situations, as performed in Chapter 6.

3.3 Trajectory Similarity

Comparing trajectories in terms of similarity is crucial in many areas. For example in the area of data mining¹⁴ in a large set of trajectories, cluster analysis¹⁵ is a very common method. Here, a key component is a similarity measure to group similar trajectories.

Furthermore, in Chapter 6 situation-dependent, prototypically predicted spatio-temporal trajectories are compared with actually sensed and recorded trajectories of all involved traffic participants, to achieve an estimate of the occurrence probability of a certain situation. The higher the similarity value the higher is the probability that the corresponding situation holds.

Therefore, the target of this section is to derive a similarity measure for spatio-temporal trajectories in the context of traffic environments¹⁶.

In literature there are multiple measures of trajectory similarity. In [59] error measures are divided into four types, termed *scale dependent*, *percentage*, *relative* and *scale free*. An example of the first type is e.g. the mean absolute error. The authors favor a *scale free* error measure, especially the mean absolute scaled error (MASE) to compare predicted trajectories, due to its property of never resulting in infinite or undefined values. In [146] the authors compare different common similarity measures for trajectories, namely the *Euclidean distance*, *Haudorff distance*, *Hidden Markov Model (HMM)-based*, *Longest Common Subsequence (LCSS)* and *Dynamic Time Warping (DTW)*. It has been shown, that LCSS and DTW cannot take full advantage of the shape similarity for trajectories in traffic scenarios. Additionally those measures are computationally very demanding.

¹⁴Data mining describes a computational method to find patterns in large data sets [144].

¹⁵Cluster analysis describes the process of grouping objects, such that the objects in each group can be considered to be similar [67].

¹⁶The main contributions of this section have been published by the author of this thesis to the IEEE ITS Society in [31].

Traffic environments are generally highly structured and, especially in the lateral direction, constrained. This is not considered in currently available similarity measures which are therefore not well suited.

In the following, two spatio-temporal trajectories $\mathbf{x}_{a:b}^1$ and $\mathbf{x}_{a:b}^2$, e.g. one sensed and one predicted trajectory (see Figure 3.12), are assumed to be given in a time interval $[a,b]$. For trajectory comparison, only the positional information \mathbf{p} is used and expressed as an explicit function of time s

$$\mathbf{p}^{1/2}(s) \mid s \in [a,b].$$

First the lengths of the trajectories are calculated as

$$L^{1/2}(s) = \int_a^s \left| \frac{d}{ds'} \mathbf{p}^{1/2}(s') \right| ds'. \quad (3.28)$$

Then, using linear referencing methods, the spatio-temporal trajectory $\mathbf{p}^1(s)$ is projected onto $\mathbf{p}^2(s)$ using (3.28) (see Figure 3.12)

$$\mathbf{p}^{1 \rightarrow 2}(s) = \mathbf{p}^2(L^{2^{-1}}(L^1(s))),$$

where $L^{2^{-1}}$ is the inverse function of L^2 , such that

$$L^{2^{-1}}(L^2(s)) = s.$$

In the next step, as shown in Figure 3.12, the longitudinal and lateral¹⁷ distances between two trajectory points are calculated

$$\Delta_{lat}(s) = \|\mathbf{p}^{1 \rightarrow 2}(s) - \mathbf{p}^1(s)\| \quad (3.29)$$

and¹⁸

$$\Delta_{lon}(s) = \|\mathbf{p}^{1 \rightarrow 2}(s) - \mathbf{p}^2(s)\|.$$

¹⁷Here *lateral* does not mean *orthogonal*, but quantifies the difference between the original trajectory points and the corresponding points projected onto the other trajectory, as formulated in (3.29). See Figure 3.12 for a more detailed explanation.

¹⁸For a trajectory \mathbf{p}^2 with strong curvature a more accurate way of calculating is $\Delta_{lon}(s) = |\Delta L(s)|$ with $\Delta L(s) = L^1(s) - L^2(s)$. Here only the absolute value $|\Delta L(s)|$ is used. However, in general $\Delta L(s)$ can be utilized to distinguish which trajectory has traveled a longer distance at time s , e.g. for $\Delta L(s) > 0$ trajectory $\mathbf{p}^1(s)$ has traveled a longer distance than $\mathbf{p}^2(s)$.

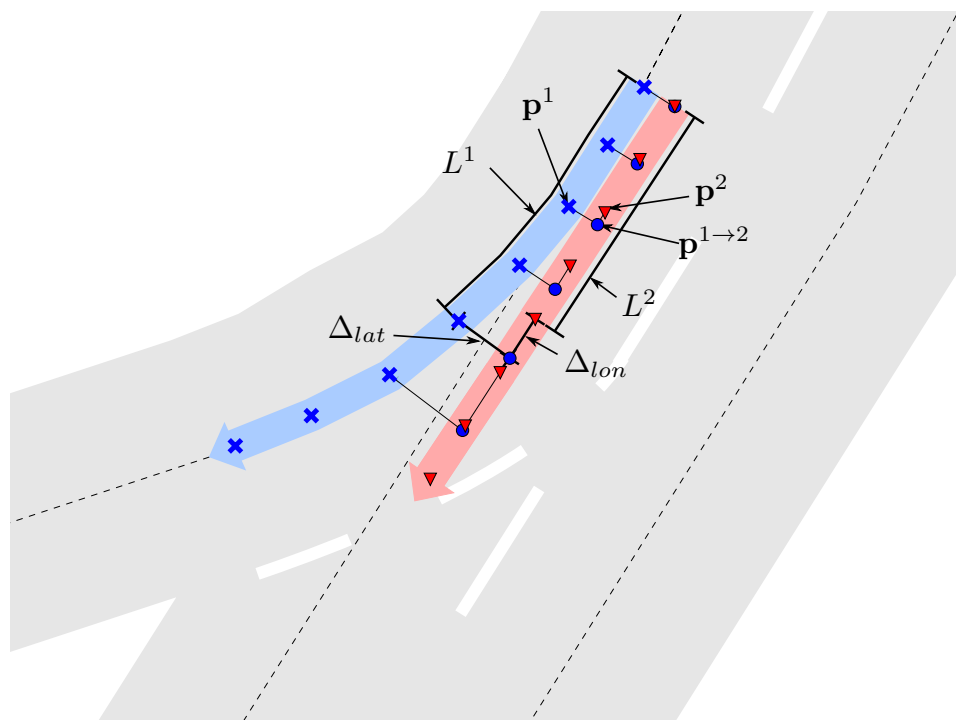


Figure 3.12: Calculation of longitudinal and lateral distances between two trajectories $\mathbf{p}^2(s)$ (red) and $\mathbf{p}^1(s)$ (blue). The blue crosses and red triangles denote points of the corresponding trajectories at the same moment in time starting from the top right. The blue circles denote the projected points $\mathbf{p}^{1 \rightarrow 2}(s)$ of $\mathbf{p}^1(s)$ onto $\mathbf{p}^2(s)$. $\Delta_{lat}(s)$ and $\Delta_{lon}(s)$ are exemplarily indicated for the 5th point in time.

Based on those distances, the following mean similarities are calculated as the mean lateral/longitudinal similarity of the trajectories

$$M_{lat/lon} = \frac{1}{b-a} \int_a^b M_{\Delta_{lat/lon}}(\Delta_{lat/lon}(s)) ds \quad (3.30)$$

and the mean similarity of the temporal derivative of lateral/longitudinal distance

$$\dot{M}_{lat/lon} = \frac{1}{b-a} \int_a^b \dot{M}_{\Delta_{lat/lon}}(\dot{\Delta}_{lat/lon}(s)) ds. \quad (3.31)$$

The single similarity values $M_{lat/lon}$ and $\dot{M}_{lat/lon}$ are derived by applying nonlinear weighted assignment functions to the lateral/longitudinal distances and their derivatives, as shown in Figure 3.13.

The resulting measure for trajectory similarity is derived as the combination of the mean similarities as

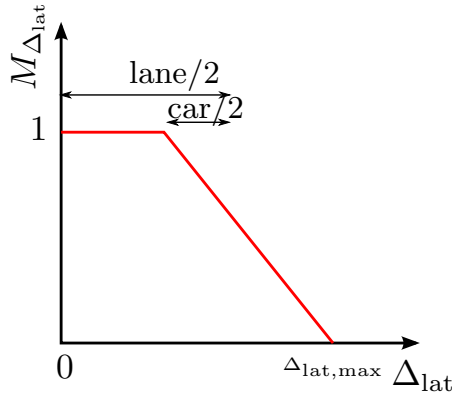
$$M_{sim} = M_{lat} \cdot \dot{M}_{lat} \cdot M_{lon} \cdot \dot{M}_{lon}. \quad (3.32)$$

For two identical trajectories the measure provides a value of $M_{sim} = 1$. For highly dissimilar trajectories the similarity value tends to $M_{sim} \rightarrow 0$.

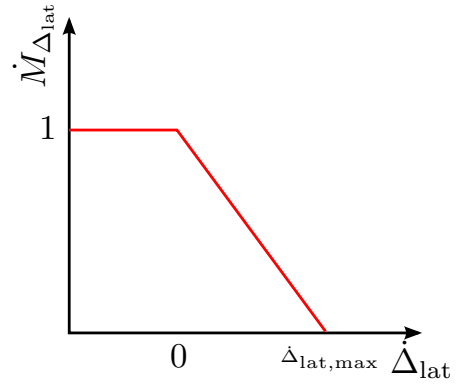
In Chapter 6, the similarity measure is applied to a situation classification system, which tries to assess the likelihood of a certain situation, by comparing situation-dependent, predicted spatio-temporal trajectories with actually sensed trajectories in terms of spatio-temporal trajectory similarity.

3.4 Conclusion

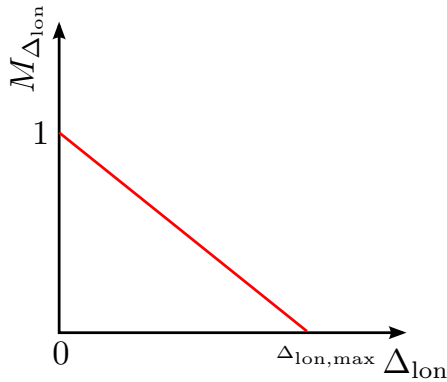
In this chapter, novel basic concepts have been proposed, which build the basis of the following thesis. In Section 3.1, the concept of situations has been presented, which define joint prototypical behavior patterns of all involved scene entities. For traffic scenarios, different spatial paths and different longitudinal behavior possibilities are separated. The longitudinal behavior separation focuses on interacting and non-interacting longitudinal behaviors. Instead of sampling a large set of possible behaviors of all involved entities and then clustering similar behaviors into situations,



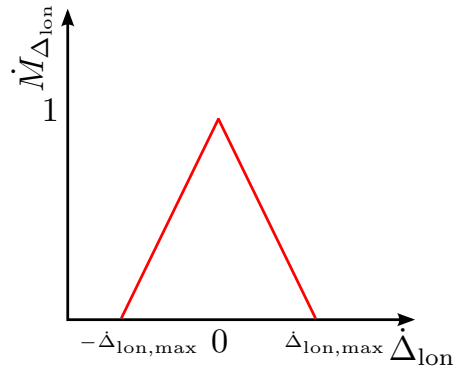
(a) Similarity assignment for the lateral distance. High assignment values are applied, while the car is still completely on the considered lane, declining constantly to zero for larger distances.



(b) Similarity assignment for the time derivative of the lateral distance. If the lateral distance of the trajectory increases fast the assignment value is reduced. For steady or even decreasing lateral distance a high assignment value is kept.



(c) Similarity assignment for the longitudinal distance. The similarity is depreciated for an increasing longitudinal distance. Above a certain maximal longitudinal distance the similarity is assumed to be zero.



(d) Similarity assignment for the time derivative of the longitudinal distance. A temporal derivative of the longitudinal distance of zero indicates equal longitudinal behavior and thus high similarity. Derivatives above $\Delta'_{lon, \max}$ are considered as not similar.

Figure 3.13: Similarity assignment functions for (a) lateral distance, (b) temporal derivative of the lateral distance, (c) longitudinal distance and (d) temporal derivative of the longitudinal distance. The used parameters are $\Delta_{lon, \max} = 50m$, $\Delta_{lat, \max} = 9.6m$, $\dot{\Delta}_{lon, \max} = 5m/s$, $\dot{\Delta}_{lat, \max} = 5m/s$, $\text{lane} = 3.2m$, $\text{car} = 2m$.

an approach has been presented to directly generate situations using road structure information and assumptions on the interaction between traffic participants.

In Section 3.2 a novel probabilistic, time-continuous model for future risk has been proposed, which targets at situation-dependent, prototypically predicted trajectories. Under the assumption that risks are caused by sparse critical events, the risk model consists of 1) the probability that a critical event will happen and 2) the expected damage in case the event actually happens. Several risk types have been considered, such as the collision risk between two cars, the risk of losing control due to heavy braking and the risk of skidding in narrow curve segments. As the proposed risk model is computationally demanding and not suitable for time critical tasks like situation-dependent scene predictions or traffic simulations, an approximate risk model, targeting only the expected risk maxima has been proposed. This approximate risk model is based on risk indicators, which can directly be extracted from the predicted trajectories with low computational costs, such as the time-of-closest-encounter (TCE) and distance-of-closest-encounter (DCE) for the car-to-car collision case.

Finally in Section 3.3 a novel similarity measure for spatio-temporal trajectories has been proposed. This measure is based on a dedicated evaluation of the longitudinal as well as lateral similarity, taking the characteristics of traffic environments into account, which are then recombined for the final evaluation.

4 Framework for Situation-based Risk Evaluation and Behavior Planning

This chapter introduces a general framework for situation-based risk evaluation and behavior planning. The target of any behavior generating system is to find a behavior that maximizes benefits and minimizes costs. For traffic scenarios this implies e.g. minimizing travel time while avoiding the risk of a collision.

The generation of an ego entity's behavior comprises an evaluation of possible behavior alternatives in terms of future risk¹ (expected costs) and future utility (expected benefits).

This evaluation requires an accurate prediction of how a scene evolves in the future for different ego behaviors. Such a prediction is uncertain and as a consequence, several possible scene evolutions have to be considered. There are basically infinite possibilities how a scene can evolve, which makes the task of finding the optimal behavior highly complex and computationally infeasible.

In order to reduce the complexity it is necessary to reduce the number of possibilities. This can e.g. be achieved by considering only scene evolutions which are relevant for the ego entity's future behavior. Also considering only significantly different scene evolutions by clustering similar ones into situations reduces the complexity. A situation² is then defined to represent exactly one prototypical scene evolution.

As possible scene evolution patterns/situations are not equally likely to happen, it is beneficial to consider a likelihood estimation³, while generating the ego entity's behavior. For traffic scenarios a suitable solution is

¹See Chapter 3.2 for more information on risk.

²Chapter 3.1 gives a more detailed introduction in the concept of situations.

³Such a likelihood estimation is e.g. the situation classification approach presented in Chapter 6

the proposed framework for *situation-based risk evaluation and behavior planning*⁴.

4.1 Framework Overview

The framework consists of the following six steps in the evaluation and planning cycle, as shown in Figure 4.1, namely 1) *scene observation*, 2) *situation classification*, 3) *trajectory prediction*, 4) *risk evaluation*, 5) *behavior planning* and 6) *behavior execution*.

1. In the **scene observation** step the system reads all sensor data to update the current state of the environment. This includes all states of dynamic objects, such as other cars or pedestrians, which are relevant for the ego car as well as infrastructure related information, like parking cars, traffic signs and map data. Here, the most important information are states of dynamic objects and the road topology delivered by map data. In the course of this work \mathbf{x}_t is referred as the measured state vector of the scene at the current time t .
2. In the **situation classification** step the current state of the scene is used to generate a set of possible prototypical situations, classify it and select those situations, which are relevant to determine the ego car's future behavior. As a result, a set of relevant situations and occurrence probabilities, one for each situation, is retrieved. A suitable approach for situation classification is presented in Chapter 6. This approach is based on similarity calculations, comparing the actually sensed, with situation-dependent, previously predicted states of the scene.
3. As presented in Chapter 3.1, each situation describes one behavior alternative for each involved scene entity. In the **trajectory prediction** step, one prototypical scene evolution is predicted for each considered situation. In the approach presented in Chapter 6.4, the Foresighted Driver Model (FDM) is applied as a prediction model in a multi-agent forward simulation of the sensed scene. For each relevant situation one prototypical state evolution is predicted, considering all involved entities. This results in one prototypically predicted, spatio-temporal trajectory for each entity in each situation.

⁴The main contributions have been published by the author of this thesis to the IEEE ITS Society in [30, 39] and patented in [28, 29].

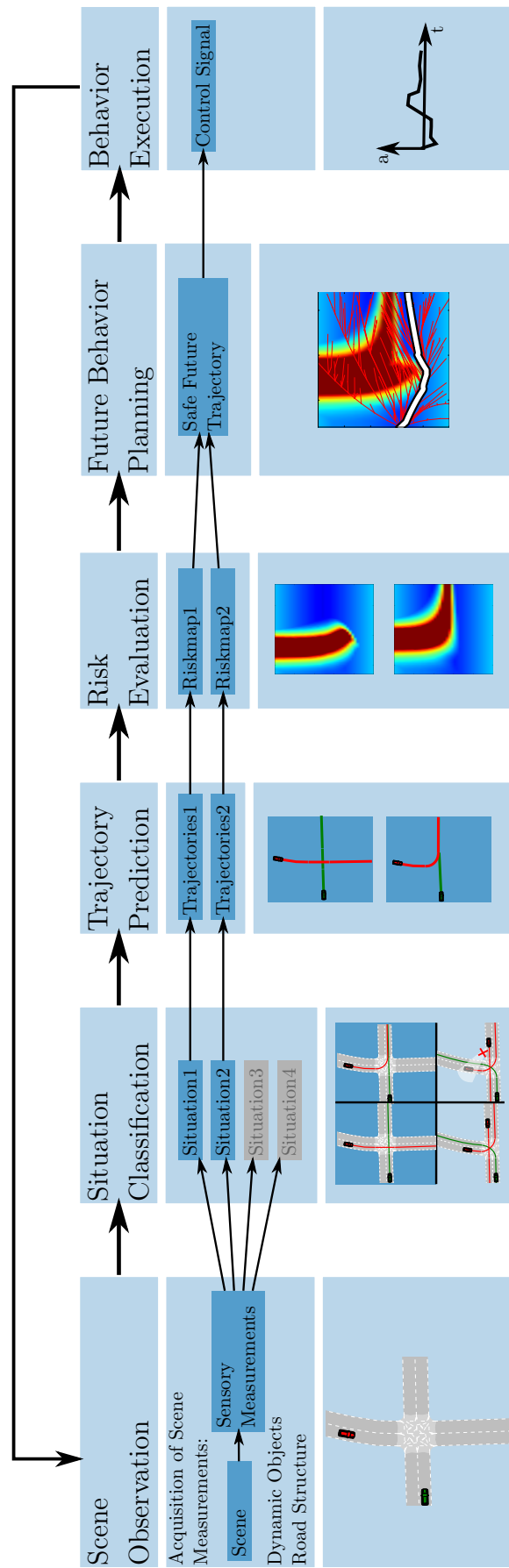


Figure 4.1: Evaluation and planning cycle of the framework for situation based risk evaluation and behavior planning consisting of the six steps 1) scene observation, 2) situation classification, 3) trajectory prediction, 4) risk evaluation, 5) behavior planning, and 6) behavior execution.

Applying the FDM in a situation-dependent forward simulation enables the incorporation of interaction, such as *one entity giving way to another approaching entity*. Additionally, the incorporation of different assumptions on how the entities interact, such as *one entity considering one other to give way, but accidentally overlooking a third entity*, is possible.

4. Next, in the **risk evaluation** step a variation of ego-car trajectories is build. The risk for each variation is evaluated, based on the predicted spatio-temporal trajectories of the other entities, according to the probabilistic model for risk, introduced in Chapter 3.2. According to Chapter 7.1, such an evaluation can be employed to generate predictive risk maps, one for each situation. A predictive risk map indicates how risky a certain behavior alternative in a certain situation will be at a certain future time and allows the determination of the best future behavior.

5. After evaluating the situation-dependent risk for possible ego behavior alternatives, the target in the **behavior planning** step is to find a future ego behavior, which minimizes risk while maximizing utility, meaning that a future behavior that is of low risk, but still efficient in terms of e.g. travel time, comfort, etc., is striven for.

Combining risk with a utility term, which defines a desired future behavior in case no or only low risk is present, allows the determination of a future behavior by finding a tradeoff between both, risk and utility. As presented in Chapter 8.1, for each situation this can be achieved in a straightforward way using a suitable planning algorithm, e.g. a sampling based approach, to find a satisfying trajectory through the risk map. Furthermore, considering several uncertain situations, as it is generally the case, the planning of a suitable future behavior has to consider the entire set of relevant situations⁵. Therefore, a behavior is necessary that is of low risk in all possible situations, but still efficient in the overall constellation of the scenario. Chapter 8.2 presents an approach to plan such a future trajectory by combining predictive risk maps for several situations, planning with regard to the estimated situation occurrence probabilities and applying a “plan B”, e.g. emergency braking, in case unlikely but risky situations suddenly occur.

6. Finally in the **behavior execution** step a control signal is generated

⁵See Chapter 3.1 for more information on how to derive this set of situations.

out of the safe future plan and applied to the dynamic system. As the system acts in a dynamically changing environment, reevaluation and replanning is necessary from time to time, using e.g. a preset time interval Δt .

The underlying idea of the presented framework is very similar to the idea of model predictive control (MPC) [99], where a time-discrete dynamic model of a system is used to predict the system's future behavior for a certain future time interval $[t, t + s]$ depending on different control inputs, starting from the current time t . This allows the calculation of a future control strategy optimizing the expected costs of the system. In general, only the next step of the control strategy is executed. Then, the sensed states of the system are updated and the prediction of a future state evolution is performed with the updated states, resulting in an adapted future control strategy. During execution the prediction horizon keeps on shifting forward, as it is also the case for the presented framework for *situation-based risk evaluation and behavior planning*.

Based on the presented framework, a system is developed by introducing approaches for *situation classification and trajectory prediction* in Chapter 6, *risk evaluation* in Chapter 7 and *behavior planning* in Chapter 8. Furthermore, in Chapter 5 the Foresighted Driver Model (FDM), a microscopic driver model based on a simplified version of the presented framework, is introduced. The driver model relies on a gradient descent and a computationally inexpensive, approximate risk model, targeting only the expected risk maxima, which has been introduced in Chapter 3.2.3.

The FDM is applied to the situation classification and trajectory prediction step of the full system. This allows the system to incorporate interaction between multiple traffic participants in the prediction task. As a consequence, the behavior prediction of the full system can be understood as a bootstrapping approach, where the prediction step comprises an approximate behavior planning system including all its steps, on a lower level, to increase the prediction performance.

For the full system, this thesis assumes an accurately sensed scene, including a precise localization of the ego and other entities⁶. Furthermore, a controller applying the planned behavior, derived from the behavior planning step in Chapter 8, to the dynamic system, is assumed to be given.

⁶Despite the assumption of an accurately sensed scene and localized scene entities, the approaches presented in this thesis explicitly consider measurement and prediction uncertainties.

Therefore, the *scene observation* and *behavior execution* steps are not covered in detail.

However, in [22] the author of this thesis proposed a method to improve the localization of scene items based on state-of-the-art map data, combined with a coarse and cheap position estimation as e.g. provided by standard GNSS (Global Navigation Satellite System). From the map data, the structure of the contextual road geometry is inferred, and aligned with the road view(s) provided by a front camera. This results in an improved relative positioning of the sensed items on the map structures, allowing a better scene interpretation. The alignment occurs by best-match search based on a feature comparison between the real road view from the camera and virtually generated road views based on the map, considering different assumed ego-vehicle positions. The method is illustrated in the Appendix A.3 in Figure A.1 and A.2. On standard road scenes, this approach has been validated and shown that it can be used as a cheap means to support intelligent Advanced Driver Assistance Systems (ADAS) and improve localization.

5 The Foresighted Driver Model

The modeling of realistic driving behavior has been heavily researched in recent years and even though there are numerous approaches targeting this problem, there are still considerable problems to solve. In the field of *situation classification and trajectory prediction*, which targets the prediction of human driving behavior, one of the main problems is the prediction of spatio-temporal trajectories of drivers, especially under consideration of interaction between several traffic participants. As discussed in Chapter 2.1, many learning-based approaches, such as [71], predict a traffic participant's behavior based on a large set of training data and features indicating the future behavior. Furthermore, there are approaches that use driver models, such as the Intelligent Driver Model (IDM) [133], in a forward simulation to predict how a traffic situation evolves into the future, which is a required technology for the support of Advanced Driver Assistance Systems (ADAS) and Autonomous Vehicles (AV). The approach for trajectory prediction that will be presented in Chapter 6.4 belongs to this category. If sufficient training data is available, learning-based approaches have the potential to perform very accurately. However, particularly in the case of a highly general driver model, the model-based approaches are applicable to a wider range of different scenarios, especially for predicting dangerous traffic situations, where training data is often scarce. Furthermore, learning-based approaches still struggle with the consideration of interaction between acting entities in the prediction process.

Modeling vehicle behavior always implies modeling the behavior of the vehicle's driver (human or machine), along with its specific driving style and driving preferences. An important aspect is that a realistic driver model has to capture the causes that lead to the driver's decisions. Usually, these are related to concepts of driving progress, risk and safety, parametrized e.g. by the distance traveled per time or by velocity differences and time-gaps to other traffic participants.

Furthermore, driver models can be utilized to determine the current maneuver or driving situations by analyzing and comparing the actual

behavior of a driver with “how the driver should behave” followed by an early warning to provide time to react, as done in [31, 87, 101]. In Chapter 6 the Foresighted Driver Model, introduced in this chapter, is applied to the task of situation classification in order to achieve a suitable model of *how the current scene will evolve in the future*.

In addition to prediction purposes, microscopic driver models are commonly applied in simulation tasks. In this case, they aim at describing the dynamics of driving vehicles reasonably well in terms of realistic single entity behavior, but they also allow the simulation of collective traffic flow properties, like traffic breakdown in high density situations.

The Intelligent Driver Model (IDM) is a simple yet seminal microscopic model for the simulation of free driving and car-following, longitudinal behavior in freeway and urban traffic (see Section 5.1). It has a low number of parameters that can be related to the driving dynamics and the driver preferences. Its extension MOBIL [68] further allows the application to lane change decisions. Nevertheless, the IDM is lacking several properties that are required in prediction models for future ADAS and autonomous driving, as e.g. for situations which involve the handling of multiple other traffic participants, the consideration of non-longitudinal risks, the behavior at unmanaged intersections, and the incorporation of road structure and geometry.

This chapter introduces a novel microscopic driver model, the **Foresighted Driver Model (FDM)**, for the description of driving dynamics, which is able to handle such situations. The model is targeted to capture the risk-dependent aspects of driving, assuming that a driver is influenced in its driving behavior decisions mainly by the consideration of future utility/benefits and the risks that he/she may encounter along his/her intended driving route. In such a case, the benefits will be mainly expressed by factors related to the driving goal, such as driving speed, time to arrival, driving economy, etc., whereas the risks will be related to (excessive) driving speed and accelerations as well as potential collisions with road structure elements and other traffic participants. In short, we assume that drivers have a strong tendency to avoid potential risks like upcoming collisions and adjust their behavior accordingly. This assumption is also considered in other works, trying to improve prediction accuracy, e.g. in [61].

The presented FDM straightforwardly and explicitly captures a number of properties of driving dynamics that are related to the predicted risk of situations, while retaining a simplicity that allows for efficient simulation

and its application in ADAS and autonomous driving scenarios¹.

5.1 The Intelligent Driver Model

As the Foresighted Driver Model (FDM) is inspired by the Intelligent Driver Model (IDM), its properties are briefly discussed, before advancing to the more general FDM. The Intelligent Driver Model, introduced in [133], combines realistic simulation properties with a simple formulation and calculation, and has been used in numerous scientific studies related to driver modeling, driver assistance systems and collective traffic simulations. It has a low number of parameters which can be related naturally with driver- or car-specific properties. In addition, it is deterministic and is evaluated continuously for its input variables.

Its formulation for the longitudinal behavior is in form of a differential equation for the longitudinal ego car velocity change

$$\frac{dv}{dt} = a \left[1 - \left(\frac{v}{v_0} \right)^\beta - \left(\frac{d^*(v, \Delta v)}{d} \right)^2 \right], \quad (5.1)$$

with

$$d^*(v, \Delta v) = d_0 + vT + \frac{v\Delta v}{2\sqrt{ab}}.$$

Here, the ego-car is described by longitudinal position and velocity, x and v . The distance $d = |x - x^1|$ and the velocity difference $\Delta v = v - v^1$ are measured between the first leading car with position x^1 and velocity v^1 and the ego car. It applies only for cars in front and ego car velocities larger than the velocity of the leading car ($\Delta v > 0$). The parameters v_0 , d_0 , T , a and b are related to the driving style, and express desired free cruising velocity, minimal gap distance and minimal time gap to the leading car, maximal acceleration and comfortable deceleration, respectively. The exponent β describes how the entity approaches the free cruising velocity v_0 . Typically used parameters can be found in [133].

With no car in front of the ego-car, the last term from (5.1) vanishes and the driving velocity adjusts to the desired free driving velocity v_0 with acceleration a . For short distances to the car in front and/or large speed difference Δv , the last term from (5.1) dominates the dynamics, leading to a deceleration with factor b . The IDM does not consider risks explicitly.

¹The main contributions of this chapter have been published to the IEEE ITS Society in [38].

However, some aspects of criticality are handled implicitly by the terms and parameters related to the time gap T and the deceleration factor b .

5.2 The Foresighted Driver Model

Generally, driver dynamics are assumed to be best modeled by considering the driver as being aware of the risks of the upcoming situations (to the best of his/her knowledge and subject to sensory and cognitive limitations) and comparing those risks with the benefit he/she gets when choosing a particular driving behavior.

This allows to incorporate such a model directly into ADAS considerations, either by simulating other traffic participants with FDM in a realistic fashion, as a prediction model for actual planning (see Chapter 6), or by comparing the proposed dynamics with assistance functions that also have to find a tradeoff between utility and risk.

However, such a risk- and utility-aware driving behavior generally needs appropriate optimization and planning methods. It additionally requires elaborate probabilistic prediction schemes of the other traffic participants, since their true intention is unknown and measurements are uncertain and noisy. The general framework for *situation-based risk evaluation and behavior planning*, introduced in Chapter 4, includes such a detailed approach for risk prediction with uncertainty and is used for planning the best behavior in terms of expected risk and utility.

The following builds on this framework to propose a driving model that is comparable in simplicity to microscopic models like the IDM, but which is based explicitly on future risk and utility factors. It is called the Foresighted Driver Model, because it requires the consideration of predicted critical points along a driver's future trajectory. Given the risk, it is assumed that the driver behaves in a way that tries to avoid critical points while maximizing utility.

Since the FDM is based on the same underlying framework of *situation-based risk evaluation and behavior planning*, it comprises the following six steps, which are simplifications of the steps presented in Chapter 4:

1. Since the FDM is a longitudinal driver model, generally applied to simulate or predict longitudinal behavior, the step of **scene observation** is usually handled by the simulation/prediction environment, which provides the current state (longitudinal position and velocity) and a possible drivable path for each considered entity.
2. The **situation classification** step is in general a highly complex

task. In the FDM, only a fixed set of situations, separating longitudinal behavior alternatives of the involved entities, is considered. Furthermore, situations in the FDM always consider bilateral relations between the ego and one other entity. Nevertheless, multiple other entities can be considered by superposing risks caused by different sources. In order to avoid the computationally expensive, probabilistic estimation of a situation's occurrence probability, a preset weighting of the different considered situations is applied.

3. The goal of the **trajectory prediction** step is generally to provide one possible prototypical trajectory for each entity in each situation. Here, only computationally inexpensive, longitudinal prediction models are considered, such as *constant velocity* and *constant deceleration*. Unlike in the full framework for *situation-based risk evaluation and behavior planning*, interaction between the involved entities is not considered in the prediction process due to high computational costs.
4. In the **risk evaluation step**, the upcoming risk of the ego entity has to be evaluated. This evaluation has to comprise the risk of all involved risk sources and all considered situations, according to the general definition of risk in Chapter 3.2. Here, the approximate risk model, introduced in Chapter 3.2.3, which targets only risk maxima is applied. By a bilateral evaluation of the predicted ego entity's trajectory and the predicted trajectory of another traffic participant or road structure element, the predicted points in time with maximal risk can be extracted. For collision risks, this is the point-of-closest-encounter, typically expressed by the risk indicators time-of-closest-encounter (TCE) and distance-of-closest-encounter (DCE).
5. The aim of the **behavior planning** step is to find a future behavior that minimizes risk and maximizes utility. To arrive at a computationally inexpensive behavior adaptation, finding a tradeoff between risk and utility, the longitudinal velocity is adjusted using a gradient descent on a cost function combining both, risk and utility.
6. The **behavior execution** step is of low importance, as the FDM is generally applied in simulation or prediction tasks. The derived velocity change can directly be applied to the dynamic system.

The Foresighted Driver Model is a longitudinal microscopic driver model mainly applicable to traffic simulation and prediction tasks. The scene

observation is generally assigned to the simulation or prediction environment. Therefore, the current state of the traffic scene \mathbf{x}_t , including the states of the ego entity \mathbf{x}_t^0 and other traffic participants \mathbf{x}_t^i , constitute a first step into the driver modeling. For the FDM, the spatial positions and longitudinal velocities are important.

Furthermore, as common in microscopic driver modeling [133], a known spatial path χ_t^0 and χ_t^i for the ego- and each other entity, on which they act longitudinally, is assumed.

The risk evaluation, according to Chapter 3.2, relies on prototypical predictions on how the current scene state \mathbf{x}_t evolves into the future. Both, state measurement uncertainty and the propagated state uncertainty in the prediction process are explicitly handled by the risk model. However, uncertainty arises also in the estimation of drivers' intents. This usually results in fundamentally different behaviors of the involved entities, considered in separate situations. To cope with this uncertainty, the full framework for *situation-based risk evaluation and behavior planning* estimates the occurrence probabilities of relevant situations. Such an evaluation is a computationally complex task. Therefore, relevant situations for the use in the FDM are predefined in a fixed set of considered situations. In the FDM the general definition of situations is reduced to represent only bilateral relations between the ego- and one other entity. For each involved other entity i , the set \mathbb{H}^i of the following three bilateral situations with adequate prediction models is considered:

1. Both entities keep on driving with constant longitudinal velocity.
2. The ego entity keeps on driving with constant velocity, while the other entity performs a sudden stop.
3. The other entity keeps on driving with constant velocity, while the ego entity performs a sudden stop.

This results in the total set of considered situations $\mathbb{H} = \bigcup_i \mathbb{H}^i$.

Assuming a risk-averse behavior of the FDM, the first situation mainly defines the general behavior e.g. to avoid collisions at intersections or rear-end collisions for the car-following case. Considering only the first situation would result in a risky behavior, as no safety distance to a leading vehicle would be kept. The decisional uncertainty in the behavior of involved entities is not considered.

By taking the second situation into consideration, driving very close to a leading vehicle would result in high risk for the situation that the

other entity suddenly brakes. In the same way the third situation results in an FDM behavior keeping a safety distance to a vehicle approaching from behind. For other scenarios such as intersections, situation 2 and 3 also result in an increasing distance kept by the FDM to the other acting entities.

The risk evaluation according to Chapter 3.2 relies on situation-dependent, prototypically predicted scene evolutions $\hat{\mathbf{x}}_{t:t+s}(\mathbf{x}_t, h_t)$. For traffic scenarios this mainly involves a prediction of prototypical trajectories of the considered entities in each evaluated situation. For the FDM the three previously introduced bilateral situations are considered. Thus each other entity results in an evaluation of three situations. For each of the considered situations $h_t \in \mathbb{H}$, a prediction of the ego- and the other entity's trajectory, $\hat{\mathbf{x}}_{t:t+s}^0(\mathbf{x}_t, h_t)$ and $\hat{\mathbf{x}}_{t:t+s}^i(\mathbf{x}_t, h_t)$, is performed. Longitudinal *constant velocity* and *maximal deceleration*² models, according to the three situations, are applied for prediction. More sophisticated prediction models can be used as well.

Recapitulating Chapter 3.2, the definition of risk is the expectation value of the cost or benefit related to critical future events. A computationally inexpensive way to derive a measure for future risk is the approximate model for accumulated future risk, introduced in Chapter 3.2.3. Given the current state of the scene \mathbf{x}_t at current time t and the situation-dependent predicted trajectories of the ego- and another entity, $\hat{\mathbf{x}}_{t:t+s}^0(\mathbf{x}_t, h_t)$ and $\hat{\mathbf{x}}_{t:t+s}^i(\mathbf{x}_t, h_t)$, a suitable model for the approximate accumulated future risk considering any “maximal risk” (mr) event for a bilateral situation h_t , is derived in (3.27) as

$$\begin{aligned} r_\infty(\mathbf{x}_t, h_t) &= \sum_{\mathbf{e}_{mr}} \hat{c}_{mr}(\mathbf{e}_{mr}, \hat{\mathbf{x}}_{t+TMR}(\mathbf{x}_t, h_t)) \cdot P^\infty(\mathbf{e}_{mr} | \text{IVMR}(\mathbf{x}_t, h_t), \text{TMR}(\mathbf{x}_t, h_t)). \end{aligned}$$

Considering purely collision risks and only a single possible collision with one other entity i this simplifies to

$$\begin{aligned} r_\infty^{co}(\mathbf{x}_t, h_t) &= \sum_i \hat{c}_{co}^i(\mathbf{e}_{co}^i, \hat{\mathbf{x}}_{t+TCE^i}(\mathbf{x}_t, h_t)) \cdot P^\infty(\mathbf{e}_{co}^i | \text{DCE}^i(\mathbf{x}_t, h_t), \text{TCE}^i(\mathbf{x}_t, h_t)), \end{aligned}$$

²The maximal possible deceleration is set to $8m/s^2$.

with

$$\begin{aligned} & \hat{c}_{co}^i(\mathbf{e}_{co}^i, \hat{\mathbf{x}}_{t+TCE^i}(\mathbf{x}_t, h_t)) \\ &= \frac{1}{2} \frac{m_0 m_i}{m_0 + m_i} \|\hat{v}_{t+TCE^i}^0(\mathbf{x}_t, h_t) - \hat{v}_{t+TCE^i}^i(\mathbf{x}_t, h_t)\|^2 \end{aligned}$$

and

$$\begin{aligned} & P^\infty(\mathbf{e}_{co}^i | \text{DCE}^i(\mathbf{x}_t, h_t), \text{TCE}^i(\mathbf{x}_t, h_t)) \tag{5.2} \\ &= F_{co}^i \cdot e^{-\frac{\max(\text{DCE}^i(\mathbf{x}_t, h_t) - d_0, 0)}{\sigma_d}} \cdot e^{-\frac{\text{TCE}^i(\mathbf{x}_t, h_t)}{\sigma_{co}}} \\ & \quad \cdot B(\text{TCE}^i(\mathbf{x}_t, h_t), \text{DCE}^i(\mathbf{x}_t, h_t)). \end{aligned}$$

The parameters and $B(\dots)$ are defined according to Chapter 3.2.3. The risk indicators $\text{TCE}^i(\mathbf{x}_t, h_t)$ and $\text{DCE}^i(\mathbf{x}_t, h_t)$ are derived from the situation-dependent, predicted trajectories of the ego car and another entity i .

Furthermore, it is assumed that risk for the ego-car exerted by each other entity can be modeled separately with a different bilateral situation, and that it is sufficient to consider the set of most critical predicted future events corresponding to the discrete points in time of maximal future risk, as introduced in Chapter 3.2.3. Therefore, by integrating the considered bilateral situations, pairwise the ego with each other entity, the total accumulated risk is

$$r_\infty^{co}(\mathbf{x}_t) = \sum_{h_t \in \mathbb{H}} r_\infty^{co}(\mathbf{x}_t, h_t) \cdot P(h_t | \mathbf{x}_t).$$

In order to achieve a computationally cheap expression of the total future risk, a parametric, preset prior for the different situations is assumed, such that the three different situations are weighted according to

$$r_\infty^{co}(\mathbf{x}_t) \sim \sum_{h_t \in \mathbb{H}} r_\infty^{co}(\mathbf{x}_t, h_t) \cdot S_{h_t}^{co}.$$

The collision risk used in the FDM that explicitly considers the three bilateral situations between the ego- and each other vehicle denoted by h_1^i, h_2^i, h_3^i is

$$\begin{aligned} r_\infty^{co}(\mathbf{x}_t) \sim & \sum_{u \in [1,2,3]} \sum_i \hat{c}_{co}^i(\mathbf{e}_{co}^i, \hat{\mathbf{x}}_{t+TCE^i}(\mathbf{x}_t, h_u^i)) \\ & \cdot P^\infty(\mathbf{e}_{co}^i | \text{DCE}^i(\mathbf{x}_t, h_u), \text{TCE}^i(\mathbf{x}_t, h_u^i)) \cdot S_u^{co}, \end{aligned}$$

where S_u^{co} a preset prior for the individual bilateral situations.

In the risk model of Chapter 3.2 several different types of risk are allowed, beyond the car-to-car collision risk. For the approximate risk model used in the FDM, a consideration of multiple risk types is also possible, by summing over the different risk types

$$r_\infty(\mathbf{x}_t) = r_\infty^{co}(\mathbf{x}_t) + r_\infty^{cv}(\mathbf{x}_t) + \dots, \quad (5.3)$$

where $r_\infty^{co}(\dots)$ expresses the car-to-collision risk using the time-of-closest-encounter (TCE) and the distance-of-closest-encounter (DCE) as risk indicators. $r_\infty^{cv}(\dots)$ expresses the risk of skidding off the road when driving too fast through narrow curves (cv), where the time-of-maximal-curvature (TMC) and the indicator-value-of-maximal-curvature (IVMC) are applied as risk indicators³. The full expression of the approximate accumulated curvature risk $r_\infty^{cv}(\dots)$ can be found in the Appendix A.1. Further risk types can be applied in the same way, as explained in Chapter 3.2.3.

Recapitulating, the risk equation (5.3) involves a prediction step generating situation-dependent, prototypically predicted trajectories of the involved entities, including the ego entity. The risk indicators, which are used for the approximate risk model, express critical future events and rely on the performed trajectory predictions. Furthermore, each predicted trajectory relies on the current states of the scene \mathbf{x}_t . As the FDM acts longitudinally on an intended path the most important states are the ego entity's longitudinal velocity as well as its current position. The future risk, based on risk indicators, implicitly results from the different trajectory predictions and is thus heavily depending on the ego entity's longitudinal velocity, and therefore also controllable by a velocity adaptation. Therefore the future risk is expressed as an explicit function of the longitudinal ego velocity $r_\infty(\mathbf{x}_t, v)$.

A risk-averse behavior of the ego entity (FDM) can be achieved by performing a gradient descent on the risk function, respective the ego entity's velocity v . In this way, the ego entity adapts its velocity to minimize the expected future risk

$$\frac{dv^{\text{risk}}}{dt} = -\eta \frac{dr_\infty(\mathbf{x}_t, v)}{dv}, \quad (5.4)$$

where η is the gradient descent constant, defined in the Appendix A.2.

³More information about modeling the risk of skidding in curvy segments can be found in Chapter 3.2.3.

A purely risk-averse behavior is not sufficient to achieve a realistic driving behavior. Furthermore, efficiency resp. utility considerations have to be incorporated to arrive at a realistic behavior, finding a tradeoff between risk and utility. For a utility term, the free-driving term of the original IDM (5.1) is borrowed. In case of low risk, this term tries to approach a preset cruising velocity v_0 ,

$$\frac{dv^{\text{free}}}{dt} = a \left[1 - \left(\frac{v}{v_0} \right)^\beta \right]. \quad (5.5)$$

Throughout the simulations $a = 1.25 \text{ m/s}^2$ is used, which is a typical value for the acceleration/deceleration to cruising speed used in IDM simulations.

The total velocity change is given by a combination of free-driving (5.5) and the foresighted minimization of predicted risks (5.4), according to

$$\frac{dv}{dt} = \frac{dv^{\text{free}}}{dt} + \frac{dv^{\text{risk}}}{dt}. \quad (5.6)$$

Since the trajectory velocity parameter v may depend on a non-analytical path geometry, the velocity gradient of the risk $r_\infty(t, \mathbf{x}_t, v)$ is calculated numerically, with the benefit that it can be applied to arbitrary scenarios.

Equation (5.4), (5.5), and (5.6) can be further adapted to achieve physically realistic driving velocity curves, e.g. by using constraints on dv/dt to adjust to the maximally possible acceleration and braking deceleration. For low risk scenarios the free driving term outweighs the risk term and the entity tries to optimize for utility considerations. However for risky scenarios, the most important term driving the model dynamics, is given by the risk minimization.

5.3 Results

In the following, the FDM is applied to three different scenarios, two inner-city scenarios and one highway scenario. In the first inner-city scenario, a car drives along a route comprising several turns with different curvature and no other traffic. The second inner-city scenario is based on an intersection with several other traffic participants in the way of the ego car. In the highway scenario, the ego car is accessing a highway and adapting its velocity according to the general traffic flow. All scenarios are based

on simulations on real-world maps with realistic road map structure taken from augmented OpenStreetMap data, as shown in Figure 5.5.

Two types of risk have been modeled, namely collision risk of the three different bilateral situations (ego- and each other entity) from Section 5.2, and one risk type which models the criticality from exceeding the safe velocity in curves, which enforces a smooth anticipatory longitudinal velocity adaptation at turns with high curvature.

The FDM parameters for the risk types can be found in the Appendix A.2. For the three different bilateral situations, 1) ego/other constant velocity, 2) ego constant velocity/other sudden stop and 3) ego sudden stop/other constant velocity, different parameters have been used in (5.2), indexed by 1-3. The time constant $\sigma_{co,1} \in \{0.5, 1.0, 1.5\}$ s is utilized to model the general look-ahead time for any possibly upcoming collision in case that the velocity is not adapted. $\sigma_{co,2} = 0.5$ s is used to model the time gap/safety distance to a leading car in front. Analogously, a suitable time gap to a car following behind is modeled using $\sigma_{co,3} = 0.5$ s. The parameters $S_{1,2,3}^{co} = 1.0$ are used to weight the different risks of the considered situations.

Likewise, for the risk of skidding in a curvy road segment, $\sigma_{cv} \in \{0.5, 1.0, 1.5\}$ s is used to define the look-ahead time, i.e. when to start adapting the velocity for a safe driving along the curve. The approximate risk formula for skidding in a curvy road segment is defined in the Appendix A.1.

The maximally allowed lateral acceleration is $a_{c,\max} = 0.9 g$ ⁴, with the actual centrifugal acceleration while driving along in the curve.

5.3.1 Curve Driving Scenario

In Figure 5.1 the FDM is applied to a scenario where a car is driving along a route with several turns of different curvature. The centrifugal risk term now *foresees* risks due to a predicted velocity that is too high for an upcoming curve, enforcing an appropriate deceleration in these cases. In Figure 5.2, the red curve represents the maximally allowed velocity for driving through a curve before losing control,

$$v_{c,\max} = \sqrt{a_{c,\max} \cdot R},$$

where $a_{c,\max}$ is the maximally allowed lateral acceleration (mainly a property of car and tires) and R the curve radius along the route.

⁴with $g = 9.81$ m/s²



Figure 5.1: Curve driving scenario.

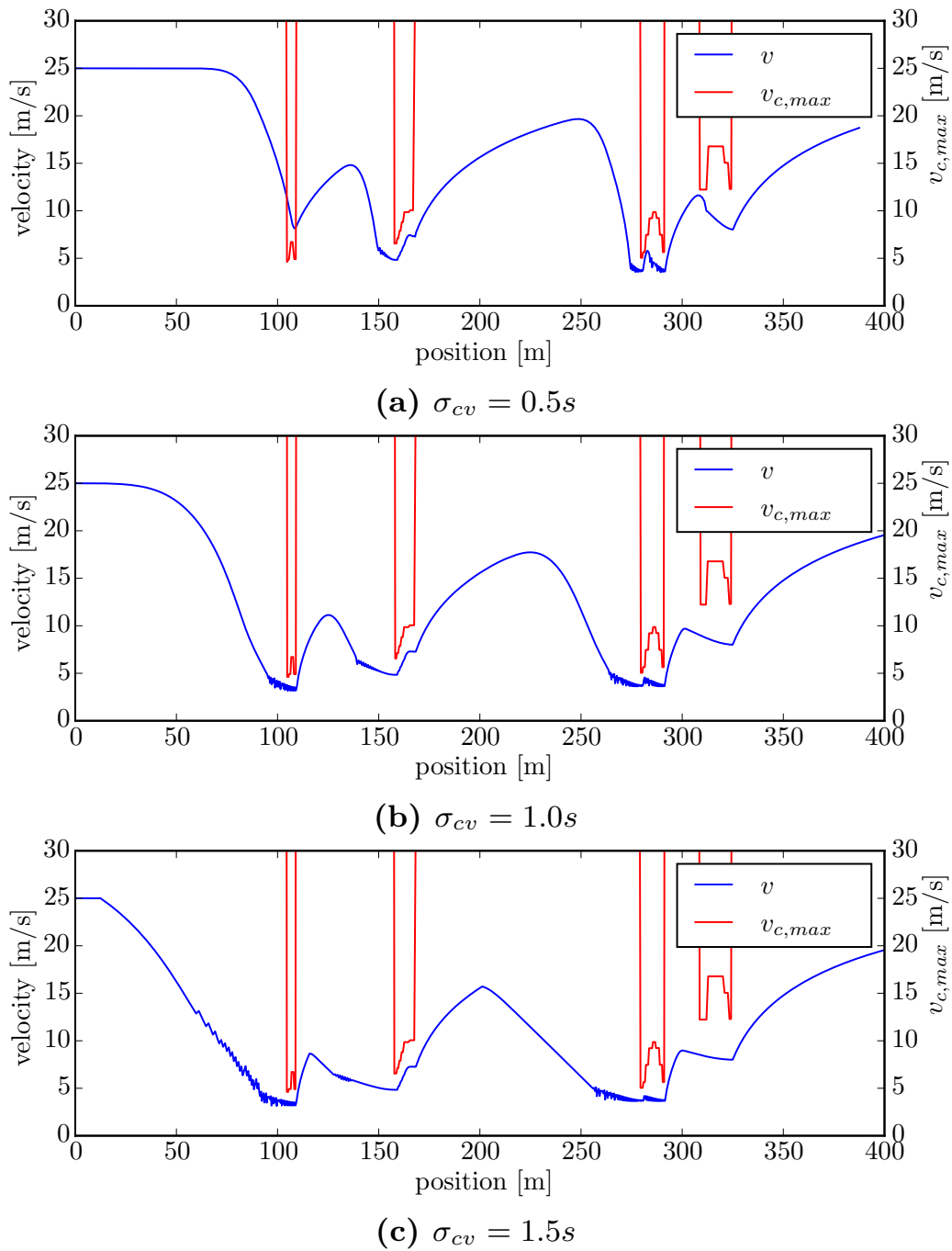


Figure 5.2: Curve driving scenario. Results for the FDM with different σ_{cv} time constants, $v_0 = 25m/s$. Higher σ_{cv} result in an earlier consideration of upcoming curve risks. Red lines indicate the maximally allowed longitudinal velocity, depending on the turn curvatures. Blue curves show the resulting FDM velocity. If σ_{cv} is too short, even maximal braking is not sufficient to mitigate the risk in the first curve, (a). For larger prediction horizons, however, the FDM results in smooth and continuous velocity profiles that reliably avoid risks by the parametrized safety margins, (b) and (c).

The driving behavior has been evaluated for different look-ahead times σ_{cv} . By comparing the velocity profiles (blue), it can be easily seen that a larger time window results in an earlier consideration of the upcoming curvature risk so that the car starts to brake earlier, resulting in a lower necessary deceleration and a globally smoother velocity course. Once the point of maximum curvature is approached, the velocity reaches a value which allows to drive out of the curve at low risk. In Figure 5.2(b) and (c), it can be seen that the velocity is reliably reduced before the curves, so that it always remains below the critical $v_{c,\max}$. In Figure 5.2(a), due to the limited temporal look-ahead the braking phase is not sufficient to reach below the critical maximal velocity in the first curve. The reason for that is the incorporation of a constraint on the maximal acceleration and deceleration to physically realistic values.

5.3.2 Intersection Scenario

In Figure 5.3 the FDM model is applied to an intersection scenario, where the ego car approaches from the left and has to give way to cars approaching from the right, if no safe crossing is possible. As the distance between the first two and the second two crossing cars is sufficiently large, the ego car chooses to cross during this gap. By comparing the velocity profiles (blue) in Figure 5.4 it can be seen that a large time constant $\sigma_{co,1}$ results in an earlier incorporation of the upcoming risky event related to the crossing cars. Thus in Figure 5.4(c), the ego car starts earlier to slow down in order to cross in the gap. By adapting the velocity earlier to the risky upcoming events the ego car does not have to slow down as much as in Figure 5.4(a), where the time constant is smaller. Additionally it can be seen that the resulting risk (red) in 5.4 a) is much higher compared to the risk in 5.4(b) and (c).

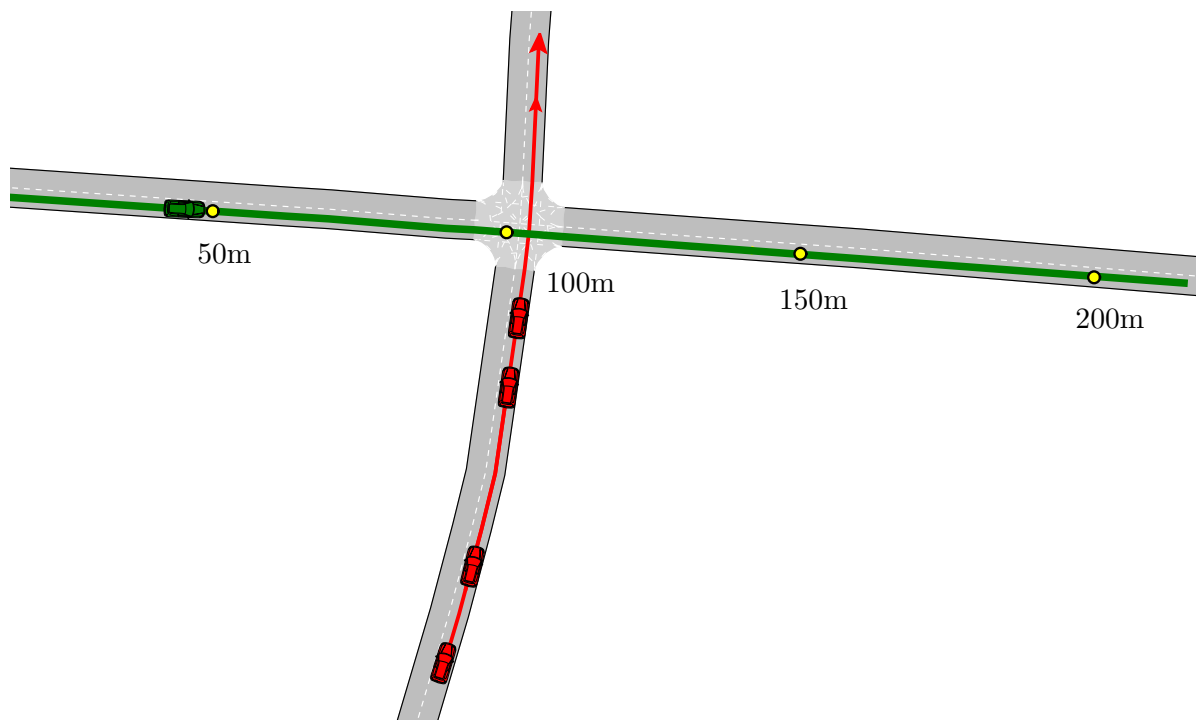


Figure 5.3: Intersection scenario.

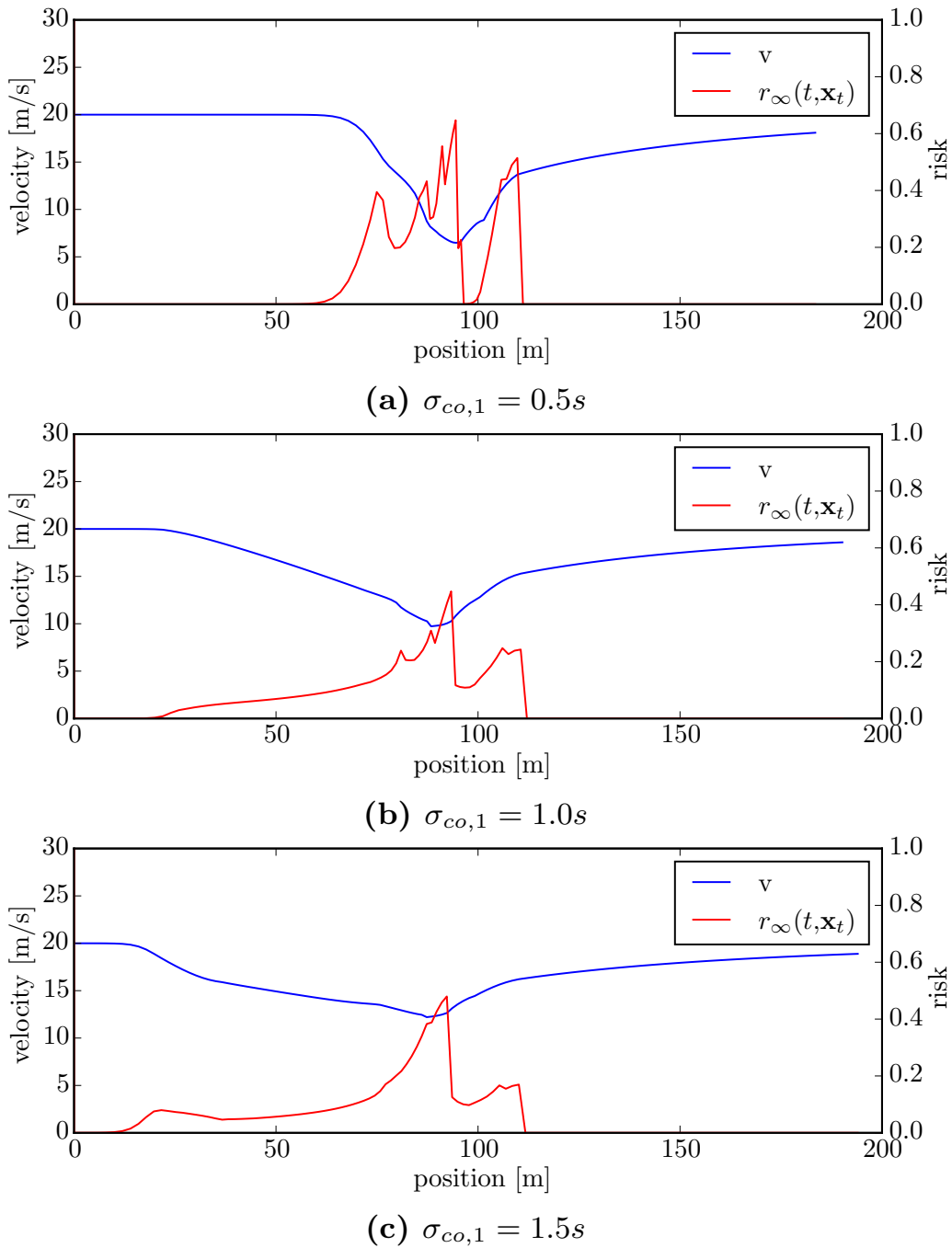


Figure 5.4: Intersection scenario. Results for the FDM with different $\sigma_{co,1}$ time constants, $v_0 = 19m/s$, $v_{others} = 10m/s$. The ego-car approaches a crossing with 4 other cars and adjusts its velocity to fit in the gap between the two groups of approaching cars. Velocity (blue) and risk (red) profiles are shown. Higher $\sigma_{co,1}$ result in an earlier consideration of upcoming risky events.

5.3.3 Highway Accessing Scenario

In Figure 5.5 the ego car intends to access a highway (see also the satellite view), on which three other cars are driving with almost the same speed. As the gap between the second and the third car is sufficiently large, the ego car adapts its speed in order to pull in. Figure 5.7 shows a temporal sequence of the scenario.

It can be seen in 5.6 that a larger time constant $\sigma_{co,1}$ results in an earlier adaptation of the velocity and a smoother highway accessing with lower risk. Once the car is on the highway it adapts its velocity to the general traffic flow, while keeping a safety distance to the car in front (defined by $\sigma_{co,2}$) and to the car behind (defined by $\sigma_{co,3}$). The curvy segment when accessing the highway is also incorporated into the risk calculation, but does not dominate the car dynamics since the curvature is quite low.

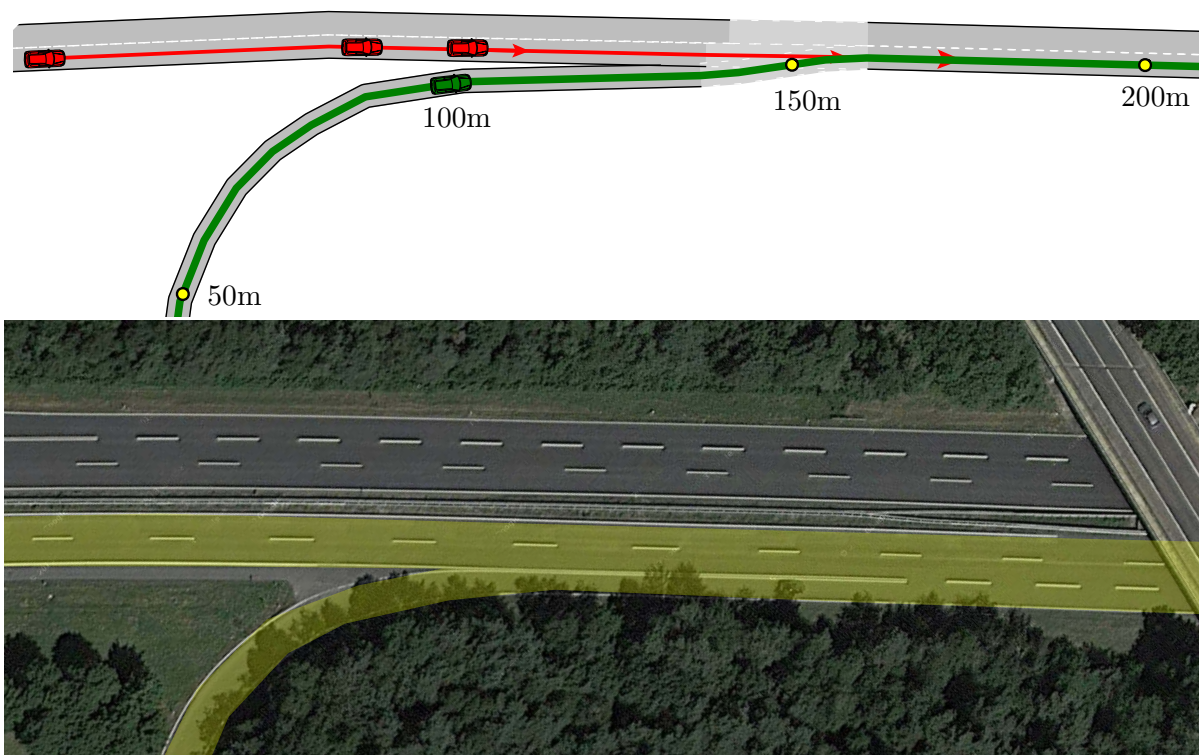


Figure 5.5: Highway accessing scenario. Real world road topology taken from augmented OpenStreetMap data.

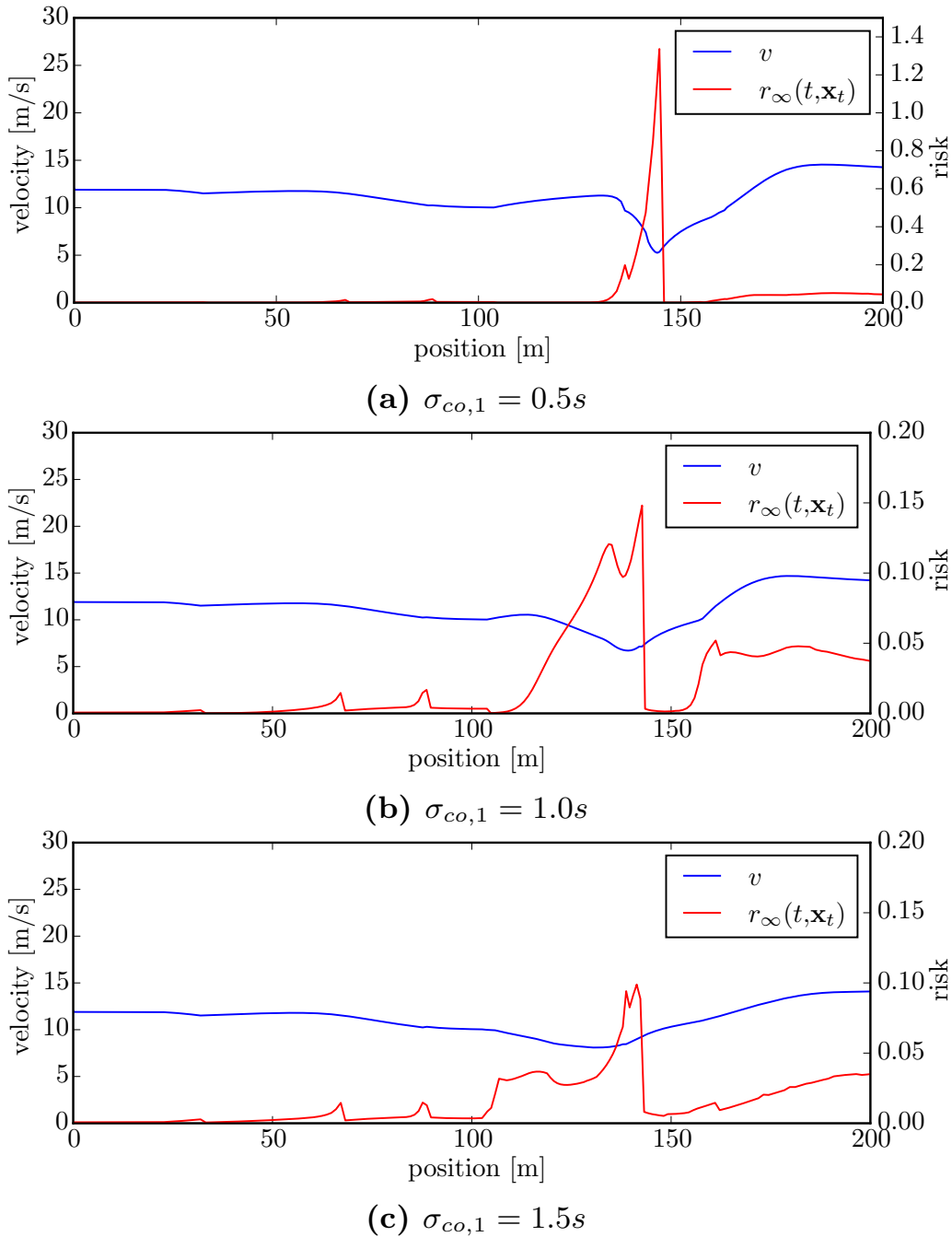


Figure 5.6: Highway accessing scenario. Results for the FDM with different $\sigma_{co,1}$ time constants, $v_0 = 12m/s$, $v_{others} = 14m/s$. Velocity (blue) and risk (red) profiles are shown. Higher $\sigma_{co,1}$ results in an earlier consideration of upcoming risky events. The ego-car tries to find the right low-risk gap between the approaching highway cars, braking and accelerating accordingly. Note the different scales of the risk plots.

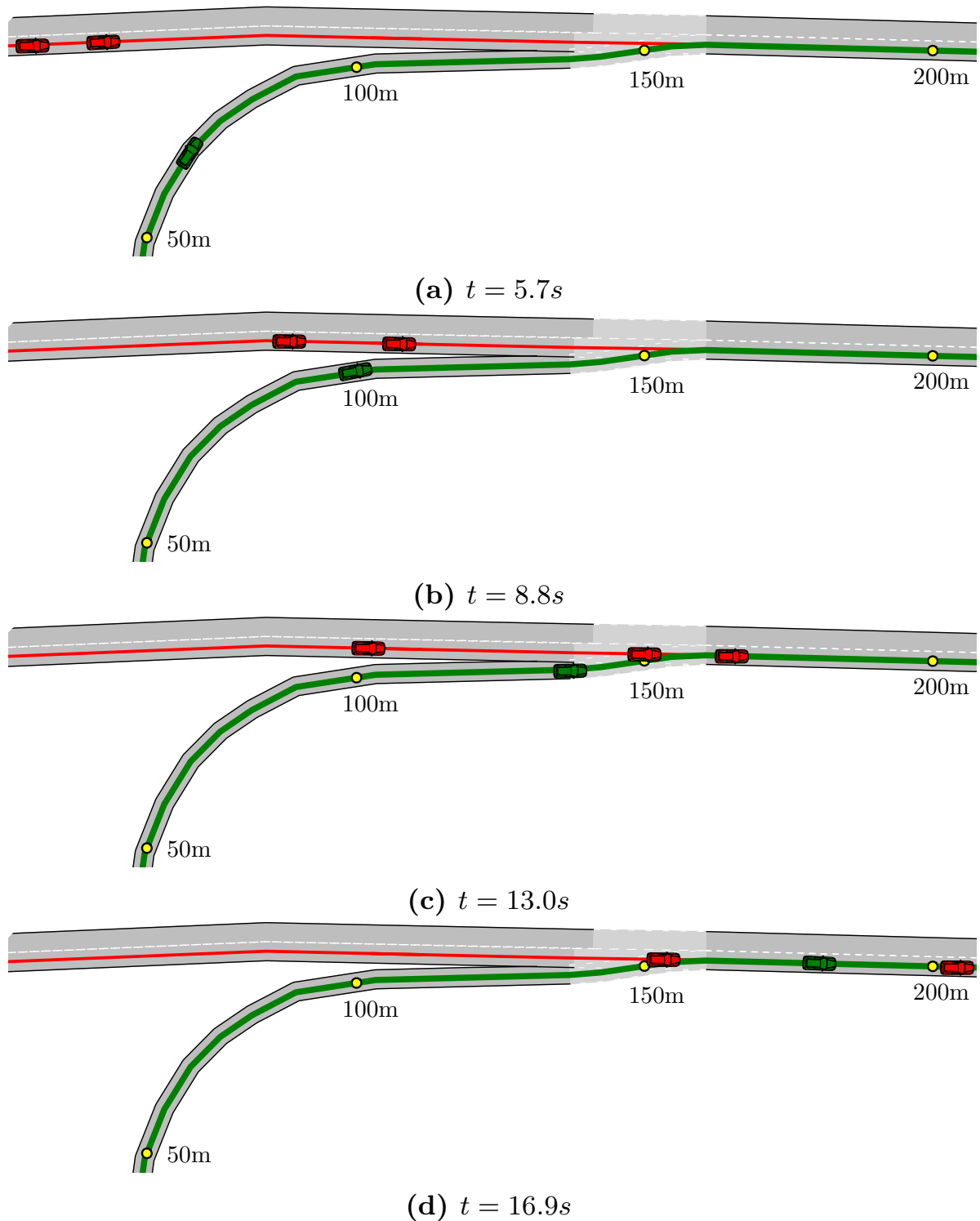


Figure 5.7: Highway accessing scenario for $\sigma_{co,1} = 1.0$. Cut-in behavior at different moments in time. The ego car (green) adapts its velocity to access the highway safely between the second and third car on the highway.

5.4 Conclusion

This chapter presented a novel microscopic driver model, the Foresighted Driver Model (FDM), which exhibits a behavior that is defined in terms of different types of risk, with the assumption that a driver's behavior mainly targets at minimizing risk while maximizing driving utility. The risks explicitly covered are collision risk with other traffic participants and risks caused by narrow curves in the road structure. The FDM is able to handle open traffic scenarios with an arbitrary number of risk types and risk causes (e.g. other traffic participants) by superposition, as well as with longitudinal and lateral collision risk components. Furthermore, it can be implemented in a very efficient way, compared to full behavior planning approaches.

Compared to the well-known Intelligent Driver Model IDM, the FDM is expressed in a similar way to control the longitudinal cruising velocity. Its model parameters are easy to adjust since they reflect risk- or dynamics-related factors with direct link to behavior. The influence of risk is implemented by adjusting to the velocity that minimizes the overall risk. Differently to the IDM, the FDM is easily generalizable to other risk types, such as traffic lights, without gaining much more complexity.

The FDM is able to generate realistic velocity profiles in a wide range of scenarios, such as traffic flow adaptation incorporating safety time gaps to a leading car and a following car (similar to the two seconds traffic rule), intersection behavior with multiple traffic participants, cut-in situations and curve driving. In this chapter, one curve driving scenario has been presented, where the FDM adapts its speed in order to drive safely and efficiently. Furthermore, the capability of the driver model to safely cross an unmanaged intersection with multiple other traffic participants, where it is necessary to brake or to choose a sufficiently large gap between crossing cars to pass through, has been presented. Finally, the approach has been applied to a highway accessing scenario, which requires the combined ability of adapting to the general traffic flow and safely cutting in, which is also a required skill for lane change maneuvers.

In [33] and [37], the author of this thesis has presented extensions to the FDM with a special focus on lateral positioning scenarios, such as lane changes in highway traffic. Differently to previous models (see e.g. [68]), those lateral extensions do not rely on indirect features like gap lengths, TTC or decelerations, but model the lane change process by explicitly calculating the involved risks and benefits of the different trajectory alternatives. The lane change decision occurs by searching a tradeoff between

the anticipated risks and the utility of the maneuver for the driver. In such a way, the model generalizes to a large variability of lane-change situations with varying number of involved traffic participants, since their states are incorporated into the risk estimation.

In [37], the author of this thesis has shown that with the presented lane change model, regular lane change processes can be reliably captured. Furthermore, the model has shown to react in plausible ways in complex traffic scenarios which are not covered by previous models. This is the case e.g. when an emergency lane-change is forced by another vehicle approaching fast from the rear-end, or when a lane change occurs in anticipation to an expected merge-in at an entrance.

When driving at high speeds, tactical preparation for a safe lane change is of high importance. In [33], the author of this thesis has presented more advanced driving maneuvers that allow for lane changes to be planned well in advance and carefully made without the restraint of requiring immediate action. Furthermore, the publication presents a continuous lateral control which allows driving on arbitrary paths other than the centerline, depending on the current traffic situation. Since more complex lateral maneuvers require more detailed considerations of the environment, an approach is presented to model the lane and the environmental influences. This paves the way for a modeling of variables such as lane markings, roadblocks, hard shoulders and more. Simulations illustrated how the introduced maneuvers allow successful preparation for upcoming lane changes and how traffic obstructions can be bypassed without performing a lane change but by using the continuous lateral control.

Future work on the FDM could include the incorporation of further risk types, as well as the link to properties of collective traffic dynamics.

6 Situation Classification and Trajectory Prediction

Humans in general not only “react”, but also behave proactively. They are able to look ahead and react to events that they expect will happen, but which have not yet occurred. They reflect their intentions and expectations as well as the actual events [55], which makes the prediction of their future behavior and the detection of faulty or unexpected, abnormal behavior a highly complex task.

Especially the breakdown of interaction between traffic participants is identified to be a major reason for collisions, see e.g. [130]. According to the authors, the most common errors are *faulty interpretations*, *observation errors*, *misplanning* or *distractiveness* and *inattentiveness*.

This chapter addresses the problem of situation classification in general and its application to detect that a traffic participant does not interact when it should interact due to criticality reasons. For this purpose, a situation classification approach is proposed, comparing the actually sensed behavior with different expected behavior alternatives, which were predicted under different situation-dependent assumptions. The more an expectation resembles the sensed behavior, the better the considered assumptions of this expectation serve as a suitable model for the considered entities’ behaviors¹.

As the behavior of traffic participants is mainly represented by spatio-temporal trajectories, the measure for trajectory similarity, introduced in Chapter 3.3, is applied to compare sensed and predicted trajectories.

By defining situations in a way that they differentiate between interacting and non-interacting behavior, according to Chapter 3.1, the system for situation classification can be applied to detect the *lack of interaction*. This could e.g. be the case when a vehicle does not brake, when it should in order to give way to another vehicle.

As discussed in Chapter 2.1, there are several approaches using evidence

¹The main contributions of this chapter have been published to the IEEE ITS Society in [31].

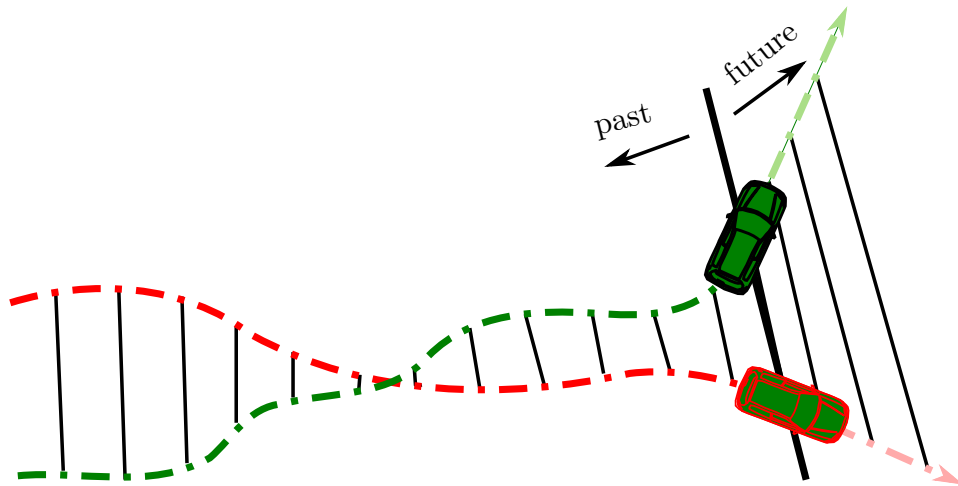


Figure 6.1: Schematical illustration of the similarity evaluation for spatio-temporal trajectories. Measured (vivid green) and formerly predicted (vivid red) spatio-temporal trajectories are compared to evaluate the past trajectory similarity. The expected future trajectory similarity is derived by extrapolating the measured trajectory into the future using kinematic short term prediction models (pastel green) and comparing it with the predicted trajectory reaching into the future (pastel red). The current position of the vehicle is indicated with black wire frame, while the expected position at current time is indicated with a red wire frame.

theory to map different features indicating the similarity of measured trajectories in the past and features indicating the similarity of a possible future evolution of trajectories to a maneuver occurrence probability and a lane assignment. Such features with predictive character are e.g. the time-to-lane-crossing (TLC) [134], the angle between vehicle and lane orientation [82, 102], and tangential velocity [101].

It is additionally common to use the minimal distance to the lane centerline for probabilistic lane assignment [101]. Especially for lane assignment in highway scenarios the velocity, gap distance, and conflict resolution can be used to classify maneuvers such as free, forced, and cooperative lane changes [53].

Instead of using several different features indicating the future trajectory similarity, *kinematic short term prediction models* are applied here, to directly evaluate the future trajectory similarity on the spatio-temporal distance level. This is a more general approach which allows the incorporation of more complex kinematic predictions for trajectory similarity. In Figure 6.1, the past (vivid) and future (pastel) trajectory similarity is indicated by the equi-time connections (black).

This chapter utilizes the general measure for trajectory similarity, introduced in Chapter 3.3, to propose a model- or prediction-based approach for situation classification. Actually sensed and situation-dependent, prototypically predicted, spatio-temporal trajectories of all involved entities are compared. As a result, for each situation a similarity measure is derived, which can be employed to estimate the probability that entities will keep on behaving according to the prototypically defined prediction of the considered situation.

Extrapolating the sensed trajectories using simple kinematic short term prediction models enables the incorporation of indicators for the expected future evolution of similarity. In Section 6.3, this system is applied to detect the *lack of interaction* between traffic participants. This is especially important for cases, where interaction is necessary to avoid upcoming risks, such as car-to-car collisions.

6.1 Prediction-based Situation Classification

In Chapter 4, a framework for *situation-based risk evaluation and behavior planning* has been introduced. The framework consists of the six steps shown in Figure 6.2, executed repetitively. In the first step, the system acquires all relevant data of the current scene from sensor measurements. The following step performs a situation classification to determine situations, relevant for the ego vehicles behavior, for which the third step then predicts prototypical state evolutions. Based on those predictions, the future risk is estimated, e.g. car-to-car collision risk. The ego behavior is then planned in a risk-averse way.

This chapter introduces an approach for situation classification that seamlessly fits into this framework (see Figure 6.2, green part).

According to Chapter 3.1, the acquired sensor data, such as the current road structure and dynamic entities including their current states, is utilized to generate a set of situation hypotheses based on the different possible behavior alternatives of the involved entities. A situation represents a specific assumption on how the entities possibly behave, e.g. if an entity does give way to another entity or not. For each of those situations a trajectory prediction is performed to get situation-dependent prototypical future state evolutions (more precisely, to get future spatio-temporal trajectories of the considered entities). The sensed trajectories as well as the situation-dependent expected or predicted trajectories in combination with the considered situation-dependent assumptions are continuously

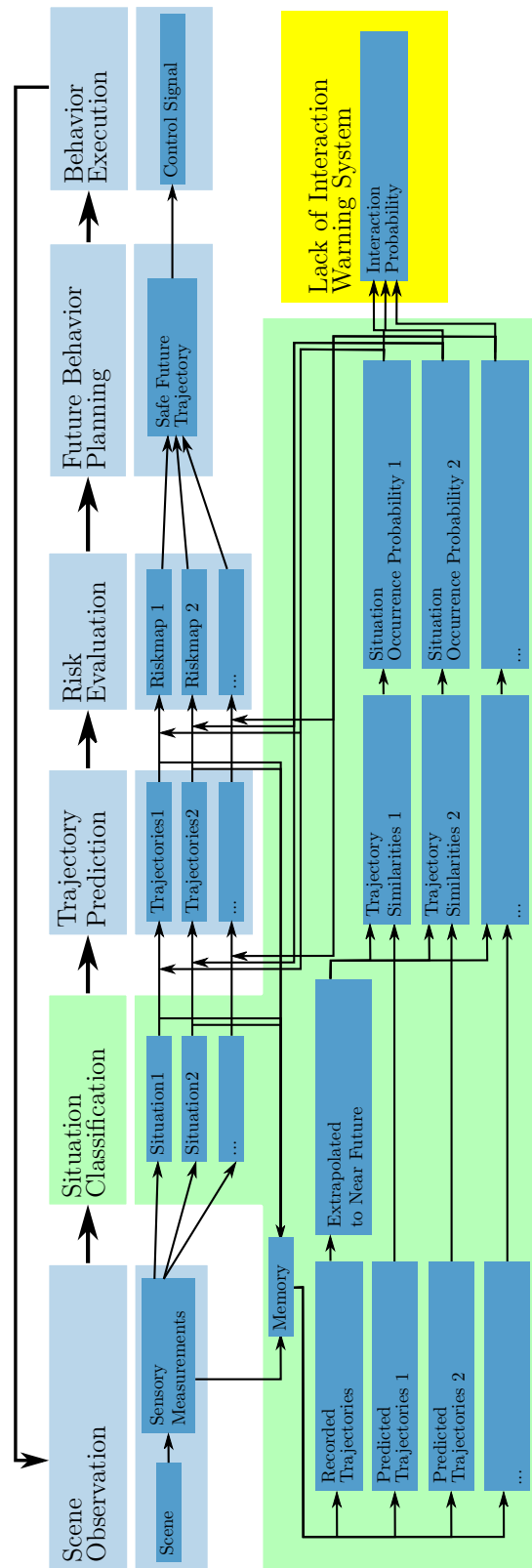


Figure 6.2: Integration of the *situation classification* approach into the framework for *situation based risk evaluation* and *behavior planning*. The situation classification approach is based on a trajectory similarity evaluation (green), between situation-dependent, prototypically predicted and actually measured trajectories of all entities involved in a situation. The approach is then applied to detect the *lack of interaction* in right-of-way violation scenarios (yellow).

stored for comparison.

To evaluate the likelihood that a certain situation applies to the current scenario, it is evaluated which situation-specific prediction fits best to the sensed and recorded trajectories of the present entities. First, the trajectory similarity (see Chapter 3.3) between each situation's predicted trajectories and the recorded trajectories is calculated. The result is processed to estimate the occurrence probability of each situation. To increase the prediction capability of the situation analysis, future trajectory similarity indicators (e.g. current driving orientation) are naturally incorporated, by means of *kinematic short term prediction models* to extrapolate the recorded trajectories into the near future.

By defining situations such that they differentiate between interacting and non-interacting behavior and using an interaction-aware trajectory prediction approach (see Section 6.4), the situation classification approach can be applied to detect situations, which are lacking interaction, e.g. the violation of the *right-of-way* rule (see Figure 6.2, yellow part). For the trajectory prediction, a forward simulation of the given situation hypothesis is performed by modeling each entity as an interaction-aware Foresighted Driver Model.

6.2 Situation Classification based on Trajectory Similarity Evaluation

The target of situation classification is to find a suitable model to explain the scene evolution, including the involved entities' behaviors. A situation according to Chapter 3.1 provides such a model. By generating situations, different assumptions on how each entity i could possibly behave, are incorporated. Situation-dependent assumptions on the selected spatial path of an entity and on how the entities interact, e.g. by incorporating right-of-way, are made. A trajectory prediction step, as introduced in Section 6.4, can be employed to generate prototypical behaviors/spatio-temporal trajectories by combining the different behavioral assumptions with suitable prediction models and an initial state of the scene.

As a result, one prototypical state evolution per involved entity i per situation h_t is achieved. The target is to compare situation-dependent predicted trajectories with actually measured trajectories. Therefore, predicted trajectories, initialized with the state of the sensed scene at the past

time \mathbf{x}_{t-T_p} , reaching into the future until $t + T_f$, are considered as

$$\hat{\mathbf{x}}_{t-T_p:t+T_f}^i(\mathbf{x}_{t-T_p}, h_t).$$

Additionally, the actually driven trajectories are sensed and recorded,

$$\mathbf{x}_{t-T_p:t}^i.$$

The recorded trajectories are then extrapolated into the future, as shown in Figure 6.3 using kinematic short term prediction models. Here, a simple *constant velocity, constant orientation* model is used

$$\mathbf{x}_{t:t+T_f}^i.$$

For each entity i in each situation h_t , the trajectory similarity between the recorded trajectory $\mathbf{x}_{t-T_p:t+T_f}^i$ and the (under the situation's assumptions) predicted trajectory $\hat{\mathbf{x}}_{t-T_p:t+T_f}^i(\mathbf{x}_{t-T_p}, h_t)$ is calculated according to (3.32), as $M_{sim}^i(h_t)$.

Based on those trajectory similarities, the situation's occurrence probability is estimated as

$$P(h_t|\mathbf{x}_t) \sim \frac{M_{sim,total}(h_t)}{\sum_{h'_t \in \mathbb{H}_t} M_{sim,total}(h'_t)} \quad (6.1)$$

with

$$M_{sim,total}(h_t) = \prod_{i \in I(h_t)} M_{sim}^i(h_t),$$

where $M_{sim,total}(h_t)$ is a situation's prediction similarity, considering all involved entities $I(h_t)$. \mathbb{H}_t represents the set of relevant situations according to Chapter 3.1.

The situation occurrence probability is then an indicator for *how good the situation-dependent assumptions on the involved entities' behaviors fit to the actually sensed behaviors* and can be utilized to further predict the evolution of the current traffic scene. A simple example with a single car and two situations is shown in Figure 6.3.

In the following, particularly the other entity's behavior alternatives are considered, because the target is to estimate if another entity interacts with the ego entity when it should, due to traffic rules and criticality considerations.

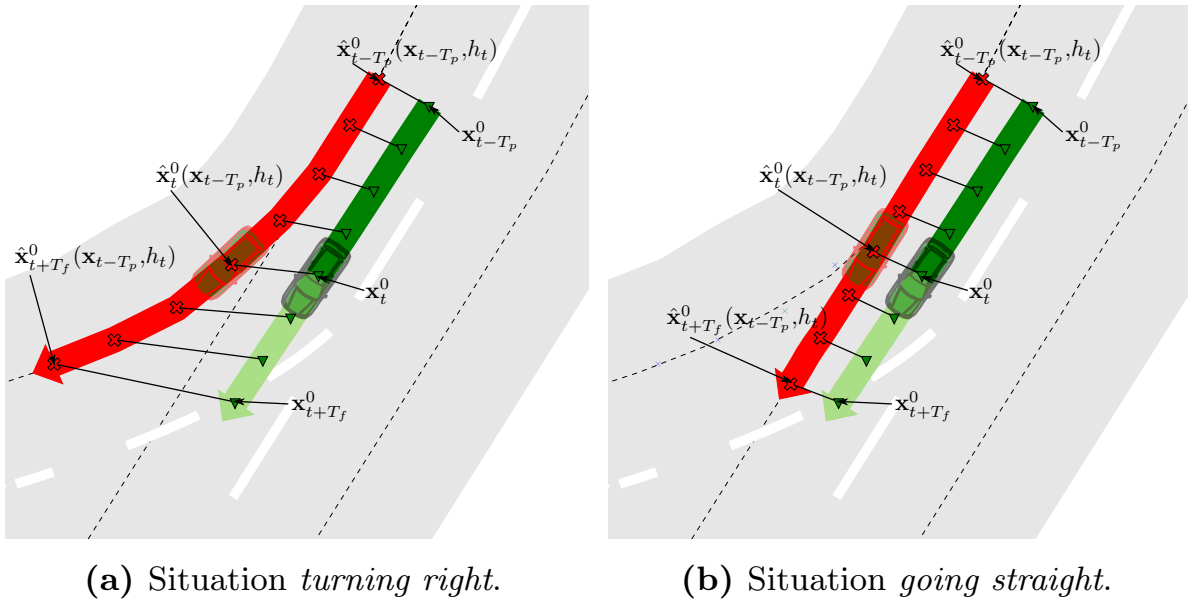


Figure 6.3: Similarity evaluation of two situations: (a) car predicted to turn right, (b) car predicted to continue straight. The measured trajectory (vivid green) extrapolated into the near future (pastel green) is compared to situation-dependent predicted trajectories (red) using the similarity measure introduced in Chapter 3.3. The measured and predicted position at current time is indicated by the cars. In this example the *going straight* trajectory is more similar to the measured and extrapolated trajectory and thus more likely to happen than the *turning right* situation.

6.3 Situation Classification for Interaction Detection and Lane Assignment

As initially motivated, situations where another entity does not consider the ego entity for interaction when it should, e.g. violations of right-of-way, are potentially highly risky and therefore very important to be detected as early as possible. In Chapter 3.1 situations are defined such that they differ in terms of their involved entities' possible drivable paths and longitudinal behaviors. For the longitudinal behavior alternatives, especially interacting and non-interacting behavior is differentiated. More precisely, it is analyzed, if the other entity does or does not interact with the ego vehicle. This is particularly important in traffic scenarios where the ego car has right-of-way, but has to detect if another car actually gives right-of-way.

To estimate the probability for non-interactive (~~inter~~) behavior, the occurrence probabilities of all situations are accumulated, according to (6.1), where no interaction is considered in the prediction of the other entity as

$$P(\mathbb{H}_t^{\text{inter}} | \mathbf{x}_t) = \sum_{h_t \in \mathbb{H}_t^{\text{inter}}} P(h_t | \mathbf{x}_t). \quad (6.2)$$

Likewise, the probability for interactive (inter) behavior is determined as

$$P(\mathbb{H}_t^{\text{inter}} | \mathbf{x}_t) = \sum_{h_t \in \mathbb{H}_t^{\text{inter}}} P(h_t | \mathbf{x}) = 1 - P(\mathbb{H}_t^{\text{inter}} | \mathbf{x}_t). \quad (6.3)$$

Besides the recognition of faulty behavior due to a lack in interaction, the situation classification system can also be applied for lane or path assignment. The target is to estimate the likelihood of an entity (here the considered other entity) choosing a certain path. For this purpose, the occurrence probabilities of all situations in \mathbb{H}_t^χ for a certain other entity's path alternative χ , neglecting different longitudinal behavior alternatives, are accumulated. Thus, we obtain the probability of the other entity choosing path χ as

$$P(\mathbb{H}_t^\chi) = \sum_{h_t \in \mathbb{H}_t^\chi} P(h_t | \mathbf{x}_t). \quad (6.4)$$

6.4 Situation-based Trajectory Prediction

A situation h_t contains all the information needed to predict the evolution $\hat{\mathbf{x}}_{t:t+s}(\mathbf{x}_t, h_t)$ of the situation by a forward simulation using the future time s and the current state of the scene \mathbf{x}_t . The evolution of the entire situation is a combination of one behavior evolution $\hat{\mathbf{x}}_{t:t+s}^i(\mathbf{x}_t, h_t)$ per involved entity i ,

$$\begin{aligned}\hat{\mathbf{x}}_{t:t+s}(\mathbf{x}, h_t) &= \bigcup_{i \in I(h_t)} \hat{\mathbf{x}}_{t:t+s}^i(\mathbf{x}_t, h_t) \\ &= \text{FS}(\mathbf{x}_t, h_t),\end{aligned}$$

where $\text{FS}(\mathbf{x}_t, h_t)$ denotes the forward simulation of the current scene \mathbf{x}_t for the future time interval $[t, t + s]$, according to the situation h_t .

In the forward simulation of the scene, each entity's prototypical behavior is modeled using a Foresighted Driver Model (FDM). Each entity's path, the way of interaction and the model parameters are chosen according to the predicted situation h_t (see Chapter 3.1).

The FDM, introduced in Chapter 5, is a highly general, longitudinal, interaction-aware driver model, which is able to provide realistic, long term stable predictions of traffic scenes, including intersection scenarios. It determines the velocity change by a gradient descent on a cost function combining a simplified risk evaluation and utility terms.

During the forward simulation of a situation, assuming interaction, the evolution of each interaction-aware entity is dependent on the evolution of other entities. For situations where none of the entities considers any other entity for interaction, the trajectories of each entity $\hat{\mathbf{x}}_i(s, t, h, i)$ can also be predicted independently from of each other.

6.5 Results: Interaction Detection applied to Real World Crash Scenarios

This section first guides through the procedure of situation classification and interaction detection on the example of an intersection crash scenario, followed by a statistical evaluation of the approach analyzing several real-world and simulated crash scenarios. The used parameters can be found in the Appendix A.2.

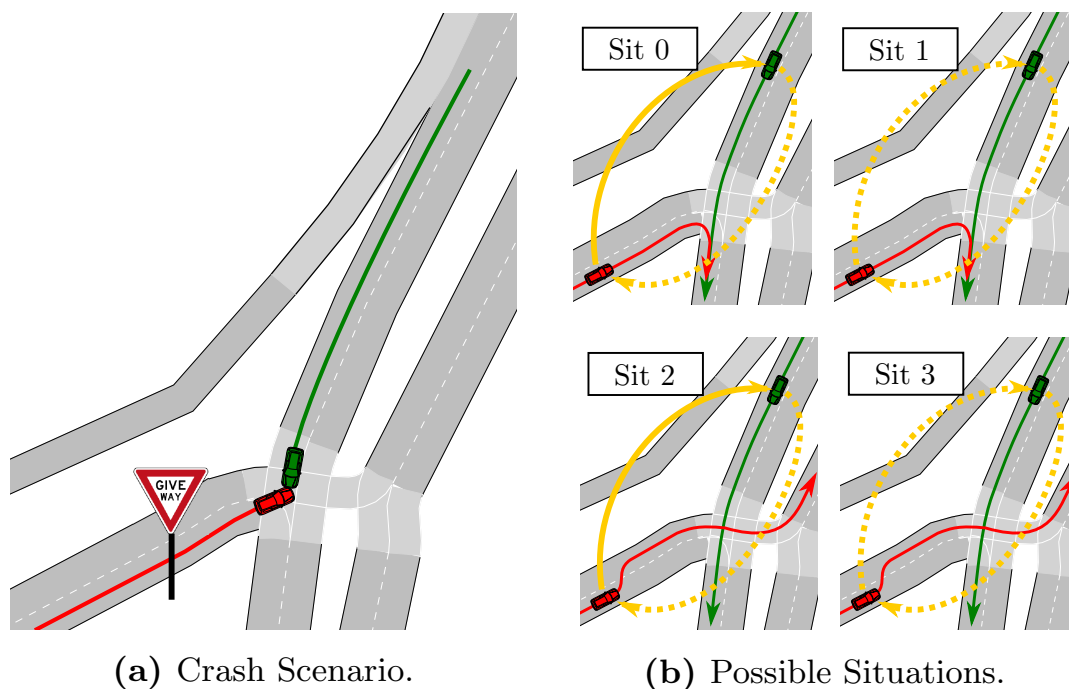


Figure 6.4: Multi-Lane Intersection Crash Scenario. The ego vehicle (green) and another car (red) approach an intersection, while the ego vehicle is on a priority road. Path alternatives for the other car are, staying on the right lane and turning right, or performing a lane change to the left lane and driving straight over the intersection. As behavior alternatives it is taken into account that the other car does consider the ego car and interacts, or that it violates the *right-of-way* and does not interact. A solid yellow arrow from vehicle A to vehicle B denotes that vehicle A considers B for interaction, while a dashed arrow indicates no interaction. This results in the 4 situations shown in (b).

6.5.1 Evaluation of a Multi-Lane-Intersection Scenario

To illustrate the general procedure, a complex intersection scenario with multiple crossing lanes is evaluated, as shown in Figure 6.4. The examined scenario is taken from the real-world crash database GIDAS-PCM (German In-Depth Accident Study - Pre-Crash-Matrix [41]), which contains reconstructed trajectories of involved entities leading to the observed crash. In the analyzed crash case, a violation of right-of-way and thus a *lack of interaction* has been identified as the main cause. The presented approach is not only able to estimate if another vehicle does not interact with the ego vehicle, but it can also determine how likely it is that the other entity will choose a certain spatial path. To show this combined estimation of *which path the other entity will choose* and *how the other entity will behave along that path*, the intersection scenario in Fig-

ure 6.4(a) is evaluated. Figure 6.4(b) illustrates four possible situations in this scenario. For the ego car, it is assumed, that the spatial path as well as the longitudinal behavior are known. The resulting situations arise from the other entity's path and behavior alternatives, namely turning right on the right lane (situations 0 and 1), turning left on the left lane (situations 2 and 3), as well as interaction-awareness (situations 0 and 2) or non-interacting behavior (situations 1 and 3).

The assigned longitudinal prediction similarities (3.31) of all situations in Figure 6.5(a) start with a value close to one, because the prediction model for interaction and non-interaction both predict that keeping the velocity constant is an appropriate behavior, which also fits well to the actually measured behavior of the other car. At around $t = -3s$ before the crash, the prediction models of the situations assuming interaction, start to predict a reduction of the other vehicle's velocity in order to reduce the collision risk. However, the actually measured trajectory does not fit well to those predicted trajectories and the assigned longitudinal prediction similarities of the two interaction-aware situations start to drop.

Looking at the assigned lateral prediction similarity (3.30) in Figure 6.5(b) it can be seen, that all situations with a path on the left lane have a lower similarity, compared to situations with a path on the right lane, where the other car is currently driving. Here the lane assignment character of the lateral similarity measure can be observed.

Figure 6.5(c) shows the occurrence probabilities of all four situations, which combine the contributions of the longitudinal and lateral prediction similarity. By combining the occurrence probabilities of all interaction-aware situations and all non-interaction-aware situations, according to (6.2) and (6.3) in Figure 6.5(e), an estimation of the *lack of interaction* in this scenario can be estimated. Similarly, by combining situations with the same spatial paths (6.4), standard lane assignment can be achieved in Figure 6.5(d).

6.5.2 Statistical Evaluation

After presenting the general approach, the lack of interaction for 12 different intersection scenarios from the GIDAS-PCM crash database is evaluated with the target to show that the system is able to correctly detect and warn in dangerous situations where a lack of necessary interaction was detected. Similarly to the intersection scenarios discussed above, in all the cases the violation of right-of-way caused the accident (at $t = 0s$). Additionally, the same cases are simulated with an interaction-aware driver

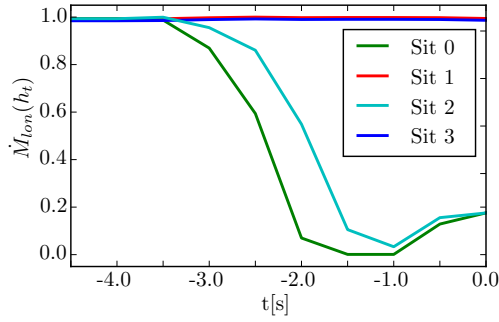
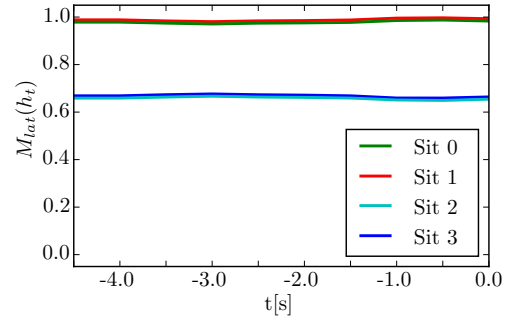
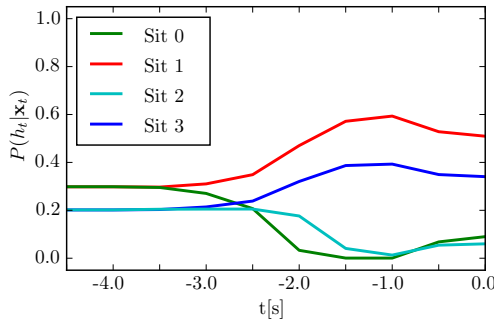
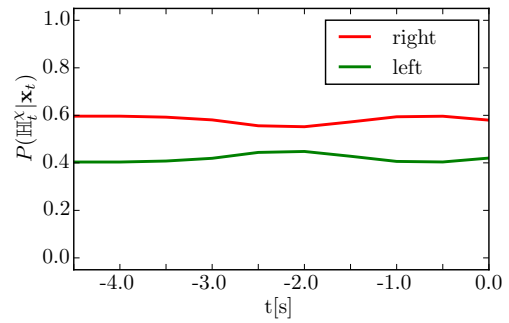
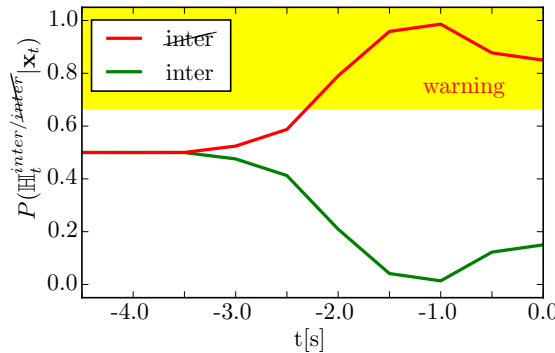
(a) Longitudinal trajectory similarities $\dot{M}_{lon}(h_t)$.(b) Lateral trajectory similarities $M_{lat}(h_t)$.(c) Situation occurrence probabilities $P(h_t | \mathbf{x}_t)$.(d) Path probabilities $P(\mathbb{H}_t^x | \mathbf{x}_t)$.(e) Interaction probabilities $P(\mathbb{H}_t^{inter} | \mathbf{x}_t)$ and $P(\mathbb{H}_t^{inter/inter} | \mathbf{x}_t)$.

Figure 6.5: Multi-Lane Intersection Crash Scenario. The longitudinal similarities $\dot{M}_{lon}(t, h)$ in a) show a decline for the interaction-aware situations as the other car does not start braking. The lateral similarities $M_{lat}(t, h)$ in b) show lower values for situations on the left lane, as the other car currently drives on the right lane. c) shows the occurrence probabilities of each situation combining longitudinal and lateral similarity. d) shows the probability of each spatial path to be chosen by the other entity according to (6.4). e) shows the probability according to (6.3) and (6.2) for the situations assuming the other car to interact or to not interact. The outcome of this real-world GIDAS scenario analysis is an early crash prediction, because of the other car violating the *right-of-way*. The crash occurs at $t = 0s$.

model, namely the Foresighted Driver Model (FDM), to achieve realistic trajectories with the same start constellation but which, due to considered interaction, avoid the crash. Here, a randomized parameter set for the driver models is used to include a higher variability in our tests. In those non-crash cases our system should correctly recognize the non-dangerous situations, which do not lead to any crash and should thus not give a warning. A selection of the analyzed scenarios is shown in Figure 6.6. It can be seen that intersections of highly diverse road structures have been evaluated.

From Figure 6.7, showing the *lack of interaction* probabilities for scenarios that actually did lead to a crash (red), it can be seen, that around three seconds before the occurring crash (at $t = 0s$), the probability for *lack of interaction* starts to rise and about two seconds before the crash the system determines the correct situation with high confidence and gives a warning.

It can also be seen, that the *lack of interaction* probabilities for the

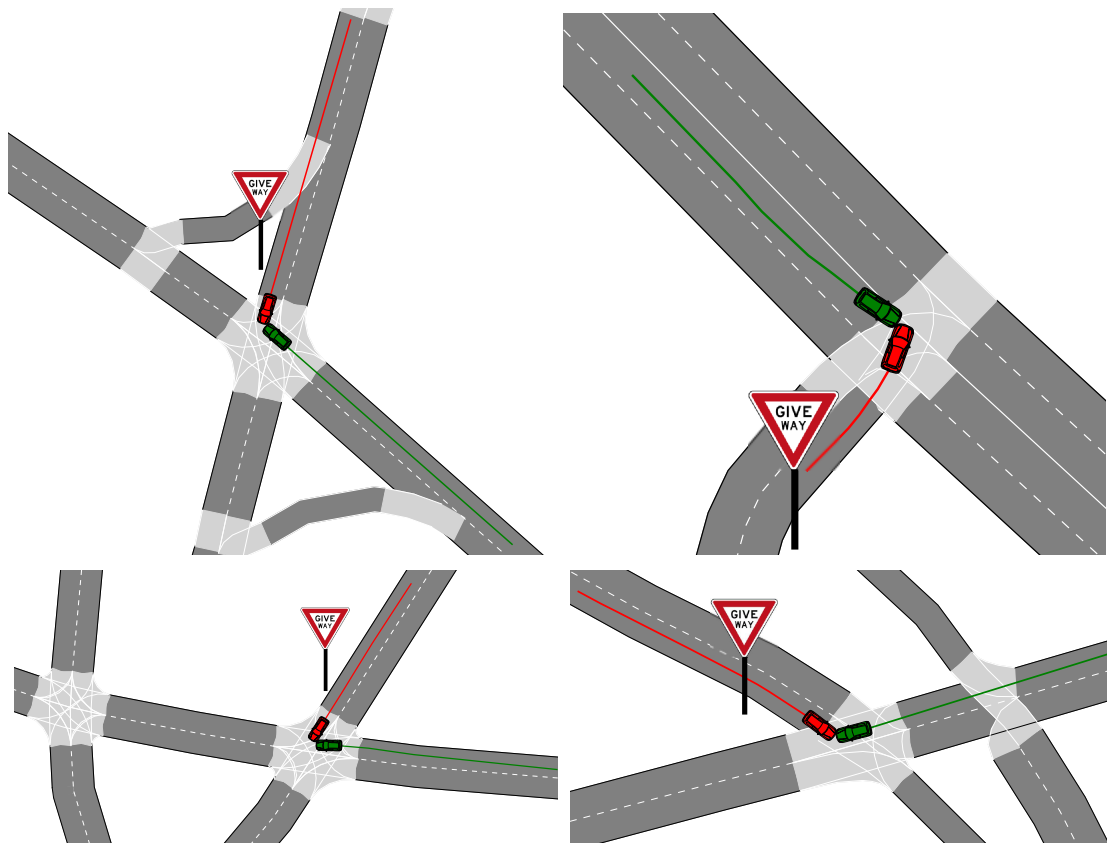


Figure 6.6: Exemplary crash scenarios analyzed in the statistical evaluation of several simulated and real-world scenarios.

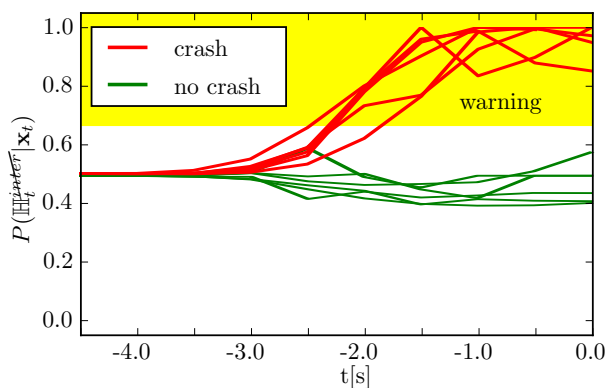


Figure 6.7: Lack of interaction evaluation $P(\mathbb{H}_t^{inter} | \mathbf{x}_t)$ of several simulated and real-world scenarios.

crash scenarios are in general more distinct, compared to the probabilities in case of non-crash scenarios in Figure 6.7 (green). This can easily be explained. The system evaluated the prediction similarity for different assumptions (here interaction and non-interaction). The evaluation of the situation occurrence probabilities for the crash cases lead to the following result: As one gets closer to the actual crash, the prediction assuming interaction predicts increasing interaction (e.g. deceleration), as this would be necessary to avoid the crash. Thus, the prediction similarity for the interaction-aware prediction heavily decreases compared to the prediction assuming non-interaction and thus the system becomes very certain that there is a lack of interaction.

In the non-crash cases, once the observed (other) vehicle starts to interact (e.g. brake), the situation becomes safer and further interaction becomes less necessary. Thus, the predictions with and without interaction are similar and do not diverge as heavily as for the crash-cases.

Furthermore, in Figure 6.7 of the non-crash cases (green), it can be seen that in one case the system first tends to favor *non-interaction* although interaction takes place. This can be understood as a consequence of the limited set of prediction models. In this case, the prediction model assuming interaction estimates an acceleration of the other car to act in a safe manner (to pass in front of the ego vehicle). In fact, the other car behaves more defensive than assumed by the prediction model and stops at the intersection. As only *interaction* (here acceleration) and *non-interaction* (here constant velocity) is considered, the real behavior of braking fits better to the *non-interaction* prediction. At a certain point in time the prediction model adapts and starts to predict a deceleration and the system correctly favors *interaction*.

The yellow area in Figure 6.7 symbolizes a warning system, which warns the ego driver in case the probability for *lack of interaction* crosses a threshold, $P(\mathbb{H}_t^{inter} | \mathbf{x}_t) \geq 0.65$. The threshold is chosen such that no false warning occurs in the evaluated cases. The system is able to warn about 2 seconds before the crash actually occurs, which would in general be sufficient to avoid the upcoming collision.

6.6 Conclusion

This chapter has presented a prediction-based approach for situation classification and interaction detection. The general measure for similarity of spatio-temporal trajectories, introduced in Chapter 3.3, is based on a decomposition into lateral and longitudinal trajectory similarity. Using this similarity measure, the current traffic situation can be evaluated by performing situation-dependent predictions of prototypical trajectories for each involved entity and by comparing those predictions to the actually sensed trajectories.

By defining situations as interacting and non-interacting, according to Chapter 3.1 and using an interaction-aware prediction model for the trajectory prediction, the system can be used to evaluate a *lack of interaction* in another entity's behavior. The Foresighted Driver Model, introduced in Chapter 5, is such a suitable, interaction-aware prediction model. Additionally, the situation classification system can be applied to estimate lane assignment, as the used situations also differentiate between various drivable paths. Applying the approach to real-world crash cases, as well as partially simulated cases, confirmed that the presented system is able to warn the ego driver about 2 seconds ahead of upcoming risks caused by *lack of interaction*.

The subsequent steps of the framework for situation-based risk evaluation and behavior planning, introduced in Chapter 4, rely on such a situation classification. Chapter 8 confirms that especially the behavior planning step benefits from the presented approach. Detecting dangerous near-crash situations is highly crucial to plan the future behavior and, due to a lack of real-world training data, a challenging task for learning-based situation assessment approaches. Collision warning systems often neglect interaction in behavior prediction. As a consequence, a reduction of false-positive warnings can be expected by applying the presented approach.

7 Risk Evaluation

A major target of the future risk estimation in terms of the own and other entities' predicted behaviors is the evaluation, selection and planning of the ego entity's future behavior. In this chapter an efficient representation of the future risk evaluation that allows direct behavior planning is introduced¹.

7.1 Predictive Risk Maps

Chapter 3.2.2 has introduced a general model for time-continuous predictive risk (3.8), which can be applied to evaluate an entity's future risk, based on situation-dependent, predicted trajectories of the entity itself and other involved entities, $\hat{\mathbf{x}}_{t:t+s}^0(\mathbf{x}_t, h_t)$ and $\hat{\mathbf{x}}_{t:t+s}^i(\mathbf{x}_t, h_t)$, as shown in Figure 7.1 (top row).

It has been argued in Chapter 6, that interaction between traffic participants is crucial for an accurate prediction of the future evolution of a sensed scene, including its traffic participants. Therefore, in Chapter 6.4, the interaction-aware Foresighted Driver Model has been applied to predict situation-dependent spatio-temporal trajectories of all entities involved in a considered situation. The risk evaluation does rely purely on the predicted trajectories and not on a specific prediction model. Therefore, any trajectory prediction approach, generating future spatio-temporal trajectories of the involved entities, can be applied.

To analyze different behavior alternatives of an ego entity, the ego entity's trajectory is varied systematically using its variation parameters q , such that

$$\hat{\mathbf{x}}_{t:t+s}^0(\mathbf{x}_t, h_t, q).$$

Here, the ego entity's longitudinal velocity $q = v^0$ is used to evaluate

¹The main contributions of this chapter have been published to the IEEE ITS Society in [26, 30] and patented in [28, 29].

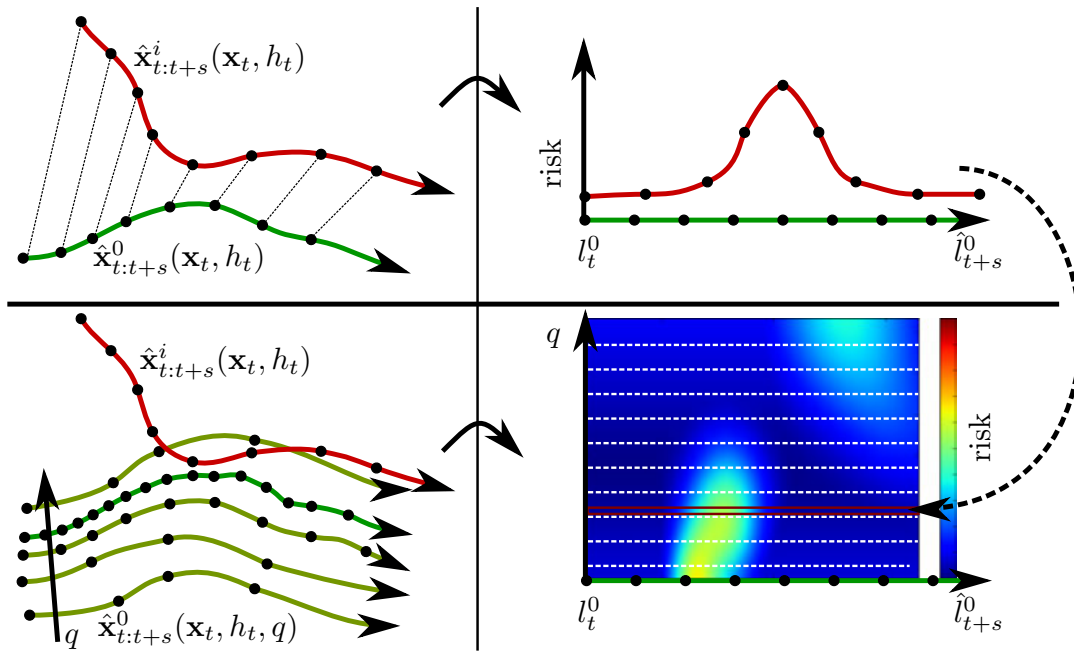


Figure 7.1: Predictive risk map - Top: evaluation of risk (top right) based on predicted ego car (green) and other car (red) trajectories (top, left) - Bottom: Generation of predictive risk map (bottom, right) based on risk evaluation of a variation of ego car trajectories and other car trajectory (bottom, left).

different velocity alternatives². For each selection of q , the future trajectory is estimated and the risk function $r(t + s, \mathbf{x}_t, h_t)$ is calculated according to (3.8) in Chapter 3.2.2. This risk function mainly depends on the situation-dependent predictions of all involved entities' trajectories, $\hat{\mathbf{x}}_{t:t+s}^i(\mathbf{x}_t, h_t)$ and the ego trajectory variations $\hat{\mathbf{x}}_{t:t+s}^0(\mathbf{x}_t, h_t, q)$.

This results in a temporal representation of the situation-dependent, predictive risk map as

$$R^{tmp}(t + s, q, \mathbf{x}_t, h_t).$$

In the following, the predictive risk map is expressed alternatively as

$$R(\hat{l}_{t+s}^0, q, \mathbf{x}_t, h_t),$$

where \hat{l}_{t+s}^0 is the future driven longitudinal distance, derived from the spatio-temporal trajectory $\hat{\mathbf{x}}_{t:t+s}^0(\mathbf{x}_t, h_t, q)$. For a given situation h_t and an initial state \mathbf{x}_t , the predictive risk map indicates how risky a certain

²If we assume a predicted constant ego velocity profile along a pre-defined spatial path we would vary the velocity, such that we get variation of multiple constant velocity profiles with different velocities.

behavior/velocity (q / v^0) will be at a certain longitudinal position (\hat{l}_{t+s}^0) on the future path³.

In Figure 7.1 (lower left), a set of possible trajectories of the ego entity, varied by q , is shown. From each of them, in combination with the predicted other entities' trajectories, the time-continuous future risk is evaluated. Composing this set of risk functions into a *predictive risk map*, allows to localize the future risks for different ego car behavior options, shown in Figure 7.1 (lower right).

Predictive risk maps can then be employed to plan future behavior/future velocity profiles, by searching for the most favorable path across the map, from the current state to a desired target region, considering risk and efficiency minimization constraints along the path, as illustrated in Figure 7.2. This can be achieved by using standard planning algorithms or other minimization techniques. In Chapter 8, a globally optimizing, sampling-based method for the evaluation of predictive risk map-based behavior for different typical traffic situations is introduced.

In the risk maps, each traffic scene entity results in a risk spot or risk area. Due to the time dependency in the risk model (TCE-influence for the simplified risk model, escape rate for the general risk model), risk spots further away in time are lower and broader. As they come closer, they get higher and sharper, i.e. more localized. This has the desirable effect that it allows to plan more coarsely for a distant time horizon and re-adjust planning when the risks become more sharply localized.

Generally, several risk functions that correspond to a set of other cars' hypothetical behavior options, represented by its predicted trajectories, as it would be the case for sampling-based prediction methods, can be superposed. This leads to a larger spread of the peaks in the risk function. However, the risk model (3.8) is targeted for prototypical situations. If the other traffic participants exhibit completely different behaviors (e.g. continuing straight at an intersection instead of turning), this should be considered in a separate situation. For each situation, including multiple entities, a *predictive risk map* is generated to evaluate the ego car's future behavior in terms of risk. Chapter 8.2 introduces a method for behavior

³The representation of the predictive risk map in terms of the traveled longitudinal distance instead of the future time is chosen due to the fact, that mainly innercity scenarios with a focus on intersections are targeted. The risk spots, which arise in such scenarios are generally spatially fixed (around the intersection point). Therefore, the illustration of a spatial representation is clearer. As spatio-temporal trajectories are applied, spatial and temporal representations provide equal information and can be exchanged.

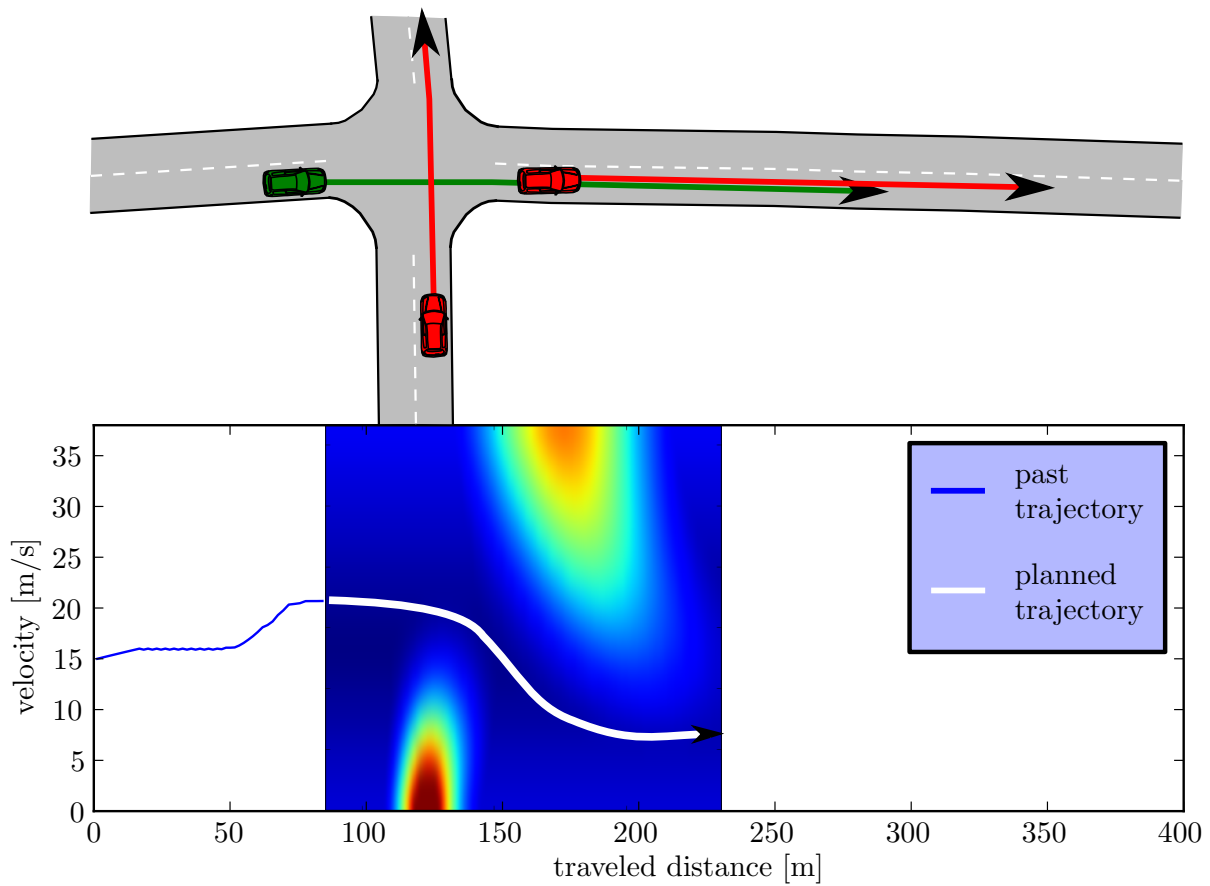


Figure 7.2: Behavior planning using predictive risk maps. Blue curve: The past driven trajectory. White curve: The future cost-optimized trajectory resulting from the selection or planning using the predictive risk map, which allows the evaluation of future risk for different behavior alternatives.

planning for the case of several possible, but competing situations and thus multiple separately considered predictive risk maps.

Nevertheless, as introduced in Chapter 3.2, different risk sources can be combined in one risk function. This applies to risks of different type, like the risk of crashing without external interaction when driving too fast on a curve or collisions with additional traffic participants, like other cars, pedestrians or road and infrastructure elements. Chapter 3.2 has shown that the critical event rates from different risk sources and types can be added, since at an accident usually only a single risk kicks in.

Here, predictive risk maps are generated by a set of ego trajectories varied by the longitudinal ego velocity as a variation parameter $q = v^0$. This is then a set of trajectories with different constant velocity profiles, as shown in Figure 7.1(bottom right). If a velocity profile through the risk map is planned which differs from the constant velocity profiles used to build the risk map, the risk evaluation is not precise, because a certain position in the risk map is reached within a different time as originally predicted.

In general, planned velocity profiles vary only smoothly and thus do not differ strongly from the velocity profiles used to generate the risk map. In this case the timing error⁴ and its influence on the risk map is sufficiently small to be neglectable. To further reduce this timing error the ego entity's dynamics are considered during the risk map generation. As shown in Figure 7.3, the variation parameter is then the target ego velocity $q = v_{target}^0$. The velocity profiles are generated by a controller adapting the current ego velocity to the target velocity,

$$\frac{dv^0}{dt} = \begin{cases} \text{sign}(v_{target}^0 - v^0) \cdot a_{comf}, & \text{for } v^0 \neq v_{target}^0 \\ 0, & \text{for } v^0 = v_{target}^0 \end{cases} .$$

To completely eliminate the timing error, a large set of ego trajectories/velocity profiles could be sampled under consideration of the system's dynamics to select the best future trajectory. However, on one hand predictive risk maps reduce the computational effort drastically, as only a small set of ego trajectories has to be evaluated and on the other hand, predictive risk maps are highly beneficial to illustrate the situation-based risk evaluation and behavior planning approach presented in this thesis.

⁴For planned velocity profiles, which vary significantly from the trajectories which were used to build the risk map there is an error in the prediction time, when the vehicle will be at a certain position.

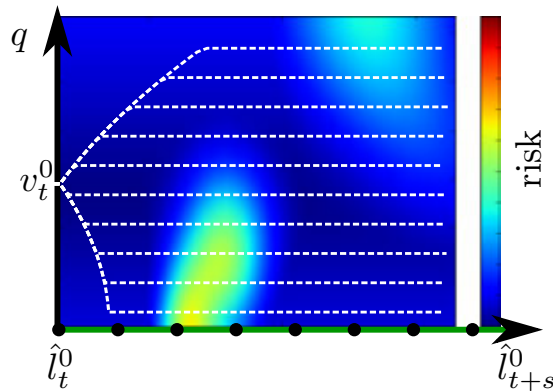


Figure 7.3: Consideration of vehicle dynamics (maximal possible acceleration/deceleration) in the generation of predictive risk maps.

7.1.1 Basic Risk Shapes

By applying the predictive risk map calculation to different complex scenarios, it could be noticed that some characteristic risk patterns appear frequently. Depending on the real constellation, these shapes are usually distorted. First, if another car is predicted to cross the ego car's path, an ellipsoidal risk spot, as shown in Figure 7.4(a), will occur on the risk map with its peak approximately at the ego car velocity and longitudinal path position at which the cars would actually crash. Second, the risk pattern of a car driving in front of the ego car has the shape shown in Figure 7.4(b). High ego car velocities result in high risk, since this would lead to a collision. If the ego car velocity decreases towards the velocity of the leading car the point of collision will be further away in the future and, once the ego car velocity is below the velocity of the leading car, there is no predicted collision anymore and the risk drops to zero. Third, if a car is approaching very fast from behind, there is a similar risk spot as for a leading car. But this time the high risky area is at velocities lower than the other car's velocity, as shown in Figure 7.4(c).

Finally, the risk shape for driving through a curve is shown in Figure 7.4(d). High risk appears for high velocities at locations of high curvature, since the risk is caused by centrifugal forces.

7.2 Conclusion

The focus of this chapter has been on the general problem of risk assessment in dynamic traffic environments for future behavior evaluation. The introduced method to derive so-called predictive risk maps is based on the

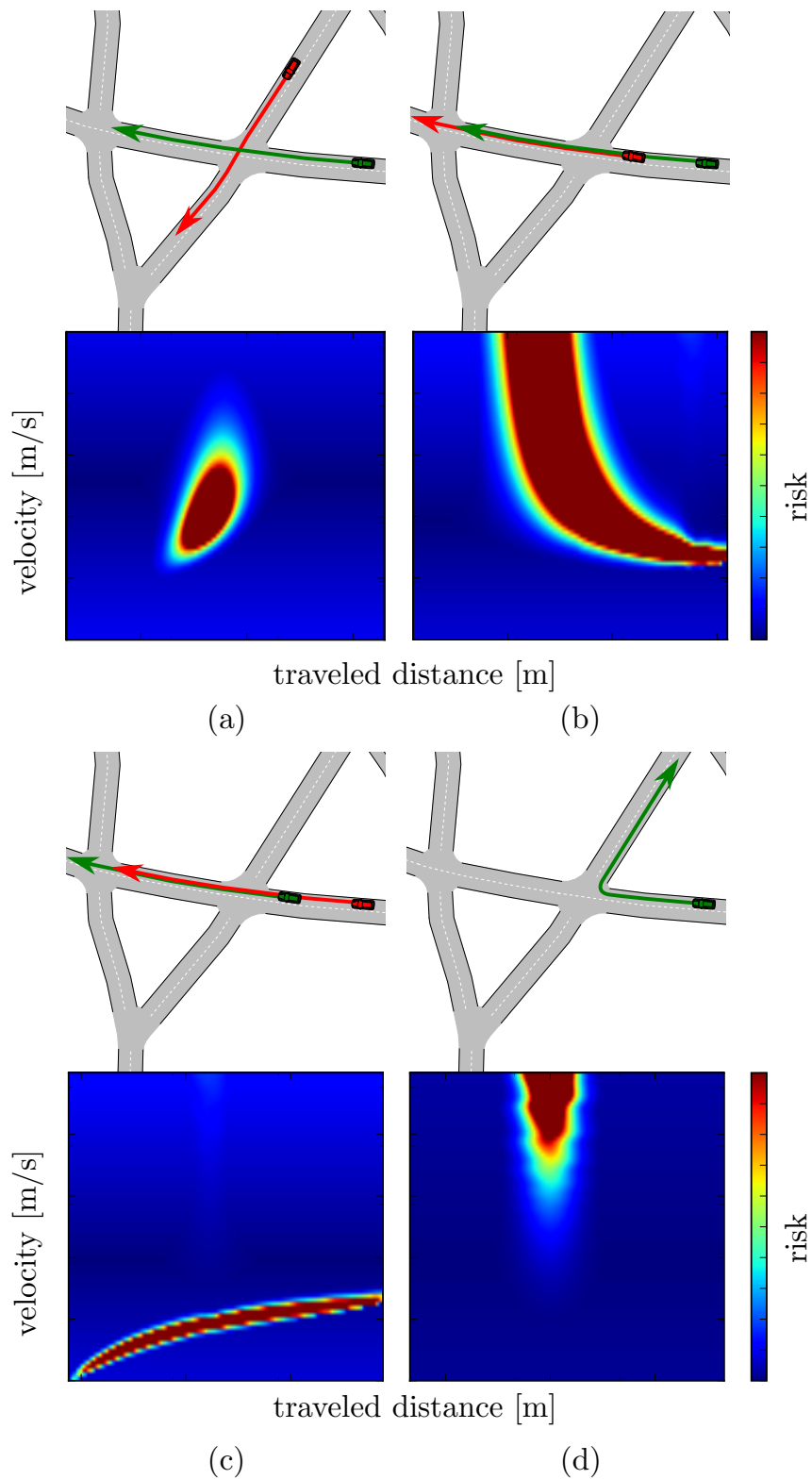


Figure 7.4: Basic risk shapes: (a) Ego car (green) crossing the path of another car (red), (b) following another car, (c) driving in front of another car and (d) passing through a narrow curve.

risk evaluation of a set of possible ego entity behavior alternatives defined by a variation parameter. The predictive risk map is created by evaluating the risk of each future ego behavior variation in relation to the other entities' predicted behaviors. For each considered situation, including the resulting set of predicted behaviors/spatio-temporal trajectories of all involved entities, one predictive risk map is derived. A predictive risk map indicates how risky a certain behavior in a considered situation will be in the future and enables the evaluation of risk-minimizing behavior.

As shown in Chapter 8, by combining the situation-dependent predictive risk maps with a utility function, behavior planning can be achieved by searching for cost-optimized trajectories/velocity profiles across the map. The resulting behavior is then beneficial in terms of risk and utility as long as the map itself is not modified considerably over time. This can be assumed, if re-evaluation times⁵ remain small compared to the time span, for which the prediction of the other entities can be considered as accurate.

Furthermore, the generated predictive risk maps can only be considered as precise, if the planned behavior is similar to one of the behavior variations used to generate the risk map. To reduce this imprecision without increasing the computational effort, the dynamic model of the ego entity is integrated into the generation process of the trajectory variations. The derived predictive risk map is then suitable to plan the ego entity's future behavior. Additionally, predictive risk maps are beneficial to illustrate the entire evaluation and planning process of the general framework for situation-based risk evaluation and behavior planning.

Applying the risk evaluation to different kind of scenarios, such as crossing vehicles at intersections or car following, revealed a set of basic risk shapes. Those risk shapes increase the intuitive understanding of the contributing risk factors in a certain scene.

⁵The time between the re-calculation of predictive risk maps using sensory updated predictions of the involved entities.

8 Behavior Planning

The target of future Advanced Driver Assistance Systems (ADAS) is to relieve the strain on the driver, starting from simple warning systems and comfort functions, such as blind spot information system or parking assistance, up to partially or fully automated driving. This thesis strives for a system that is generally able to securely support driving, especially in inner-city scenarios with multiple behavior alternatives. Traffic scene analysis for inner-city scenarios is inherently difficult, especially if more than a few traffic participants are involved. Current ADAS systems, targeting at inner-city scenarios are either mainly reactive or designed to work under very narrowly defined conditions and therefore not applicable as a general approach for risk-based behavior control.

In complex scenarios, it is unfeasible to evaluate all possible state evolutions of the involved traffic participants. A way to restrict the alternatives is to guide them by the behavioral needs¹ of one of the entities. Still, predictions of the *behaviorally relevant* future dynamics of the regarded entity and of the other traffic participants as well as their relations are required. This then leads to an evaluation of the possible future behavior in terms of risk and utility for the entity in the context of the surrounding traffic participants. Based on such an evaluation, the scope of this chapter is to plan the best possible future behavior in terms of risk and utility.

This chapter makes use of the general method for future risk estimation in dynamic scenes, introduced in Chapter 7. There, situation-dependent predictive risk maps are built by varying the ego car trajectory, defined by a variation parameter. After that, the future risk for this set of ego car trajectories is evaluated. The step of risk estimation itself is based on situation-dependent predictions of prototypical trajectories and a situation classification step, introduced in Chapter 6.

In Section 8.1, the focus lies on behavior planning for a single possible driving situation. In Section 8.2, this is then extended to the case that the situation classification provides several possible situations with uncer-

¹The term *behavioral need* describes the knowledge that is required by the ego entity to determine the own best possible behavior.

tainty, including multiple behavior possibilities of the involved entities. The main contributions of this chapter have been published to the IEEE ITS Society in [27, 30] and patented in [28, 29].

8.1 Behavior Planning under Consideration of a Single Situation

This section introduces first an approach on *how to plan the best future behavior for a single situation*, before advancing to the problem of *how to plan the best behavior for the general case of multiple possible, but competing situations*. A single situation means, that only one prototypically predicted behavior/trajectory per involved entity is considered, which results in a single predictive risk map, indicating how risky a certain behavior will be in the future.

Once the risk of possible behavior alternatives has been evaluated and composed into a predictive risk map, according to Chapter 7.1, the target is to plan the best future behavior, minimizing risk and maximizing utility.

Here, the globally optimizing, sampling-based approach rapidly-exploring random tree (RRT) is applied to obtain the best possible velocity profile through the risk map. More specifically, the extension RRT* is used, which guarantees asymptotic optimality.

In Chapter 5, the Foresighted Driver Model has been introduced, which incorporates a gradient descent-based behavior planning approach to gather a risk-averse future behavior. For simulation and/or prediction purposes a purely local risk minimization is generally sufficient. The drawback of such an approach is the lack of global optimality, which means that in certain constellations the gradient descent approach might run into local minima.

As an example we have a look at a simple turning behavior at intersections. Generally, the velocity has to be reduced in order to reduce the risk, resulting from high centrifugal accelerations when turning. At the same time, there could be a demand for a velocity increase in order to pass with reduced risk in front of a crossing car. This can end up in a constellation, where either the risk of high centrifugal acceleration or the collision risk can not be kept sufficiently small to ensure safe driving. In those cases, a globally optimizing planner is necessary to find a satisfying plan for a future behavior. In this example, slowing down to let the crossing car pass and then performing the turning with reduced velocity, would be a suitable plan for a future behavior that considers both risks adequately.

The following introduces the underlying cost function, combining risk and utility consideration, which the planner tries to minimize by finding the best possible trajectory. After presenting the rapidly-exploring random tree (RRT) and its extension RRT*, the planning algorithm is adapted to the problem of behavior planning in traffic environments.

8.1.1 General Cost Function

The target of the behavior planning stage is to find a behavior that globally minimizes risk and maximizes utility at the same time. For this purpose, the predictive risk map $R(\dots)$ is combined with a utility cost function, here travel costs $\text{TC}(\dots)$, resulting in the differential costs²

$$\text{DCost}(l_{t+s}^0, v^0, \mathbf{x}_t, h_t) = R(l_{t+s}^0, v^0, \mathbf{x}_t, h_t) + \text{TC}(l_{t+s}^0, v^0) .$$

The travel costs can be used to describe soft constraints and optimization criteria, such as time and smoothness of travel. As a simple travel cost function, $\text{TC}(l_{t+s}^0, v^0)$ is used to penalize deviations from a desired travel velocity v_{des}^0 ,

$$\text{TC}(l_{t+s}^0, v^0) = \text{TC}_0 + m |v_{des}^0 - v^0| ,$$

with a slew rate m and the minimal travel cost at the desired velocity TC_0 . In this way, the system is forced to move away from the (usually) lower risk solutions for zero velocity, arriving at solutions that balance travel costs and risk.

For one ego velocity profile $v^0(l')$ and a path of length l_{t+s}^0 , the costs integrated over the entire trajectory are

$$\text{Cost}(l_{t+s}^0, \mathbf{x}_t, h_t) = \int_0^{l_{t+s}^0} \text{DCost}(l', v^0(l'), \mathbf{x}_t, h_t) dl' . \quad (8.1)$$

In the following a sampling-based planning approach is presented, which generates a variety of ego velocity profiles where each is evaluated according to (8.1). A suitable solution for the future ego behavior should minimize both, risk and travel costs, accumulated over the future trajectory. Consequently, the planning approach is applied to find such a globally

²The differential costs represent the costs at a certain position along a given trajectory. This is then later used to derive the integral costs over the trajectory.

optimal solution.

8.1.2 Rapidly-exploring Random Tree (RRT)

The rapidly-exploring random tree (RRT) algorithm was first introduced in [79]. It is an efficient algorithm to search non-convex spaces constructing a space-covering tree by randomly sampling and forward simulation using the system's dynamic model and kinematic constraints. Starting from an initial state as a root vertex the RRT constructs open-loop trajectories for any kind of non-linear systems with state constraints.

The complexity of the dynamic model with kinematic constraints is not a restriction for the used RRT algorithm. Similar to [64], double integrator dynamics with input and state constraints (maximal acceleration, deceleration a_{max} and maximal velocity v_{max}) are used longitudinally for the dynamics of the ego car,

$$\begin{aligned} l_{t+s}^0 &= v^0, \\ \dot{v}^0 &= a^0, \end{aligned}$$

with $|v^0| \leq v_{max}$ and $|a^0| \leq a_{max}$.

The general RRT algorithm is originally designed to rapidly cover the state space (here the risk map) and is not intended to be used as a planning algorithm. Nevertheless, by defining a target region, the RRT can be used for planning purposes. Every path through the constructed tree reaching the target region defines a solution trajectory for the system from the starting region to the target region.

The basic procedure is shown in Algorithm 1, where G is the RRT tree containing *vertices* (here e.g. in the (l_{t+s}^0, v^0) -plane of the risk map as introduced in Chapter 7) and *edges*. The main part of the algorithm is the **Extend** procedure in Algorithm 2, which defines how the tree is extended towards the sampled vertex z_{rand} .

In Algorithm 2, a so-called **Steer** function constructs a trajectory from the nearest vertex $z_{nearest}$ of the RRT towards the randomly sampled vertex z_{rand} by an internal forward simulation, using the dynamic model of the system. It is not required that the sampled vertex z_{rand} has to be reached. However, the finally reached vertex z_{new} is added to the tree. As a result, a tree of reachable trajectories is created, considering the systems dynamics and constraints.

In [64], a time optimal controller is applied to from the nearest vertex $z_{nearest}$ to the randomly sampled vertex z_{rand} . The resulting trajectory

Algorithm 1 RRT

```

1: procedure RRT
2:    $G.\text{init}(z_{\text{init}})$ 
3:   while  $i < N$  do
4:      $z_{\text{rand}} \leftarrow \text{Sample}(i)$ ;
5:      $G \leftarrow \text{Extend}(G, z_{\text{rand}})$ ;
6:      $i \leftarrow i + 1$ ;
7:   return  $\text{CheapestTrajectory}(G, \text{target\_region})$ 

```

Algorithm 2 Extend RRT

```

1: procedure EXTEND( $G, z_{\text{rand}}$ )
2:    $z_{\text{nearest}} \leftarrow \text{Nearest}(G, z_{\text{rand}})$ ;
3:    $z_{\text{new}} \leftarrow \text{Steer}(z_{\text{nearest}}, z_{\text{rand}})$ ;
4:    $G.\text{add\_vertex}(z_{\text{new}})$ ;
5:    $G.\text{add\_edge}(z_{\text{nearest}}, z_{\text{new}})$ ;
6:   return  $G$ 

```

would be a sequence of maximal acceleration and deceleration, which is not suitable for the purpose of this chapter, namely the velocity control of a vehicle acting in a traffic environment.

Assuming double integrator dynamics, the controller used in the presented approach determines a constant acceleration/deceleration, such that the target state (longitudinal position and velocity) is reached by,

$$a^0 = \frac{v_{\text{init}}^0(v_{\text{trg}}^0 - v_{\text{init}}^0) + \frac{1}{2}(v_{\text{trg}}^0 - v_{\text{init}}^0)^2}{l_{t+s,\text{trg}}^0 - l_{t+s,\text{init}}^0}, \text{ with } \begin{cases} l_{t+s,\text{trg}}^0 \geq l_{t+s}^0 \\ v^0 \geq 0 \\ v_{\text{trg}}^0 \geq 0 \end{cases}.$$

a^0 is the acceleration used as the input signal for the dynamic vehicle model. $l_{t+s,\text{trg}}^0$ and v_{trg}^0 are the longitudinal position and velocity of the target vertex, and $l_{t+s,\text{init}}^0$ and v_{init}^0 the position and the velocity of the starting vertex.

8.1.3 Asymptotic Optimal Extension RRT*

As stated in [64], the RRT algorithm used for kinodynamic³ planning with consideration of a cost function does not guarantee asymptotic optimality.

³Kinodynamic motion planning describes a class of planning problems, where kinematic constraints, such as avoiding obstacles, and dynamics constraints, such as bounds on velocity, acceleration, and force, have to be fulfilled simultaneously.

Since the target is to find a trajectory through the predictive risk map, minimizing a risk and maximizing utility, the RRT* extension [64] of the RRT is applied. This extension enables asymptotic optimality by re-wiring the constructed tree based on a considered cost function.

For this purpose, the **Extend** function is enhanced, as shown in Algorithm 3. From line 6 to 11, all connections from nearby vertices Z_{nearby} to the new vertex z_{new} are checked and the connection with minimal cost z_{min} is added to the tree G . Additionally, from line 13 to 19 all connections from the new vertex z_{new} to nearby vertices Z_{nearby} are checked and if a connection with costs less than the original cost is found, z_{new} is made the new parent of z_{near} . The original RRT* also checks for collision while extending the tree. As collisions are represented in a continuous cost function in terms of risk, collision checking is not considered.

Algorithm 3 Extend RRT*

```

1: procedure EXTEND( $G, z$ )
2:    $z_{nearest} \leftarrow$  Nearest( $G, z$ );
3:    $z_{new} \leftarrow$  Steer( $z_{nearest}, z$ );
4:    $G.add\_vertex(z_{new})$ ;
5:    $z_{min} \leftarrow z_{nearest}$ ;
6:    $Z_{nearby} \leftarrow$  NearVertices( $G, z_{new}$ );
7:   for all  $z_{near} \in Z_{nearby}$  do
8:      $z_{new,temp} \leftarrow$  Steer( $z_{near}, z_{new}$ );
9:     if State( $z_{new,temp}$ ) = State( $z_{new}$ ) then
10:      if Cost( $z_{near,temp}$ ) < Cost( $z_{new}$ ) then
11:         $z_{min} \leftarrow z_{near}$ ;
12:    $G.add\_edge(z_{min}, z_{new})$ ;
13:   for all  $z_{near} \in Z_{nearby} \setminus \{z_{min}\}$  do
14:      $z_{near,temp} \leftarrow$  Steer( $z_{new}, z_{near}$ );
15:     if State( $z_{near,temp}$ ) = State( $z_{near}$ ) then
16:       if Cost( $z_{near}$ ) > Cost( $z_{near,temp}$ ) then
17:          $z_{parent} \leftarrow$  Parent( $z_{near,temp}$ );
18:          $G.remove\_edge(z_{parent}, z_{near})$ ;
19:          $G.add\_edge(z_{new}, z_{near,temp})$ ;
20:   return  $G$ 

```

8.1.4 Adaptation of RRT* to Velocity Planning in Traffic Environments

The planning algorithms RRT and RRT* are already applicable to find a risk minimizing and utility maximizing behavior in form of velocity profiles through the risk map. In order to improve the general RRT* algorithm for behavior/velocity profile planning, prior knowledge is included as shown in Algorithm 4.

On one hand, this is done by incorporating predefined “typical” trajectories, which should always be considered by the planner as a possible solution, e.g. the safety solution of full braking at a largest possible deceleration.

On the other hand a bias towards low risk areas is included in the sampling procedure and the target region of the planner is adapted to allow “stop and wait” solutions (i.e., regions with zero or near-zero velocities).

Predefined Trajectories

As the RRT* algorithm is based on random sampling and an internal forward simulation, it cannot be ensured that a suitable trajectory/velocity profile can always be found within limited computation time. However, some trajectories, such as full braking, should always be considered in the planning process. Thus, to ensure the presence of such trajectories, they are added to the initial tree, before constructing the entire tree, as indicated in Algorithm 4. For this purpose, the initial vehicle state and the dynamic model are applied in an internal forward simulation.

In the presented approach, two categories of predefined trajectories are considered, emergency trajectories and comfort trajectories. When planning in the comfort region, $a_{max} = a_{max,comfort}$ is used for the dynamic

Algorithm 4 Predictive-Risk-RRT

```

1: procedure PREDICTIVE-RISK-RRT
2:    $G$ .init( $z_{init}$ );
3:    $G$ .add_init_trajectories( $z_{init}$ );
4:   while  $i < N$  do
5:      $z_{rand} \leftarrow$  RiskBiasedSample(RiskMap);
6:      $G \leftarrow$  Extend( $G, z_{rand}$ );
7:      $i \leftarrow i + 1$ ;
8:   return CheapestTrajectory( $G$ , target_region)

```

model in the forward simulation. However, to enable emergency trajectories, $a_{max} = a_{max,total}$, with $a_{max,total} > a_{max,comfort}$ is set, to allow the full solution space of the dynamic system. The predefined trajectories are shown in Figure 8.1.

Emergency Braking and Emergency Acceleration The emergency braking and emergency acceleration trajectories enable the planner to always find full braking and full acceleration as a solution. Since emergency trajectories are no longer in the comfortable acceleration region, the costs are increased by a penalty factor b so that $DCost_{emergency}(l_{t+s}^0, v^0) = b \cdot DCost_{comfort}(l_{t+s}^0, v^0)$ with $b > 1$, in order to avoid an unnecessary execution of those trajectories.

Comfort Braking, Comfort Acceleration, Constant Velocity and Coasting Down The constant velocity trajectory enables the planner to always consider a straightforward solution. Without the constant velocity trajectory, keeping the velocity constant, is not consistently a solution, when considering limited computation time. As a consequence, highly

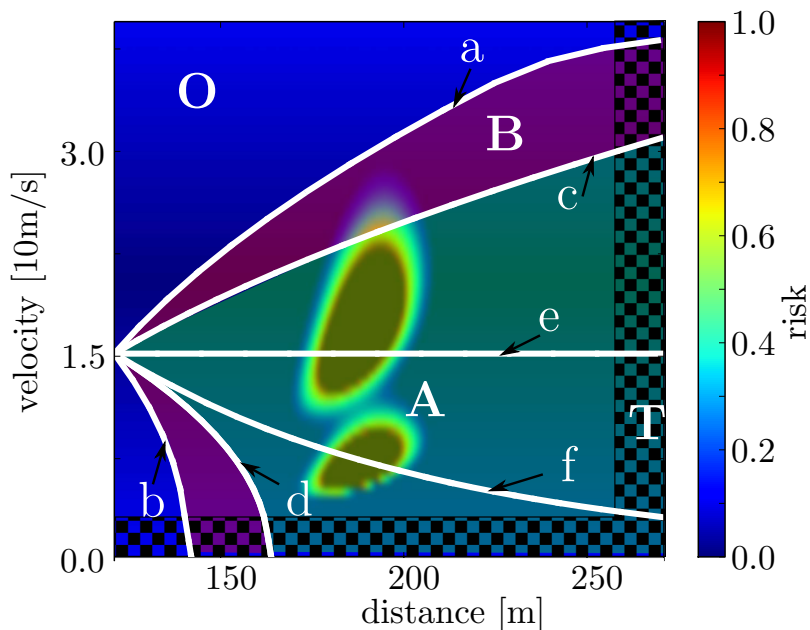


Figure 8.1: Predictive risk map. Predefined trajectories: (a) emergency acceleration, (b) emergency braking, (c) comfort acceleration, (d) comfort braking, (e) constant velocity and (f) coasting down. Regions: Comfort region (A, green), emergency region (B, violet), not reachable region (O, clear blue) and target region (T, checkerboard).

varying acceleration and deceleration might occur. A similar solution is given by the coasting down trajectory, which helps the planner to consider a coast-down for slow braking. The comfort braking and comfort acceleration trajectories define the borderline of the comfort zones, as shown in Figure 8.1, and enable the planner to faster cover the whole comfort region with comfortable solution trajectories.

As the RRT* re-wires its connections according to the cost function, a predefined comfort trajectory is usually adapted for a better fit to the risk map topology by the algorithm, avoiding risky regions.

Target Region

The aim of the algorithm is to find a trajectory from the initial state (on the left of the risk map) through the risk map to the furthest point on the future path (on the right of the risk map) with minimal cost.

Nevertheless, for the case of a crowded intersection or a red traffic light, where the ego vehicle has to stop, there is no direct trajectory through the predictive risk map with sufficiently low costs. The favored solution in terms of risk and utility would be to stop and wait until the environment changes. Thus, the target area, as shown in Figure 8.1, is the complete right area of the risk map representing the furthest predicted point along the longitudinal path and the complete area at the bottom of the risk map, representing all possible stop location along the future path. This can be extended further to include preferred stopping zones.

By including the stopping area as a target region, the problem arises that the traveled distance may be shorter if the trajectory is finalized at the stopping area, leading to overall lower costs. To overcome this problem, for all trajectories that reach a target region, the cost function $\hat{\text{Cost}}_{norm}$ is normalized by the traveled distance, such that

$$\hat{\text{Cost}}_{norm}(l_{t+s}^0, \mathbf{x}_t, h_t) = \frac{1}{l_{t+s}^0} \int_0^{l_{t+s}^0} [\text{R}(l', v^0(l'), \mathbf{x}_t, h_t) + \text{TC}(l', v^0(l'))] dl'.$$

Biased Sampling

During each execution cycle of the entire system for situation-based risk evaluation and behavior planning, as introduced in Chapter 4, a renewed predictive risk map is calculated before running the actual RRT-based planning procedure. The predictive risk map indicates how risky certain

risk map areas are. Knowing that the target is minimizing risk, the probability of sampling in risky areas is reduced by introducing a bias to the sampling procedure, such that areas with low risk are sampled more often than areas with high risk. As a result, a better coverage of low risk areas by the tree is achieved with the same computational effort. Additionally, sampling more often in the target region, generally speeds up the solution finding [21].

8.1.5 Simulation Results

Based on the predicted future dynamics of scene entities, expressed in terms of spatio-temporal trajectories, the future cost (comprising risk and other additional travel costs) can be predicted for certain behavior alternatives (here shown for ego car velocity profiles). By generating predictive risk maps, the system is able to plan a cost-optimal future behavior using a sampling-based globally optimal planning algorithm. As the system acts in a dynamically changing environment, it has to reevaluate and replan from time to time. In order to validate the approach, it is applied to a set of different simulation scenarios, including inner-city and highway scenarios.

Risk Aversive Curve Driving

In the scenario shown in Figure 8.2, the ego car drives along a curvy road, which consists basically of four main curves with different radii. As described in the previous section, the risk for driving through a curve is based on the predicted lateral acceleration. Each curvy segment generates risky areas, raising at a certain velocity. As shown in Figure 8.2, the behavior planner chooses a velocity profile that reduces risk in all of the upcoming curves in order to drive safely, but still efficiently along the road. Major risk sources are marked by circled numbers. Each risk map has a horizon range up to 150 m.

Risk-Aversive Intersection Behavior

Next, the approach is applied to the scenario shown in Figure 8.3, where the ego car (green trajectory) is intended to drive safely straight over an intersection with multiple other crossing traffic participants. The predictive risk map shows a risk peak for each traffic participant. The behavior planner constructs a velocity profile through the risk map while minimizing risk and maximizing utility. It can be seen in the velocity profile that

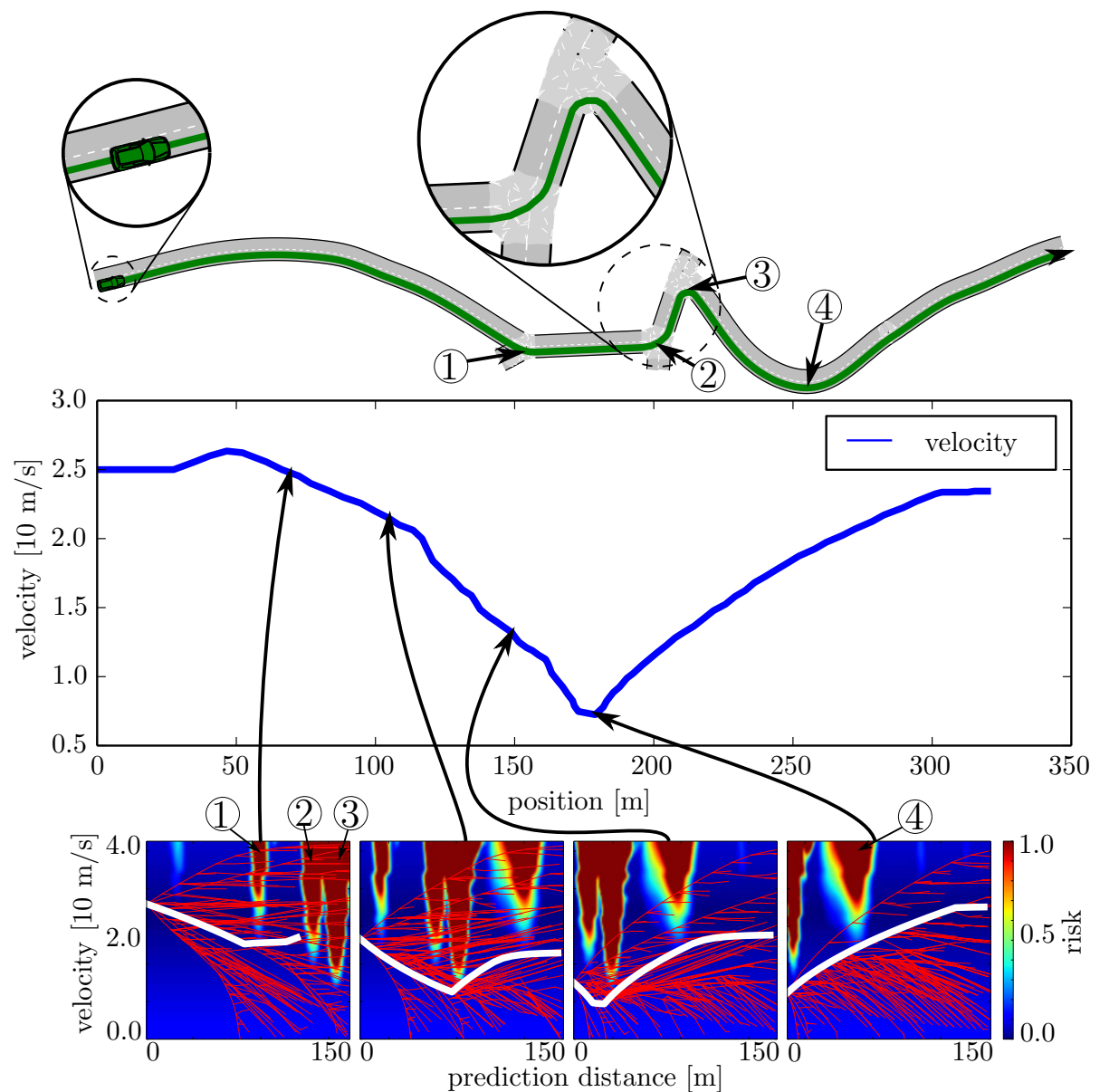


Figure 8.2: Curve driving behavior: The ego car (green) drives along a route (green path) with several curvy segments (1-4). Each curvy segment results in a risk area in the predictive risk map shown at different planning points in time while driving along the route (bottom). The constructed RRT (red) is overlaid on each risk map, where the best trajectory (white) is highlighted. The actually driven velocity profile (middle) shows a decelerating behavior, when approaching the different curves, to minimize risk while maximizing utility. The behavior planner especially targets curve segment (3), which is of highest curvature, in a foresighted manner.

the ego car slows down to let the first car pass and then speeds up to pass in front of the second car, as there is enough space to pass safely.

Risk Aversive Highway Access Behavior

In this scenario the ego car is approaching the access of a highway. Each approaching car on the highway generates a risk spot in the predictive risk map. The behavior planner determines if the gap between the first and the second car is sufficiently large for a low-risk highway access. As shown in Figure 8.4, the resulting velocity profile consists of speeding up to reach the gap, then slowing down to the same velocity of the other cars on the highway to follow the general traffic flow.

Risk Aversive Turning Behavior for Complex Intersections with Multiple other Traffic Participants

The scenario from Figure 8.5 shows a crossing, where the ego car is planning to turn left. There are four other traffic participants approaching the crossing. One car is approaching from the opposite direction planning to turn right onto the same lane as targeted by the ego car. Three other cars are approaching from the right, one driving straight and two turning left. Each of those cars generate a risk spot in the risk map. The turning process combines intersection driving with curve driving, thus a further risk spot for high velocities is caused by the curve. The behavior planner determines the velocity profile, shown in Figure 8.5, which comprises stopping at the intersection to let the other cars cross, then driving with reduced velocity through the curve, and finally speeding up to reach the desired travel velocity.

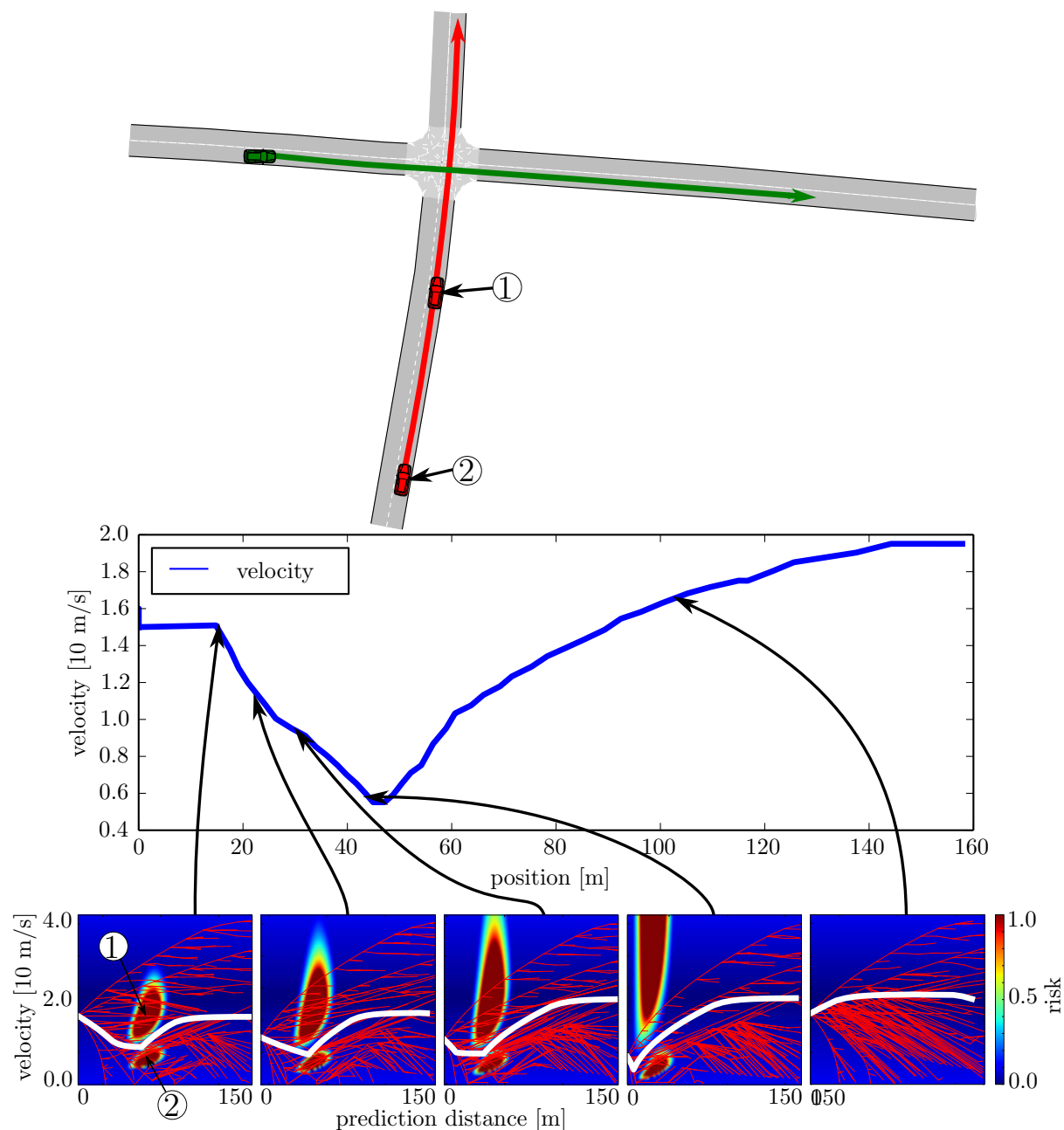


Figure 8.3: Basic intersection behavior: The ego car (green) approaches an intersection, where it has to give way to two oncoming other cars (red). Each of the other cars results in risk spots (1,2) in the predictive risk maps, shown at different planning points in time (bottom). The ego car plans to pass between the two other cars, as shown by the planned velocity profiles in the risk maps (bottom, white). As a result the driven velocity profile (middle) shows a decelerating behavior to fit through the gap between the other cars, followed by an accelerating behavior to quickly get out of the intersection and reach the desired travel velocity.

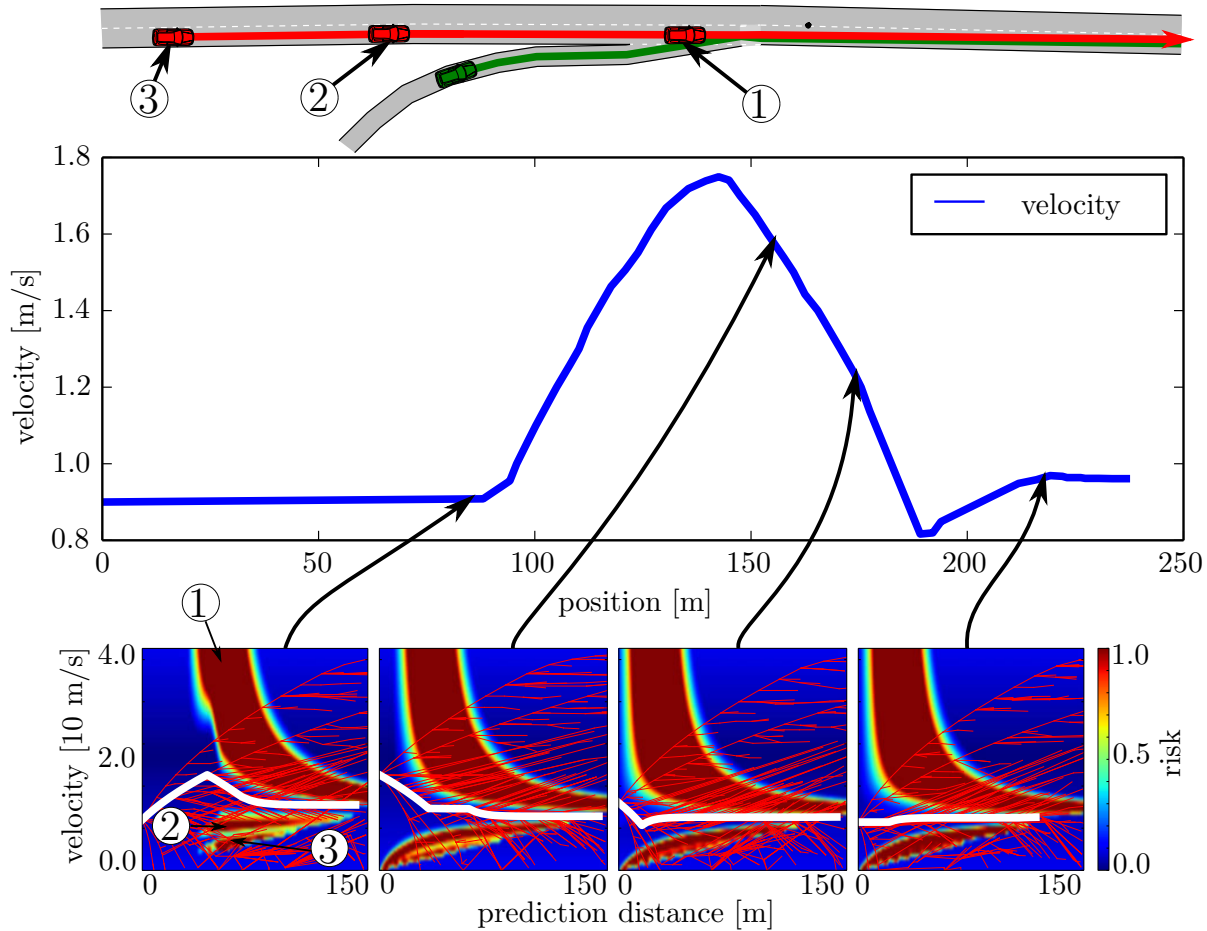


Figure 8.4: Highway access behavior. The ego car (green) accesses a highway, on which three other cars (red) are driving on the right lane. Each other car results in a risk area (1-3). The behavior planner chooses to access the highway between the first and the second car. For this purpose, the ego car first accelerates to reach the chosen gap, followed by a deceleration to adapt its velocity to the traffic flow. This is visible in the planned velocity profiles (white) of the risk maps (bottom), as well as in the actually driven velocity profile (middle).

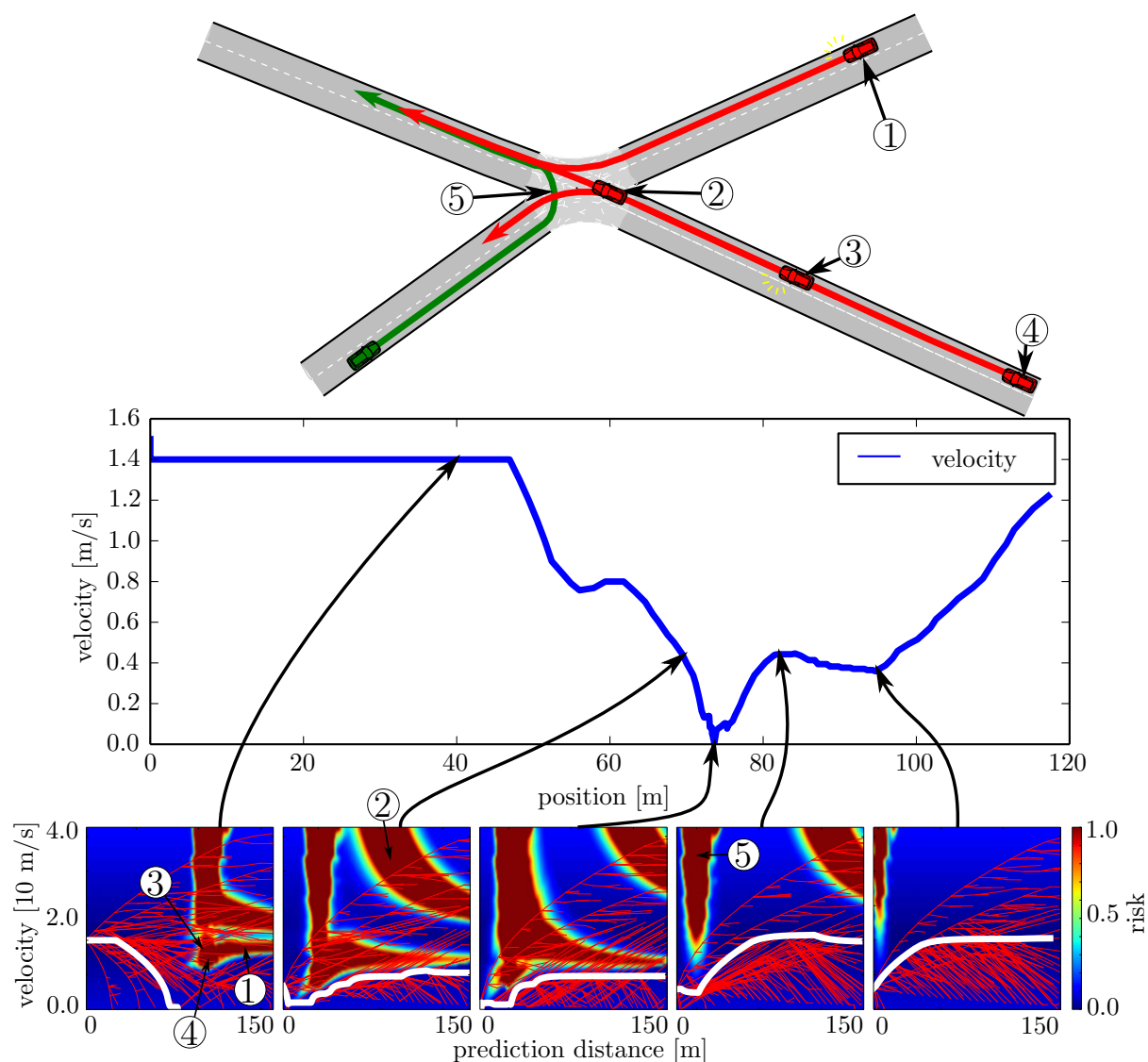


Figure 8.5: Complex turning behavior: The ego car (green) approaches an intersection and plans to turn left. Several other cars (red) to which the ego car has to give way are approaching in the meantime. Car (1) has set the indicator to turn right. Car (2) and (4) plan to drive straight over the intersection, whereas car (3) has set the indicator to turn left. Each of the other cars constitute a risk source (1-4) for the ego car. As the ego car is about to turn left, the curve segment is another risk source (5), which has to be considered. All risk sources (1-5) form the predictive risk maps, shown at different planning points in time (bottom). The planned velocity profiles (white) overlaid over the risk maps, as well as the actually driven velocity profile (middle) show an ego behavior, of stopping at the intersection to let the other cars pass, as there is no sufficient gap in between the other cars to pass through. Once the intersection is clear, the ego car turns with reduced velocity, to minimize the risk of skidding in the curve segment, followed by an acceleration to the desired travel velocity.

8.2 Behavior Planning under Consideration of Multiple Situations with Uncertainty

So far, a highly confident situation classification has been considered, providing only a single situation. Hence, the risk evaluation is purely based on one prototypical state evolution of the scene and thus the consideration of only one prototypical behavior alternative for each entity⁴. In general, the situation classification shows a certain amount of uncertainty resulting in a set of multiple possible but competing situations with different occurrence probabilities. This uncertainty arises e.g. from the uncertainty in the estimation of a considered entity's future decision, such as *will it turn left or right at an intersection*.

This causes the main problem of how to plan the best future behavior for the case that multiple possible but competitive situations arise. Incorporating every possible behavior alternative of the involved entities, the system might end up foreseeing risk everywhere and no safe or only highly inefficient future behavior can be found. In contrast, by neglecting situations with high risk and low probability the system might end up in constellations inevitably leading to a crash.

Thus, an approach is presented, where the general future behavior is planned mostly under consideration of highly probable situations, which provides an efficient behavior in those situations. Situations with lower probability are also incorporated in the behavior, but with less influence. Then, the behavior is checked on each possible situation for risky constellations and a safe “plan B” is applied to avoid such risky states in case those unlikely situations occur.

8.2.1 Approach

Each considered situation results in one prototypically predicted, spatio-temporal trajectory for each involved traffic participant. Based on those situation-dependent, predicted trajectories one predictive risk map is calculated for each situation according to Chapter 7. Additionally, the situation classification, introduced in Chapter 6, estimates for each considered situation the likelihood to occur. In detail, this means evaluating the likelihood that the involved entities will behave as assumed by the different situations.

⁴For this assumption, the rough longitudinal behavior, e.g. stopping at intersection, and the chosen spatial path of each entity have to be known in advance.

The aim is now to find a future spatio-temporal trajectory that is of low risk but still assures high utility for the finally occurring situation, which can only be estimated with uncertainty at the time of behavior planning.

The safest way would be a behavior, that minimizes risk in all possible situations, which can be understood as max-combining the risk maps of all possible situations without taking the situation occurrence probability into account. By simply combining the risk maps, the system might foresee risk everywhere and possibly no safe future trajectory can be found. If a future trajectory can be found, the resulting behavior would avoid all risky areas in all situations, also in unlikely situations, and would consequently be very safe and defensive, but in general also of low utility.

The most efficient way would be to only take the most probable situation into account and plan the future trajectory on this risk map. If this situation actually occurs, the system provides the most efficient future behavior. However, in case another situation with lower probability occurs, the system might end up in a state, where a crash is inevitable. This happens as situations with lower probability but possibly of high risk are not considered in the planning of the future behavior in this case.

Here, as shown in Figure 8.6, an approach is proposed that provides safe and efficient future trajectories taking all possible situations into account. The situation classification approach presented in Chapter 6 provides relevant situations and their respective occurrence probabilities. The trajectory prediction generates situation-dependent, prototypical, spatio-temporal trajectories, one for each considered entity. The risk evaluation step, introduced in Chapter 7, uses those predicted spatio-temporal trajectories to generate one predictive risk map for each situation. Hence, the input of the behavior planning step consists of a **set of predictive risk maps**, one for each situation and each **situation's occurrence probability**.

The trajectory/velocity profile planning phase itself consists of the following steps.

1. First a **combined risk map of all relevant situations is calculated**, to find a desired future behavior.

By simply summing up the risk maps weighted by the corresponding probability $\sum_{h_t \in \mathbb{H}_t} R(l_{t+s}^0, v^0, \mathbf{x}_t, h_t) \cdot P(h_t | \mathbf{x}_t)$ the problem occurs, that an increasing number of similarly probable situations results in a decrease of the situation occurrence probabilities. As the risk is weighted by the situation's occurrence probability the overall risk would be quite low, compared to the utility costs used during plan-

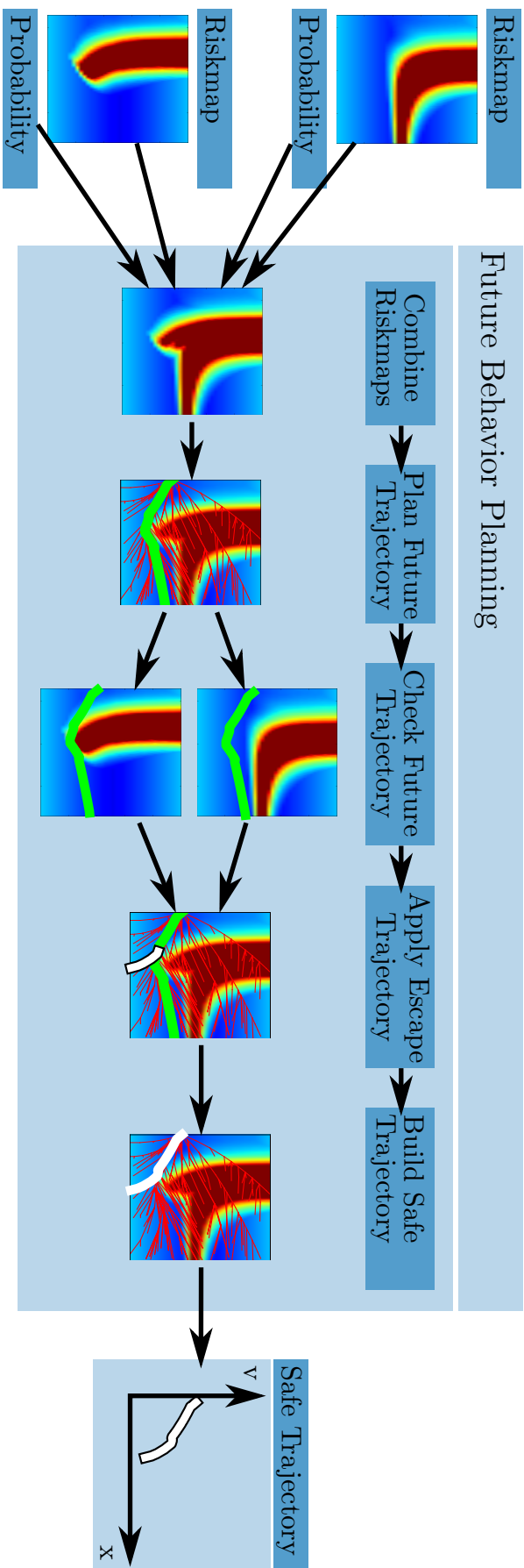


Figure 8.6: Planning of safe and efficient future behavior: Scenario with two active situations with different probabilities, generating 2 risk maps. Both risk maps are then weighted with their situation occurrence probability and combined into one risk map, which is then used to plan the future behavior. The resulting future trajectory is then checked for risk threshold violations in each situation and escape trajectories are applied. As a result, an efficient safe trajectory is achieved by using the planned future trajectory with the earliest necessary escape trajectory.

ning, but widely spread. This results in an unsuitable behavior, which would focus on the optimization of utility and highly neglecting the resulting risk. In contrast, in such a case one would expect high overall risk as this indicates a highly uncertain situation classification.

Therefore, in this approach the combined risk map is normalized by the maximal probability value of all involved situations. Normalizing the probabilities by the maximal probability has the desired effect, that the situation with highest probability is fully taken into account and, in case of an uncertain situation classification (with many equally likely situations) the system encounters an overall high risk. Thus we obtain the combined risk map

$$R_{comb}(l_{t+s}^0, v^0, \mathbf{x}_t) = \frac{\sum_{h_t \in \mathbb{H}_t} R(l_{t+s}^0, v^0, \mathbf{x}_t, h_t) \cdot P(h_t | \mathbf{x}_t)}{\max_{h_t} (P(h_t | \mathbf{x}_t))}.$$

2. In a second step, the RRT*-based behavior planning approach, introduced in Section 8.1, is applied to find a **future trajectory** (velocity profile $v^0(l)$) through the risk map, that minimizes risk and maximizes utility. The cost function for the multi-situation case is

$$\text{Cost}(l_{t+s}^0, \mathbf{x}_t) = \frac{1}{l_{t+s}^0} \int_0^{l_{t+s}^0} \text{DCost}(l, v^0(l), \mathbf{x}_t) dl,$$

with

$$\text{DCost}(l_{t+s}^0, v^0, \mathbf{x}_t) = R_{comb}(l_{t+s}^0, v^0, \mathbf{x}_t) + \text{TC}(l_{t+s}^0, v^0).$$

The RRT* based behavior planning approach generates a future trajectory by globally minimizing a cost function (risk and utility), while taking the dynamical model of the entity and its physical constraints into account.

3. As the future trajectory is planned by optimizing mainly for highly probable situations, the planned trajectory might be of high risk in improbable situations. In terms of utility it makes sense to consider situations with high probability more than situations with low probability. But in case a situation with low probability suddenly kicks

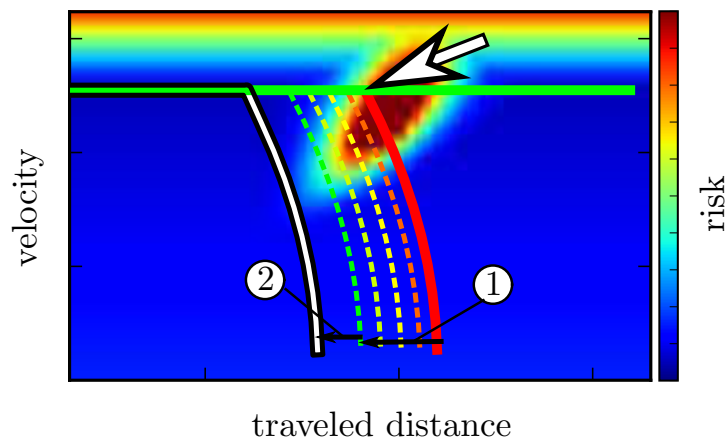


Figure 8.7: Application of escape trajectory. Starting from the risk threshold violation (white arrow) of the originally planned trajectory (green line), the execution point is shifted backwards along the path (1), while checking if a safe execution of the escape trajectory is possible. Once a safe execution point is found (green escape trajectory), an additional safety time gap t_{safety} is considered (2), resulting in the escape trajectory (white escape trajectory), which is finally applied to the planned future path. The final future plan (black outline) consists of two parts, the desired future behavior (green with black outline), followed by an escape trajectory (white with black outline).

in, the system might encounter inevitably high risks, e.g. collisions. In order to solve this problem **the future trajectory is verified on each unweighted risk map** without taking the situation occurrence probability into account. This means, for each situation assuming that it will occur, the planned future trajectory is checked for states of high risk which potentially occur when applying the planned behavior. For this purpose a maximal acceptable risk threshold is defined. As shown in Figure 8.6, the planned future trajectory is applied to each situation-dependent risk map and checked for the earliest encounter of a threshold violation.

4. If such a risk threshold violation of the planned future trajectory is detected in a certain situation, an **escape trajectory is applied** to the originally planned future trajectory, such that the final trajectory is not violating the threshold for acceptable risk and such that the escape trajectory kicks in the latest possible along the planned trajectory. Here, emergency braking is used as an escape trajectory.

Therefore, as shown in Figure 8.7, starting from the point of the first risk threshold violation, the escape trajectory is applied and checked if a threshold violation is encountered. As long as there is

still a threshold violation the escape trajectory is shifted backwards in predicted time, along the planned trajectory, until the application of the escape trajectory provides a safe behavior.

5. As a result, a **safe future trajectory** is achieved, in which the first part consists of the planned future trajectory based on the combined risk map incorporating the situation probabilities. This part is executed until the latest possible but earliest necessary state of performing the escape trajectory to avoid a risk threshold violation in any of the still possible situations is reached. The second part consists of the escape trajectory.

In Section 8.1, only one situation/setting of behavior alternatives has been used. Thus, for risk evaluation and behavior planning, only one prototypical future spatio-temporal trajectory for each traffic scene entity has been taken into account.

This section targets the problem that each other traffic participant has several possibilities to behave, meaning that the system has to cope with multiple uncertain situations.

Most of the time, unlikely but risky situation for which the escape trajectories are applied do not occur. The entire system runs in a loop, reevaluating and replanning in every cycle similar to a model predictive control strategy. As a consequence, the escape trajectory part of the plan is usually not executed. However, in case that an unlikely, risky situation occurs, the applied escape trajectory serves as “plan B” to keep the system in a safe state.

8.2.2 Results

To show the ability of the presented approach to produce efficient but still safe trajectories, it is applied to an intersection scenario (see Figure 8.9(a)). Here, the ego car (green) and another car (red) are approaching a crossing. Due to the left-yields-to-right traffic rule, the other car has to give way to the ego car. However, the other car eventually overlooks the ego car and crosses the intersection.

In this scenario two possible situations are modeled:

- The other car recognizes the ego car, lets it pass and crosses behind (other stopping).
- The other car does not recognize the ego car and violates the left-yields-to-right-rule (other not stopping).

The behavior is evaluated for the following four cases to show how our system copes with a correct and a false situation classification, where $\checkmark/\not\checkmark$ indicates a correct/false situation expectation:

| expected \ occurring | other stopping | other not stopping |
|----------------------|-------------------------|---------------------|
| | other stopping | Case 1 \checkmark |
| other not stopping | Case 3 $\not\checkmark$ | Case 4 \checkmark |

In general, the situation classification system (see Chapter 6) estimates the occurrence probabilities of all considered situations. However, to evaluate how a correct or incorrect situation classification affects the behavior planning, a probability setting for each case is modeled by hand as a function of the other car's distance to the intersection, as shown in Figure 8.8.

Case 1

The first case, shown in Figure 8.9, represents the general case, where the other car actually follows the rules and gives way, while the ego car expects correctly the other car to give way. This results in a high initial probability for the situation *other stopping*, which increases further when the other car comes closer to the intersection. The probability for the situation that the other car overlooks the ego car, namely *other not stopping*, is low and decreases further.

The risk map for *other stopping* (Figure 8.9(d), top) is of low risk, whereas the risk map for *other not stopping* (Figure 8.9(d), bottom) contains high risk around a certain velocity and position on the ego car path.

The combined risk map is dominated by the risk map for the situation with highest probability *other stopping*, while *other not stopping* is only marginally included. The resulting future velocity profile exhibits almost constant speed without deceleration.

The planned trajectory is then checked on each single situation. At planning time $t = 0s$, a risk threshold violation for *other not stopping* is detected, which results in an incorporation of an emergency braking trajectory to the originally planned trajectory to satisfy the risk conditions for this situation.

As the other car behaves as expected and brakes, the risk spot in the situation *other not stopping* decreases. Keeping the velocity constant at planning times $t = [2,4,6]s$ is not violating any risk threshold anymore and as a consequence, the planned emergency braking is never executed.

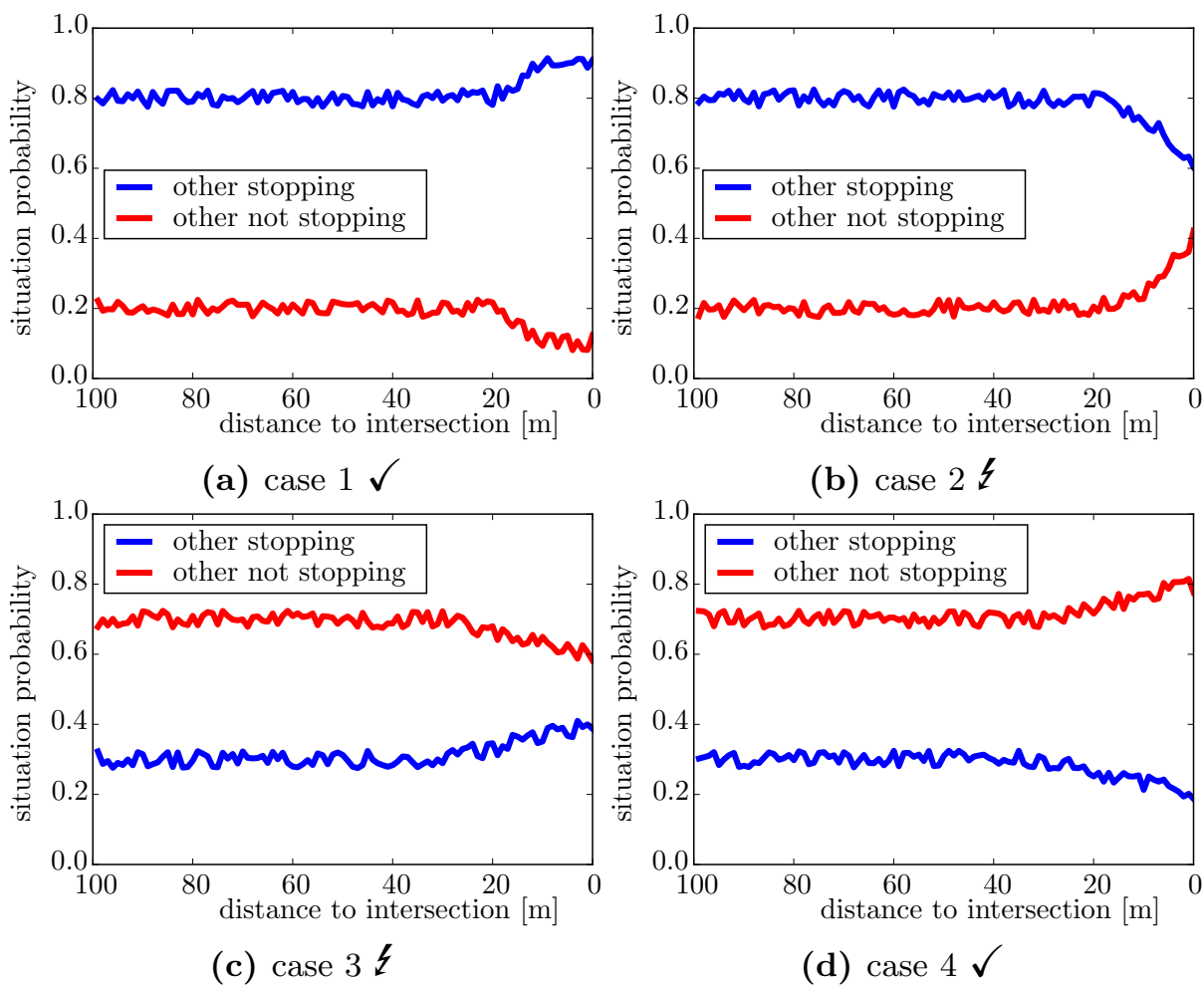


Figure 8.8: Situation occurrence probabilities, modeled by hand as a function of the distance to the intersection, for each case of the situations *other car stopping* (blue) and *other car not stopping* (red). The situation classification in (a) and (b) expects with high probability that the other car stops, whereas in (c) and (d) it expects that the other car does not stop. For (a) and (d) the expectation is correct, whereas for (b) and (c) the expectation is wrong.

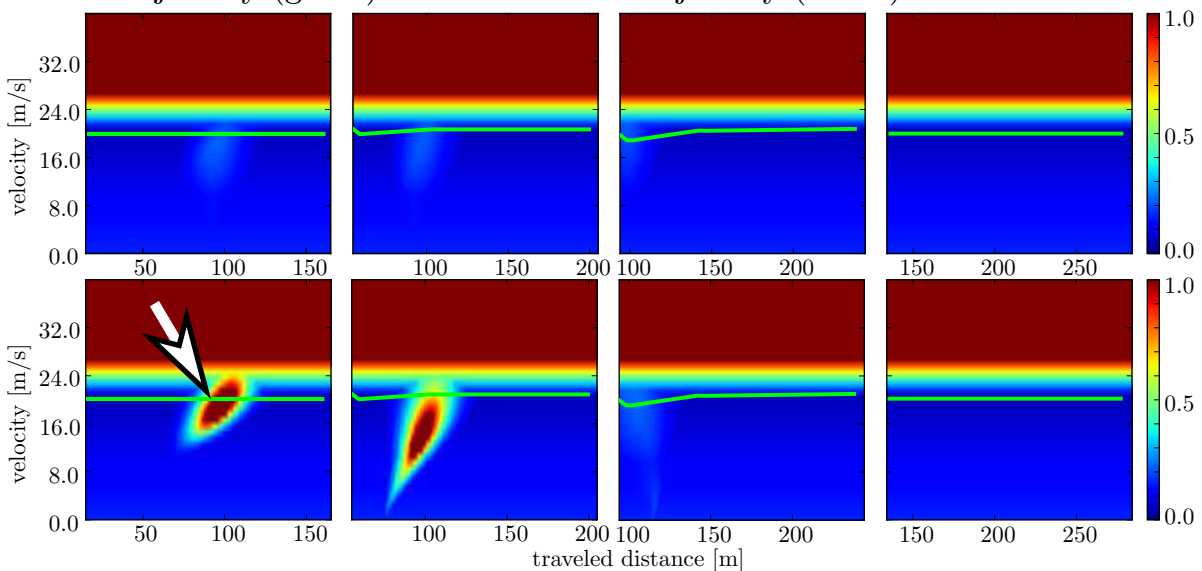
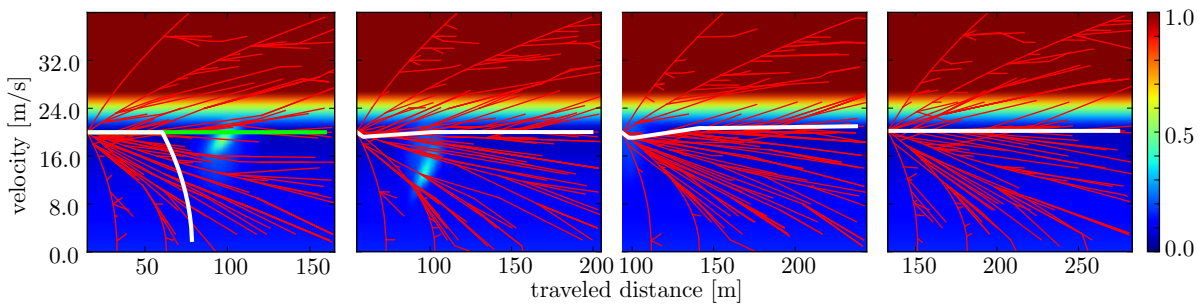
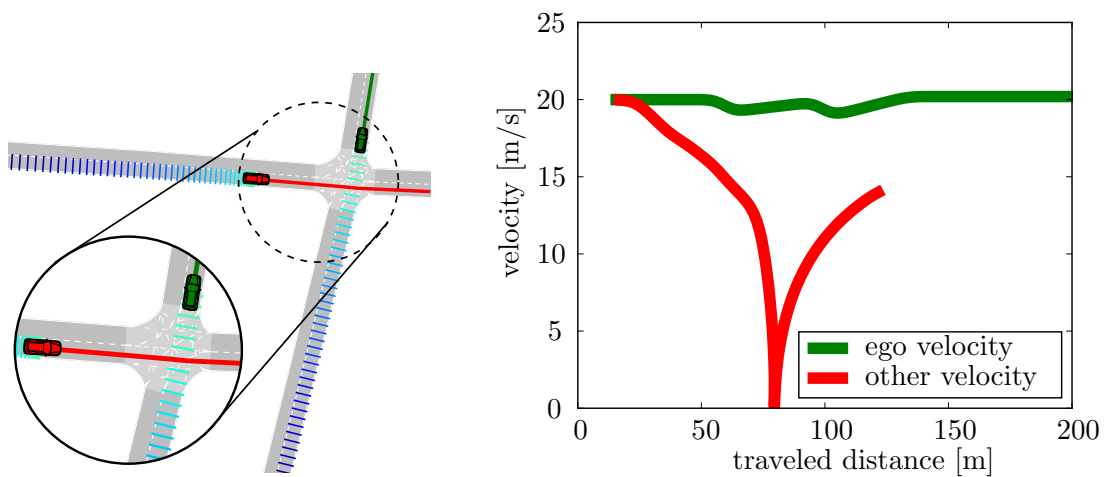


Figure 8.9: Case 1. Expected: Other car does stop. Occurring: Other car does stop.

Case 2

In the second case (Figure 8.10) the ego car expects again, here falsely, that the other car stops. But this time the other car violates the left-yields-to-right rule and drives on. The probability setting for this case shows high probability for the situation *other stopping* while the probability for this situation drops very late (too late to react).

The planned velocity profile shows only a slight deceleration, as the probability for *other not stopping* is low, but violates the risk threshold for this situation. Thus an emergency braking trajectory is applied. Even though the probability remains low for *other not stopping*, the planned trajectory still violates the risk threshold.

It can be seen in Figure 8.10 (d, top row, third risk map), that at a certain point in time even the situation *other stopping* becomes risky, since the prediction model for this situation predicts that the other car is not able to stop anymore, even if it would react to the ego car.

Once the point of executing emergency braking is reached, the situation *other not stopping* is still of high risk, even though with low probability, and emergency braking has to be executed in order to remain in an overall safe behavior.

Case 3

In case 3 (Figure 8.11), the ego car expects the other car to not stop, but in fact the other car stops.

It can be seen in the combined risk maps, that the *other not stopping* situation dominates, which results in a planned future path adapting mainly to this situation. This means, that the ego car brakes in order to avoid an upcoming crash, in case this highly probable situation occurs.

The ego car starts to brake, caused by the expectation that the other car will not brake. However, the other car does brake as well, which leads again to a further deceleration of the ego car. As this scenario (both cars brake) is of low risk, no emergency behavior is executed. However, the ego car brakes unnecessarily, which results in a behavior of low utility.

Once the other car is quite slow, both situations *other stopping* and *other not stopping* are of low risk and the ego car accelerates again to pass the intersection.

Case 4

In case 4, the ego car expects the other car to not stop, as it has potentially overlooked the ego car (Figure 8.12). The expectation is correct and the

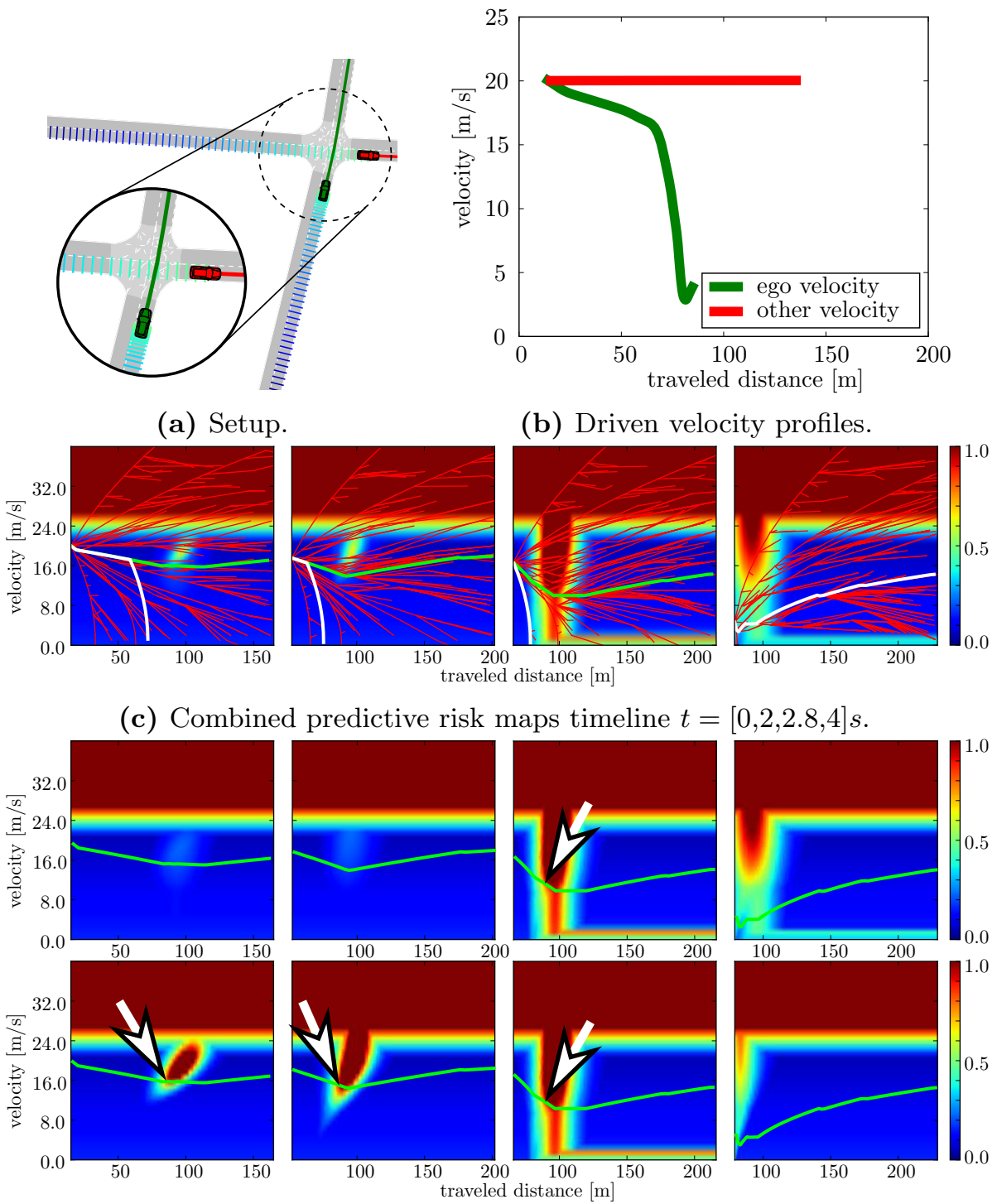


Figure 8.10: Case 2. Expected: Other car does stop. Occurring: Other car does not stop.

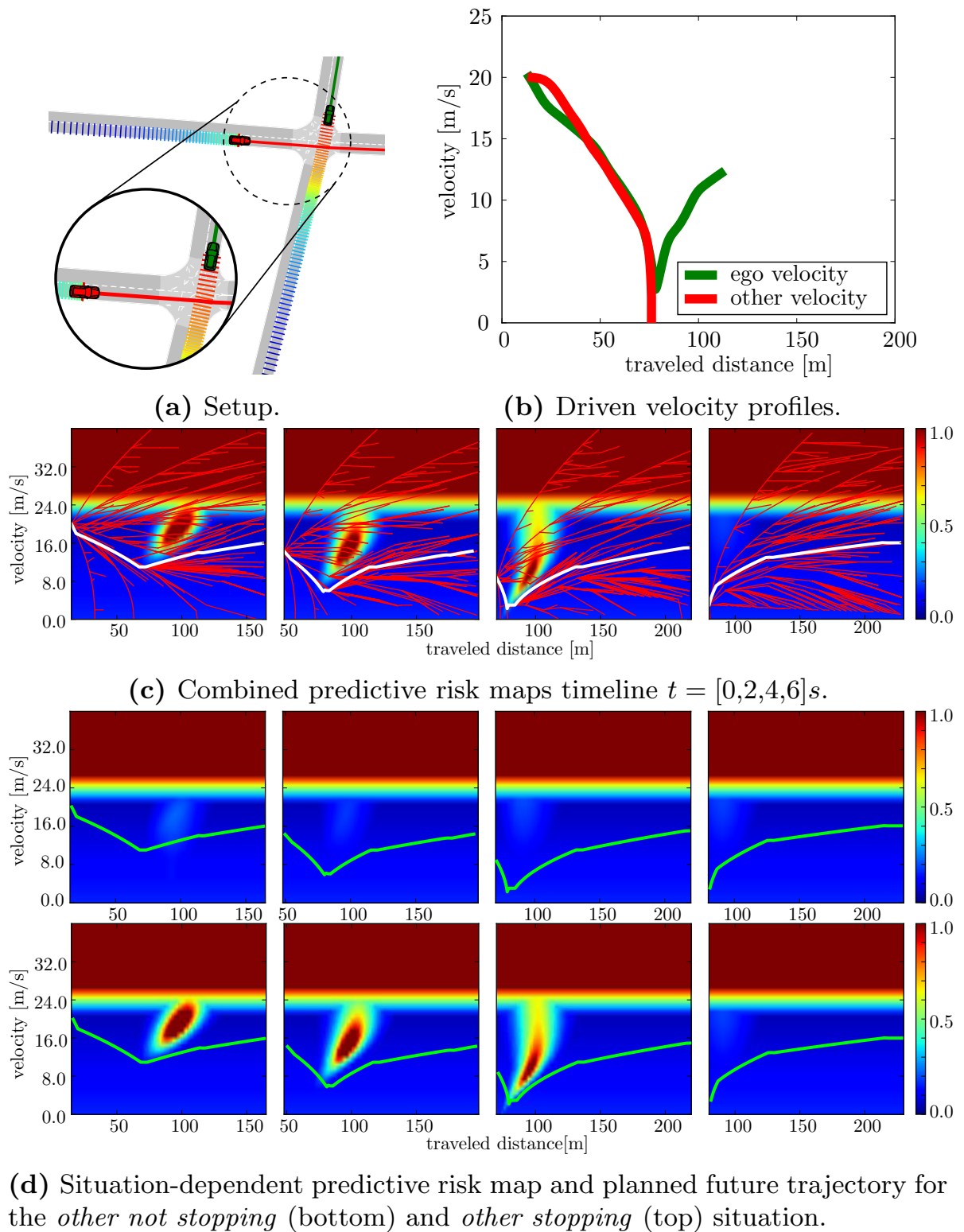


Figure 8.11: Case 3. Expected: Other car does not stop. Occurring: Other car does stop.

other car finally violates the right-of-way and drives through.

As the situation classification provides a high probability for the situation *other not stopping* this situation dominates in the combined risk maps and the planned trajectory adapts accordingly. The ego car starts early to slow down to let the other car pass (even though the other car has to give right-of-way).

The result is a velocity profile, where the ego car lets the other car pass and only brakes as much as needed and then accelerates again. This behavior is the most efficient (highest utility), while being of low risk, for this situation.

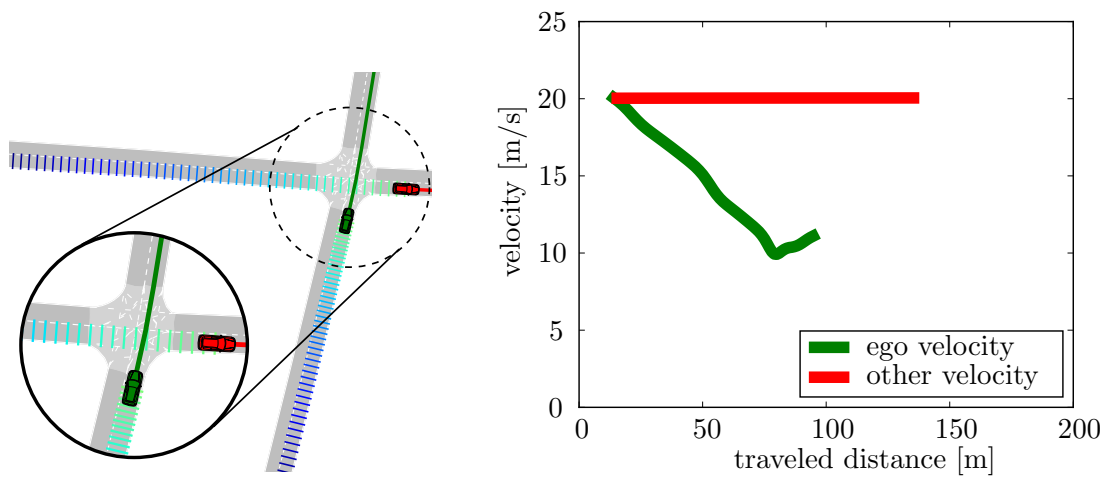
Discussion

It could be shown, that the presented approach generates a safe behavior/velocity profile in all four cases. Even in case 2 and 3, where the situation classification provides a wrong situation estimate to the system, the resulting behavior is safe.

Although safe trajectories for all four cases are achieved, it can be seen easily from the comparison of the four velocity profiles in Figure 8.13, that a correct situation classification is highly beneficial for the planned future behavior in terms of utility and comfort. For a correctly classified set of situations, the resulting behavior is highly efficient. This is for example, driving by without much braking, if the other car stops (case 1), or early braking, only to the extent to let the other car pass, if the other car does not stop (case 4). For the other two cases with incorrect situation classification, the resulting behavior is safe, but not of high utility for the actually occurring situation. In case 2, the ego car does not brake enough at the beginning to let the other car pass. Therefore, an emergency braking has to be performed to keep the situation safe. In case 3, the ego car unnecessarily brakes almost down to full stop, even though the other car stops as well.

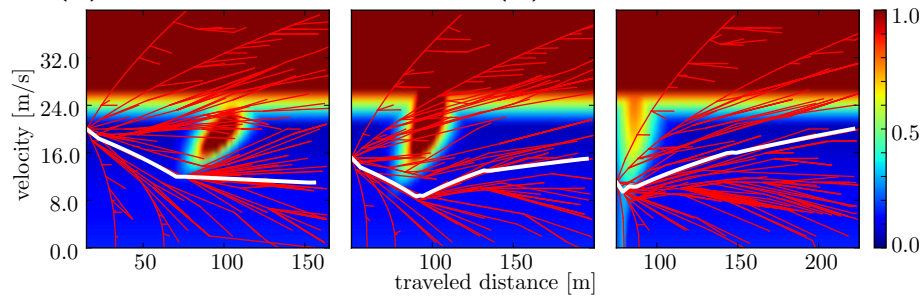
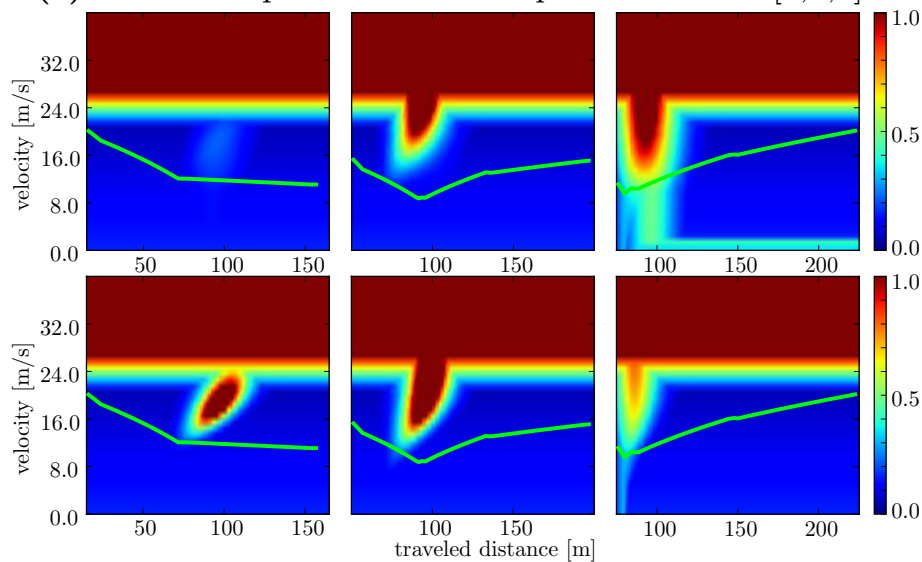
8.3 Conclusion

This chapter has focused on the problem of risk-based behavior planning in dynamic scenarios. By using the continuous, predictive risk measure, introduced in Chapter 3.2, so-called predictive risk maps are generated. Predictive risk maps are then used to plan the future behavior. Here an RRT*-based algorithm is adapted to the problem of behavior planning in



(a) Setup.

(b) Driven velocity profiles.

(c) Combined predictive risk maps timeline $t = [0, 2, 4]s$.(d) Situation-dependent predictive risk maps and planned future trajectory. *other stopping* situation (top) and *other not stopping* situation (bottom).**Figure 8.12:** Case 4. Expected: Other car does not stop. Occurring: Other car does not stop.

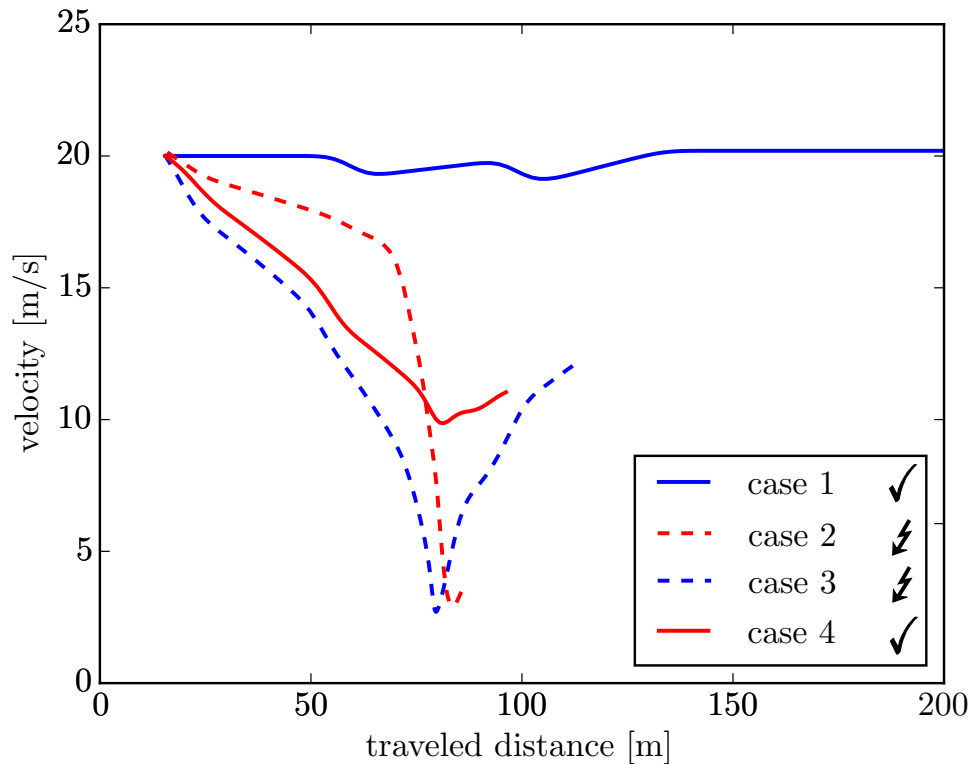


Figure 8.13: Comparison of ego velocity profiles. ✓ indicates a correct situation classification, whereas ⚡ indicates a wrong situation classification. The comparison of the ego velocity profiles of all four cases shows that the system with a reliable situation classification (solid lines) provides safe and highly efficient behavior. However, even if the situation classification provides wrong estimates of the occurring situation (dashed lines), the behavior is safe, but not necessarily efficient.

traffic environments and used to generate future velocity profiles, which minimize risk and maximize utility.

Combining predictive risk maps with a utility measure, a sampling based globally optimal planner (RRT*) is used to find cost-optimal velocity profiles through the future risk landscape. By integrating a-priori knowledge in form of typical trajectories into the algorithm, both efficiency and quality of the planning results can be increased.

At first, by considering only a single situation, the planning algorithm is applied to different scenarios, such as an inner-city intersection, curve driving, a turning scenario with several other traffic participants and an outer-city highway accessing scenario. The high generality of the approach could be shown. Even for complex scenarios, where a gradient-descent-like approach would encounter problems of local minima, the RRT* behavior planner in combination with the general predictive risk estimation scheme is able to find safe and still efficient velocity profiles.

The single-situation case is then extended by an approach to plan safe, but still efficient future trajectories under consideration of multiple uncertain situations. Based on the outcome of a situation classification step, the approach evaluates ego behavior alternatives in relation to situation-dependent predicted trajectories of other entities in terms of risk and represents the result in so-called predictive risk maps, one for each situation. By combining the risk maps for all possible situations, taking the situation probabilities into account, an efficient trajectory is planned, which adapts mainly to highly probable situations. In a further step, this efficient future plan is checked for risk violations in unlikely situations. A “plan B” is applied in form of escape trajectories to provide a safe future behavior even if an unlikely but risky situation occurs.

The evaluation of this approach on an intersection scenario shows that the resulting behavior is safe, even for a wrong situation classification. However, for a correct situation classification the behavior is additionally of high utility. This confirms that behavior strongly benefits from a good situation classification in terms of utility and comfort.

9 Summary and Outlook

This chapter summarizes and discusses the presented thesis comprising the framework for *situation-based risk evaluation and behavior planning* in combination with the individual realizations of its different steps. The summary is followed by an outlook on subsequent future work, focusing on requirements for the online application of the system in real traffic.

9.1 Summary

The overall target of this thesis is the increase of traffic safety. It has been determined that human misbehavior is still the major reason for accidents. To further increase traffic safety, the area of advanced driver assistance systems (ADAS) and autonomous driving (AD) targets at increasing the level of driving automation to relief the strain on the human driver.

A wide range of currently used systems has been developed to work under narrowly defined conditions. Consequently, those methods are only applicable to specific tasks, such as lane-keeping or highway distance control. The increasing number of specialized ADAS has raised the problem of how to combine a large number of functionalities with potentially conflicting targets. A framework that allows an integrated consideration of all the different systems such that it is applicable to the full variability of traffic scenarios is still missing but highly relevant to increase the level of driving automation towards SAE-4 and 5, namely *high- and full automation*.

This thesis has introduced such a general framework, comprising an integrated method for behavior planning and evaluation, which includes the estimation and evaluation of possible future hazards. The fundamental questions this thesis has answered are:

- How can an entity's behavior be generated in a way to minimize risk and maximizing utility?
- How can an entity's future behavior possibility be evaluated in an integrated way in terms of behavioral risk and utility?

- How can the complexity of the behavior evaluation be reduced to allow a computationally efficient evaluation of behavioral risk and utility?

The framework and system for *situation-based risk evaluation and behavior planning*, introduced in Chapter 4, has been structured by the six subsequent steps: 1) scene observation, 2) situation classification, 3) trajectory prediction, 4) risk estimation, 5) behavior planning, and 6) behavior execution. The individual realizations have been developed in a way to interlink naturally with each other.

In Chapter 3, novel basic concepts have been derived which build the foundation of the framework. This is on the one hand a situation representation applicable to reduce the complexity of a traffic scene and on the other hand a highly general risk model considering different types of risk in an integrated way.

To reduce the complexity of a sensed traffic scene and all its possible evolutions into the future, situations have been defined such that they group similar and separate dissimilar scene evolutions. A situation represents then such a cluster of similar evolutions and is treated as a prototypical scene evolution pattern. As a result, a general and compact representation of possible future scene evolutions has been achieved, that allows an efficient analysis of a traffic scene.

To evaluate possible scene evolutions as well as different behavior alternatives of a considered ego entity, a probabilistic model for future risk has been developed. Risk in general is the expectation value of the cost related to critical future events. Consequently, the proposed risk model consists of two parts: 1) the probability that a critical event will occur and 2) the expected damage in case the event occurs. The event probability term has been modeled probabilistically using a so-called “survival function” in combination with instantaneous events rates, considering different types of risk, e.g. car-to-car collisions or control loss due to heavy braking. The damage term has been modeled deterministically using e.g. a 2D-inelastic collision model. This novel risk model enables a time continuous estimation and evaluation of critical future events. Furthermore, it is not restricted to certain risk- or scenario types and generalizes many of the currently used risk evaluation methods.

In Chapter 6, an approach for the situation classification and trajectory prediction step has been presented. For the prediction of future scene- or trajectory evolutions, the Foresighted Driver Model (FDM) has been applied in a multi-agent forward simulation of a sensed scene. The FDM is a

novel microscopic driver model, introduced in Chapter 5, that is based on a computationally inexpensive, simplified version of the behavior planning framework comprising an approximate risk model targeting only risk maxima and a gradient-descent method for behavior generation. In this forward simulation, situation-dependent behavior assumptions such as “car A gives way to car B while turning left” are considered to generate prototypical scene evolutions. Due to its generality the FDM can be applied to predict or simulate a wide range of traffic situations and allows the incorporation of interaction between traffic participants in the prediction step.

By comparing the actually sensed behavior of all involved entities with the situation-dependent, prototypically predicted behavior patterns using a novel measure for trajectory similarity, the system is able to quantify how good a situation-dependent behavioral assumption fits to the current scene. This has then been employed to estimate the likelihood that the involved entities will continue to behave according to the different considered situations, the so-called situation occurrence probabilities.

By utilizing situation models that differentiate between interacting and non-interacting behavior in combination with the FDM-based prediction approach that allows the consideration of interaction, this situation classification system is applicable to detect the “lack of interaction” in critical scenarios. In a variety of real-world crash scenarios, it has shown to reliably warn the driver about two seconds ahead an upcoming crash.

Chapter 7 has introduced a computationally inexpensive approach to evaluate possible behavior alternatives in terms of future risk. Under consideration of situation-dependent, prototypically predicted trajectories derived from the previous step of situation classification and trajectory prediction, the risk for a set of ego behavior variations has been evaluated. As a result, for each situation a so-called predictive risk map is calculated, which indicates how risky a certain behavior variation will be in the future for the considered situation. A risk map can then be used to plan the best future behavior, by finding a way through the risk map. By using the ego velocity as a variation parameter, a planned “way” through the risk map represents a longitudinal velocity profile. The evaluation of different scenarios has shown that basic risk map shapes arise for different kind of scenarios, such as car-following and intersections. Those basic shapes have been shown to be very effective to enable the human analysis of the different risk causes in complex scenarios.

In Chapter 8, a novel, sampling-based, globally optimizing approach for behavior planning (RRT*) has been proposed and adapted to the problem

of behavior planning in traffic situations, especially planning velocity profiles along predefined spatial paths. The approach has shown to reliably generate a behavior or velocity profile, finding a tradeoff between risk and utility, in a wide range of complex scenarios and situations with a complex topology of the cost function.

In general, situation classification is uncertain and can only provide a set of possible situations with an estimation of their occurrence probabilities. Consequently, the behavior planning step has to cope with several possible scene evolution patterns, which result in several predictive risk maps. In Section 8.2, an approach has been presented to plan the future behavior while considering several possible situations and risk maps. The influence of the different situations on the planned behavior is dependent on the estimated occurrence probabilities. The more likely a situation is to occur, the stronger it is considered during behavior planning. This results in a behavior that is most efficient, if the most likely situation matches well with the actually occurring situation. To ensure that the planned behavior is of low risk in case an unlikely but risky situation occurs, a “plan B” is derived by checking for high risks of the planned behavior in unlikely situations. This “plan B” only considers the minimization of risk while neglecting any utility evaluations and is executed the latest possible but the earliest necessary to keep the overall situation safe. The presented approach has shown the ability to always act in a safe way. Additionally, in collaboration with a reliable situation classification, highly efficient behavior can be achieved. Furthermore, it could be shown that planning with consideration of risk and utility for the most likely scene evolutions, while considering a purely risk minimizing plan B for unlikely scene evolutions represents a highly general strategy to plan behavior in uncertain environments such as the traffic environment. This also paves the way to increase driving automation in an integrated way.

Concluding, the presented framework for *situation-based risk evaluation and behavior planning* has shown to be a highly general approach for tackling the problem of traffic scene analysis as well as behavior planning in arbitrary traffic scenarios. The realizations of the individual sub-systems are designed to naturally cooperate with each other and to be easily extendable, e.g. by further types of risk. By applying and evaluating the system in simulated as well as recorded real-world traffic scenarios, it could be shown how driving automation can heavily be increased in a safe and still efficient way with the overall target to increase driving safety.

9.2 Outlook

The presented system for situation-based risk evaluation and behavior planning has mainly been evaluated using a simulation environment and recorded real-world traffic scenarios. However, an evaluation of the individual steps as well as of the entire system on a test vehicle is missing. Here, two projects which are part of the Horizon 2020 - EU Research and Innovation programme subsequent to the presented thesis, namely inLane and VI-DAS target this issue by transferring parts of the current system onto real test vehicles.

The inLane project targets the lane-precise localization of the ego- and other vehicles using cheap GSSN-based sensors in combination with an on-board camera. The lane-precise localization is a prerequisite for the realization of the presented system for *situation-based risk evaluation and behavior planning*.

The VI-DAS project targets at transferring further steps of the system, namely situation-classification in combination with a trajectory prediction, risk evaluation and behavior planning onto a test vehicle. To apply the system online to real traffic the following aspects have to be improved:

The current computational effort for the entire system is high. This is on the one hand caused by the sampling-based, globally optimizing behavior planner RRT*, where the construction of the solution tree, to an extent where a suitable solution can be achieved, requires a large set of sampled trajectories. A way to reduce the computation effort is by including a set of predefined behavior options and simply adapting the predefined behaviors to the given problem. Furthermore the RRT* algorithm can be extended to re-use the constructed tree from the previous planning step and only reevaluating changes in the cost function. Such extensions are usually denoted as *anytime* [65]. First tests have shown promising results in reducing the computational effort.

Furthermore, it has to be evaluated if the current situation models are sufficient for the detection of all dangerous driving constellations. A more detailed situation model, e.g. by considering further driver characteristics such as aggressiveness, would improve the situation detection accuracy as well as the situation-based trajectory prediction.

In this thesis, a focus of behavior planning and prediction has been on longitudinal motion. However in certain situations, lateral maneuvers have to be considered, e.g. lane changing in highway scenarios. A first step in this direction has been proposed by the author in [33, 37], where the Foresighted Driver Model has been extended to lateral motions, by

considering lateral maneuvers as a discrete path decision process.

Another aspect, that has to be considered is the large amount of parameters which have to be tuned to achieve the desired behavior of the entire system for *situation-based risk evaluation and behavior planning*. Especially the number of parameters in the risk evaluation part is high. A way to find a suitable parameter set is comparing the system's behavior with the behavior of human drivers in a variety of traffic scenarios. However, simulations as well as the application to recorded real world scenarios have shown that the system's behavior is relatively robust for parameter changes. Furthermore many of the applied parameters are comprehensible and easy to set up.

Furthermore, the current system only acts with regard to dynamic and static objects which can be acquired by the vehicles sensors. However, risk can also occur from sources which cannot be detected by a vehicle's sensor. This is e.g. the case at intersections which are visually difficult to access. A first approach to incorporate risks caused by sensor limitation are published by the author to the Intelligent Vehicle Society (ITS) in [34]. Here, the risk arising from occluded areas at intersections is targeted. Potential risk sources are determined by combining map data with an estimation of areas which can not be captured by the vehicles sensors, e.g. areas occluded by buildings. The risk is then evaluated by assuming potentially present vehicles with a certain behavior. The system has been evaluated in recorded real-world scenarios. The resulting ego vehicle's behavior did reveal to be similar to the general human behavior at intersections of limited visibility.

A Appendix

A.1 Approximate Accumulated Curvature Risk Model

The approximate accumulated future risk for skidding off the road in curvy road segments explicitly derived according to Chapter 3.2.3 is

$$r_{\infty}^{cv}(\mathbf{x}_t) \sim \sum_{h_t \in \mathbb{H}} r_{\infty}^{cv}(\mathbf{x}_t, h_t) \cdot S_{h_t}^{cv}.$$

with the situation-dependent risk

$$\begin{aligned} r_{\infty}^{cv}(\mathbf{x}_t, h_t) \\ = \sum_j \hat{c}_{cv}^j(\mathbf{e}_{cv}^j, \hat{\mathbf{x}}_{t+TMC^j}(\mathbf{x}_t, h_t)) \cdot P^{\infty}(\mathbf{e}^j | \text{IVMC}^j(\mathbf{x}_t, h_t), \text{TMC}^j(\mathbf{x}_t, h_t)), \end{aligned}$$

the expected damage in case of skidding off the road

$$\begin{aligned} \hat{c}_{cv}^j(\mathbf{e}^j, \hat{\mathbf{x}}_{t+TMC^j}(\mathbf{x}_t, h_t)) \\ = \frac{1}{2} m_0 \|\hat{v}_{t+TMC^j}^0(\mathbf{x}_t, h_t)\|^2, \end{aligned}$$

the probability for skidding off the road

$$\begin{aligned} P^{\infty}(\mathbf{e}^j | \text{IVMC}^j(\mathbf{x}_t, h_t), \text{TMC}^j(\mathbf{x}_t, h_t)) \\ = F_{cv}^j \cdot \exp\{-\max(\hat{v}_{c,max}(\mathbf{x}_t, h_t) - v_{t+TMC}^0(\mathbf{x}_t, h_t), 0) / \sigma_c\} \\ \cdot \exp\{-\text{TMC}^j(\mathbf{x}_t, h_t) / \sigma_{cv}\} \\ \cdot B(\text{TMC}^j(\mathbf{x}_t, h_t), \text{IVMC}^j(\mathbf{x}_t, h_t)) \end{aligned}$$

and

$$v_{c,max}(\mathbf{x}_t, h_t) = \sqrt{a_{c,max} / \text{IVMC}^j(\mathbf{x}_t, h_t)}.$$

A.2 Paramters

Unless defined differently in the corresponding chapter, the parameters used for simulation and evaluation are chosen as follows:

| Symbol | Value | Chapter |
|---------------------|----------------------------------|---------|
| α | 1.5 s m^{-1} | 3.2 |
| β | 1.0 | 5 |
| $\beta_{b,0}$ | 1.0 s | 3.2 |
| $\beta_{c,0}$ | 1.0 s | 3.2 |
| $\beta_{d,0}$ | 1.0 s | 3.2 |
| β_b^{const} | $1.0 \text{ s}^2 \text{ m}^{-1}$ | 3.2 |
| β_c^{const} | 1.0 s m^{-1} | 3.2 |
| β_d^{const} | 1.0 m^{-1} | 3.2 |
| η | $1 \text{ m}^2 \text{ s}^{-3}$ | 5 |
| γ | 1.1 m | 3.2 |
| σ_{co} | 1.0 s | 3.2 |
| $\sigma_{co,1}$ | 1.0 s | 5 |
| $\sigma_{co,2,3}$ | 0.5 s | 5 |
| σ_{cv} | 1.0 s | 5 |
| σ_d | 1.0 m | 3.2 |
| τ_0^{-1} | 0.5 s^{-1} | 3.2 |
| $\tau_{d/c/b}^{-1}$ | 1 s^{-1} | 3.2 |
| F_{co} | 0.7 | 3.2 |
| $S_{1,2,3}^{co}$ | 1.0 | 5 |
| a | 1.25 m s^{-2} | 5 |
| $a_{c,max}$ | 10 m s^{-2} | 3.2 |
| $a_{max,comfort}$ | 4 m s^{-2} | 8 |
| $a_{max,total}$ | 8 m s^{-2} | 8 |
| $b_{b,max}$ | 8 m s^{-2} | 3.2 |
| b_{risk} | 0.2 | 3.1 |
| d_{min} | 1.0 m | 3.2 |
| m | 0.01 | 8 |
| m_0 | 1000 kg | 3.2 |
| m_i | 1000 kg | 3.2 |
| $s_{b,0}$ | 0.1 s | 3.2 |
| $s_{c,0}$ | 0.1 s | 3.2 |
| $s_{d,0}$ | 0.1 s | 3.2 |

A.3 Camera to map alignment

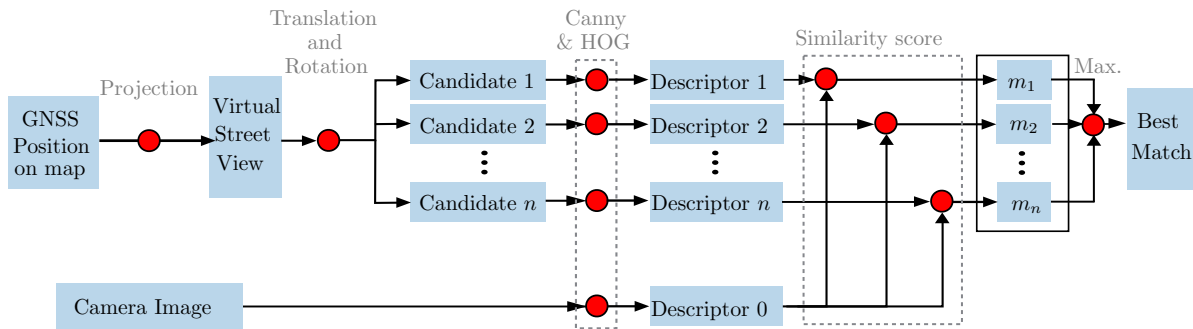


Figure A.1: Camera to map alignment approach. First, virtual street views (see Figure A.2) are generated at different poses (6 degrees of freedom) near the original GNSS-position. Then, a similarity score between each virtual view and the actual camera image is calculated, using Canny edge detection in a preprocessing step and HOG(histogram of oriented gradients) as descriptors. The camera pose, relative to the original GNSS-position, of the best matching candidate can be employed for the map-to-camera alignment.

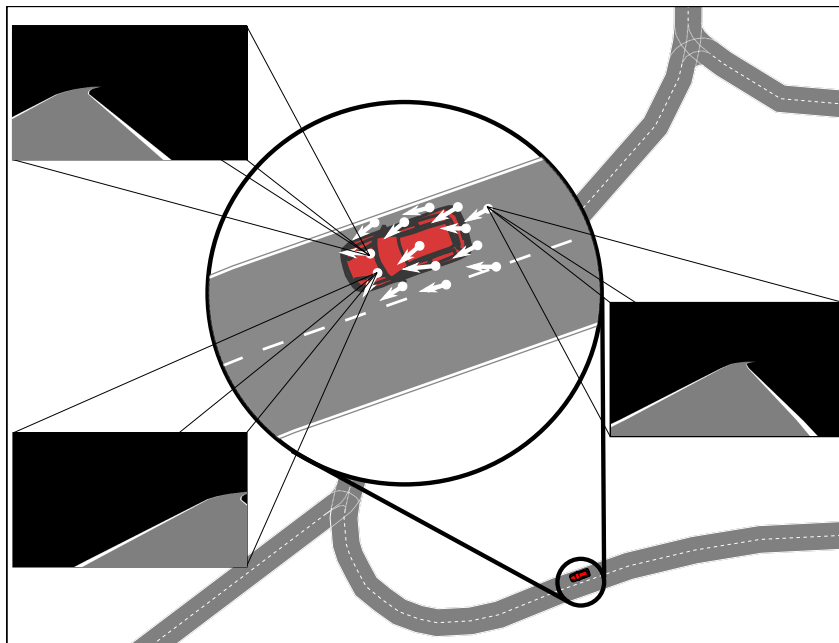


Figure A.2: Example of candidate views (white arrows), with three of them being zoomed in.

Bibliography

- [1] G. Agamennoni, J. I. Nieto, and E. M. Nebot. A bayesian approach for driving behavior inference. In *Proc. of the IEEE Intelligent Vehicles Symposium*, pages 595–600, 2011.
- [2] K. Ahmed, M. Ben-Akiva, H. Koutsopoulos, and R. Mishalani. Models for freeway lane changing and gap acceptance behavior. *Transportation and traffic theory*, 13:501–515, 1996.
- [3] D. Althoff, M. Althoff, D. Wollherr, and M. Buss. Probabilistic collision state checker for crowded environments. In *Proc. of the IEEE International Conference on Robotics and Automation*, pages 1492–1498, 2010.
- [4] M. Althoff and J. M. Dolan. Online Verification of Automated Road Vehicles Using Reachability Analysis. *IEEE Transactions on Robotics*, 30(4):903–918, 2014.
- [5] M. Althoff and A. Mergel. Comparison of Markov Chain Abstraction and Monte Carlo Simulation for the Safety Assessment of Autonomous Cars. *IEEE Transactions on Intelligent Transportation Systems*, 12(4):1237–1247, 2011.
- [6] M. Althoff, O. Stursberg, and M. Buss. Model-Based Probabilistic Collision Detection in Autonomous Driving. *IEEE Transactions on Intelligent Transportation Systems*, 10(2):299–310, 2009.
- [7] S. Ammoun and F. Nashashibi. Real time trajectory prediction for collision risk estimation between vehicles. In *Proc. of the IEEE Conference on Intelligent Computer Communication and Processing*, pages 417–422, 2009.
- [8] M. Bahram, C. Hubmann, A. Lawitzky, M. Aeberhard, and D. Wollherr. A Combined Model- and Learning-Based Framework for Interaction-Aware Maneuver Prediction. *IEEE Transactions on Intelligent Transportation Systems*, 17(6):1538–1550, 2016.

-
- [9] M. Bando, K. Hasebe, A. Nakayama, A. Shibata, and Y. Sugiyama. Dynamical model of traffic congestion and numerical simulation. *Physical Review E*, 51(2):1035, 1995.
 - [10] C. Barrios, H. Himberg, Y. Motai, and A. Sad. Multiple model framework of adaptive extended kalman filtering for predicting vehicle location. In *Proc. of the IEEE Intelligent Transportation Systems Conference*, pages 1053–1059, 2006.
 - [11] A. Barth and U. Franke. Where will the oncoming vehicle be the next second? In *Proc. of the IEEE Intelligent Vehicles Symposium*, pages 1068–1073, 2008.
 - [12] T. Basar. A New Approach to Linear Filtering and Prediction Problems. In *Control Theory*, pages 167–179. 2009.
 - [13] T. Batz, K. Watson, and J. Beyerer. Recognition of dangerous situations within a cooperative group of vehicles. In *Proc. of the IEEE Intelligent Vehicles Symposium*, pages 907–912, 2009.
 - [14] M. Behrisch, L. Bieker, J. Erdmann, and D. Krajzewicz. SUMO - Simulation of Urban MObility An Overview. In *Proc of the Conference on Advances in System Simulation*, pages 63–68, 2011.
 - [15] H. Berndt and K. Dietmayer. Driver intention inference with vehicle onboard sensors. In *Proc of the IEEE Conference on Vehicular Electronics and Safety*, pages 102–107, 2009.
 - [16] A. L. Berthaume. *Microscopic Modeling of Driver Behavior Based on Modifying Field Theory for Work Zone Application*. PhD thesis, 2015.
 - [17] A. Berthelot, A. Tamke, T. Dang, and G. Breuel. Handling uncertainties in criticality assessment. In *Proc. of the IEEE Intelligent Vehicles Symposium*, pages 571–576, 2011.
 - [18] C. Braeuchle, F. Flehmig, W. Rosenstiel, and T. Kropf. Maneuver decision for active pedestrian protection under uncertainty. In *Proc. of the IEEE Intelligent Transportation Systems Conference*, pages 646–651, 2013.
 - [19] M. Brannstrom, E. Coelingh, and J. Sjoberg. Model-Based Threat Assessment for Avoiding Arbitrary Vehicle Collisions. *IEEE Transactions on Intelligent Transportation Systems*, 11(3):658–669, 2010.

-
- [20] A. Broadhurst, S. Baker, and T. Kanade. Monte Carlo road safety reasoning. In *IEEE Proceedings. Intelligent Vehicles Symposium, 2005.*, pages 319–324, 2005.
- [21] J. Bruce and M. Veloso. Real-time randomized path planning for robot navigation. In *Proc. of the IEEE Conference on Intelligent Robots and System*, volume 3, pages 2383–2388, 2002.
- [22] G. Cao, F. Damerow, B. Flade, M. Helmling, and J. Eggert. Camera to Map Alignment for Accurate Low-Cost Lane-Level Scene Interpretation. In *Proc. of the IEEE Intelligent Transportation Systems Conference*, 2016.
- [23] D. Caveney. Numerical Integration for Future Vehicle Path Prediction. In *Proc. of the American Control Conference*, pages 3906–3912, 2007.
- [24] Z. Chen. Bayesian Filtering: From Kalman Filters to Particle Filters, and Beyond. Technical report, McMaster University, 2003.
- [25] I. Dagli, M. Brost, and G. Breuel. Action Recognition And Prediction For Driver Assistance Systems Using Dynamic Belief Networks. In *Proc. of the Conference on Object-Oriented and Internet-Based Technologies, Concepts, and Applications for a Networked World*, pages 179–194, 2002.
- [26] F. Damerow and J. Eggert. Predictive risk maps. In *Proc. of the IEEE Intelligent Transportation Systems Conference*, pages 703–710, 2014.
- [27] F. Damerow and J. Eggert. Balancing Risk against Utility: Behavior Planning using Predictive Risk Maps. In *Proc. of the IEEE Intelligent Vehicles Symposium*, pages 857 – 864, 2015.
- [28] F. Damerow and J. Eggert. Method and vehicle with an advanced driver assistance system for risk-based traffic scene analysis. *Patent, United States, Europe, US20150344030, EP2950294A1*, 2015.
- [29] F. Damerow and J. Eggert. Method for risk-based traffic scene analysis using advanced driver assistance system, and vehicle with such a system for performing such an analysis. *Patent, Japan, JP2015228204A*, 2015.

- [30] F. Damerow and J. Eggert. Risk-Aversive Behavior Planning under Multiple Situations with Uncertainty. In *Proc. of the IEEE Intelligent Transportation Systems Conference*, pages 656–663, 2015.
- [31] F. Damerow and J. Eggert. Spatio-temporal Trajectory Similarity and it’s Application to Situation Classification and the Evaluation of Lack of Interaction. In *Proc. of the IEEE Intelligent Vehicles Symposium*, 2016.
- [32] F. Damerow, J. Eggert, and A. Richter. Method and system in a vehicle for improving prediction results of an advantageous driver assistant system. *Patent, United States, Europe, US20160236683, EP3056861A1*, 2016.
- [33] F. Damerow, B. Flade, and J. Eggert. Extensions for the Foresighted Driver Model: Tactical Lane Change, Overtaking and Continuous Lateral Control. In *Proc. of the IEEE Intelligent Vehicles Symposium*, pages 168–193, 2016.
- [34] F. Damerow, T. Puphal, Y. Li, and J. Eggert. Risk-Based Driver Assistance for Approaching Intersections of Limited Visibility . In *Proc. of the IEEE International Conference on Vehicular Electronics and Safety*, page in press, 2017.
- [35] D. Dolgov, S. Thrun, M. Montemerlo, and J. Diebel. Path Planning for Autonomous Vehicles in Unknown Semi-structured Environments. *The International Journal of Robotics Research*, 29(5):485–501, 2010.
- [36] J. Eggert. Predictive risk estimation for intelligent ADAS functions. In *Proc. of the IEEE Intelligent Transportation Systems Conference*, pages 711–718, 2014.
- [37] J. Eggert and F. Damerow. Complex Lane Change Behavior in the Foresighted Driver Model. In *Proc. of the IEEE Intelligent Transportation Systems Conference*, pages 1747–1754, 2015.
- [38] J. Eggert, F. Damerow, and S. Klingelschmitt. The Foresighted Driver Model. In *Proc. of the IEEE Intelligent Vehicles Symposium*, volume 2015-Augus, pages 322–329, 2015.
- [39] J. Eggert, S. Klingelschmitt, F. Damerow, C. Methods, V. D. Control, and A. Driving. The Foresighted Driver: Future ADAS Based

- on Generalized Predictive Risk Estimation. In *Proc. of the FAST-zero Symposium*, 2015.
- [40] A. Eidehall and L. Petersson. Statistical Threat Assessment for General Road Scenes Using Monte Carlo Sampling. *IEEE Transactions on Intelligent Transportation Systems*, 9(1):137–147, 2008.
- [41] C. Erbsmehl. Simulation of real crashes as a method for estimating the potential benefits of advanced safety technologies. In *Proc. of the Technical Conference on the Enhanced Safety of Vehicles*, number 09-0162, 2009.
- [42] J. Erdmann and D. Krajzewicz. SUMO’s Road Intersection Model. In *Proc. of the Simulation of Urban MObility User Conference*, pages 3–17, 2013.
- [43] D. Fassbender, A. Mueller, and H.-J. Wuensche. Trajectory planning for car-like robots in unknown, unstructured environments. In *Proc. of the IEEE International Conference on Intelligent Robots and Systems*, pages 3630–3635, 2014.
- [44] N. Faulhaber. *Verkehrsunfallaufnahme Grundlagenwissen polizeilicher Ermittlungen ; Recht - Taktik - Psychologie*. Boorberg, 2012.
- [45] D. Ferguson, M. Darms, C. Urmson, and S. Kolski. Detection, prediction, and avoidance of dynamic obstacles in urban environments. In *Proc. of the IEEE Intelligent Vehicles Symposium*, pages 1149–1154, 2008.
- [46] T. Gindele, S. Brechtel, and R. Dillmann. A probabilistic model for estimating driver behaviors and vehicle trajectories in traffic environments. In *Proc. of the IEEE Intelligent Transportation Systems Conference*, pages 1625–1631, 2010.
- [47] T. Gindele, S. Brechtel, and R. Dillmann. Learning context sensitive behavior models from observations for predicting traffic situations. In *Proc. of the IEEE Intelligent Transportation Systems Conference*, pages 1764–1771, 2013.
- [48] P. G. Gipps. A behavioural car-following model for computer simulation. *Transportation Research Part B: Methodological*, 15(2):105–111, 1981.

- [49] D. Greene, J. Liu, J. Reich, Y. Hirokawa, A. Shinagawa, H. Ito, and T. Mikami. An Efficient Computational Architecture for a Collision Early-Warning System for Vehicles, Pedestrians, and Bicyclists. *IEEE Transactions on Intelligent Transportation Systems*, 12(4):942–953, 2011.
- [50] T. Gu and J. M. Dolan. On-Road Motion Planning for Autonomous Vehicles. In *Proc. of the International Conference on Intelligent Robotics and Applications*, pages 588–597. Springer Berlin Heidelberg, 2012.
- [51] T. Gu, J. M. Dolan, and J.-W. Lee. On-Road Trajectory Planning for General Autonomous Driving with Enhanced Tunability. In *Intelligent Autonomous Systems 13*, pages 247–261. Springer, 2016.
- [52] T. Gu, J. Snider, J. M. Dolan, and J.-w. Lee. Focused Trajectory Planning for autonomous on-road driving. In *2013 IEEE Intelligent Vehicles Symposium (IV)*, pages 547–552, 2013.
- [53] P. Hidas. Modelling vehicle interactions in microscopic simulation of merging and weaving. *Transportation Research Part C: Emerging Technologies*, 13(1):37–62, 2005.
- [54] J. Hillenbrand, A. M. Spieker, and K. Kroschel. A Multilevel Collision Mitigation Approach—Its Situation Assessment, Decision Making, and Performance Tradeoffs. *IEEE Transactions on Intelligent Transportation Systems*, 7(4):528–540, 2006.
- [55] E. Hollnagel. *Cognitive reliability and error analysis method : CREAM*. Elsevier, 1998.
- [56] Y. Hou, P. Edara, and C. Sun. Modeling mandatory lane changing using bayes classifier and decision trees. *IEEE Transactions on Intelligent Transportation Systems*, 15(2):647–655, 2014.
- [57] C. Howard. *Knowledge representation and reasoning for a model-based approach to higher level information fusion*. PhD thesis, University of South Australia, 2010.
- [58] T. Hulnhagen, I. Dengler, A. Tamke, T. Dang, and G. Breuel. Maneuver recognition using probabilistic finite-state machines and fuzzy logic. In *Proc. of the IEEE Intelligent Vehicles Symposium*, pages 65–70, 2010.

- [59] R. Hyndman. Another Look At Forecast-Accuracy Metrics for Intermittent Demand. *Foresight: The International Journal of Applied Forecasting*, 4(4):43–46, 2006.
- [60] T. JR. Tri-Level Study of the Causes of Traffic Accidents: An overview of final results. In *Proc. of the American Association for Automotive Medicine Annual Conference*, volume 21, pages 391–403, 1977.
- [61] E. Kaefer. *Situationsklassifikation und Bewegungsprognose in Verkehrssituationen mit mehreren Fahrzeugen*. PhD thesis, University of Bielefeld, 2013.
- [62] N. Kaempchen, B. Schiele, and K. Dietmayer. Situation Assessment of an Autonomous Emergency Brake for Arbitrary Vehicle-to-Vehicle Collision Scenarios. *IEEE Transactions on Intelligent Transportation Systems*, 10(4):678–687, 2009.
- [63] R. E. Kalman. A New Approach to Linear Filtering and Prediction Problems. *Journal of Basic Engineering*, 82(1):35, 1960.
- [64] S. Karaman and E. Frazzoli. Optimal kinodynamic motion planning using incremental sampling-based methods. In *Proc. of the IEEE Conference on Decision and Control*, pages 7681–7687, 2010.
- [65] S. Karaman, M. Walter, and A. Perez. Anytime motion planning using the RRT. In *IEEE International Conference on Robotics and Automation (ICRA)*, pages 1478–1483, 2011.
- [66] R. Karlsson and J. Jansson. Model-based statistical tracking and decision making for collision avoidance application. In *Proc. of the American Control Conference*, volume 4, pages 3435–3440, Boston, MA, USA, 2004.
- [67] L. Kaufman and P. J. Rousseeuw. *Finding Groups in Data: An Introduction to Cluster Analysis*. Wiley Series in Probability and Statistics. Wiley, 2009.
- [68] A. Kesting, M. Treiber, and D. Helbing. General Lane-Changing Model MOBIL for Car-Following Models. *Transportation Research Record*, (1999):86–94, 2007.
- [69] J. F. C. J. F. C. Kingman. *Poisson processes*. Wiley Online Library, 1993.

- [70] S. Klingelschmitt, F. Damerow, and J. Eggert. Managing the Complexity of Inner-City Scenes: An Efficient Situation Hypotheses Selection Scheme. In *Proc. of the IEEE Intelligent Vehicles Symposium*, pages 1232 – 1239, 2015.
- [71] S. Klingelschmitt and J. Eggert. Using Context Information and Probabilistic Classification for Making Extended Long-Term Trajectory Predictions. In *Proc. of the IEEE Intelligent Transportation Systems Conference*, pages 705 – 711, 2015.
- [72] S. Klingelschmitt, M. Platho, H.-M. Gros, V. Willert, and J. Eggert. Combining behavior and situation information for reliably estimating multiple intentions. In *Proc. of the IEEE Intelligent Vehicles Symposium*, pages 388–393, 2014.
- [73] S. Krauss. Towards a unified view of microscopic traffic flow theories. *IFAC Transportation Systems*, 2:941–946, 1997.
- [74] R. Kühne. Macroscopic freeway model for dense traffic-stop-start waves and incident detection. In *Proc. of the International Symposium on Transportation and Traffic Theory*, pages 21–42, 1984.
- [75] F. Kuhnt, J. Schulz, T. Schamm, and J. M. Zöllner. Understanding Interactions between Traffic Participants based on Learned Behaviors. In *Proc. of the IEEE Intelligent Vehicles Symposium*, pages 1271–1278, 2016.
- [76] Y. Kuwata, S. Karaman, J. Teo, E. Frazzoli, J. How, and G. Fiore. Real-Time Motion Planning With Applications to Autonomous Urban Driving. *IEEE Transactions on Control Systems Technology*, 17(5):1105–1118, 2009.
- [77] R. Labayrade, C. Royere, and D. Aubert. A collision mitigation system using laser scanner and stereovision fusion and its assessment. In *Proc. of the IEEE Intelligent Vehicles Symposium*, pages 441–446, 2005.
- [78] C. Laugier, I. E. Paromtchik, M. Perrollaz, M. Y. Yong, J. Yoder, C. Tay, K. Mekhnacha, and A. Negre. Probabilistic Analysis of Dynamic Scenes and Collision Risks Assessment to Improve Driving Safety. *IEEE Intelligent Transportation Systems Magazine*, 3(4):4–19, 2011.

- [79] S. M. LaValle and J. J. Kuffner. Randomized Kinodynamic Planning. *The International Journal of Robotics Research*, 20(5):378–400, 2001.
- [80] A. Lawitzky, D. Althoff, C. F. Passenberg, G. Tanzmeister, D. Wollherr, and M. Buss. Interactive scene prediction for automotive applications. In *Proc. of the IEEE Intelligent Vehicles Symposium*, pages 1028–1033, 2013.
- [81] S. Lefevre, Y. Gao, D. Vasquez, H. E. Tseng, R. Bajcsy, and F. Borrelli. Lane Keeping Assistance with Learning-Based Driver Model and Model Predictive Control. In *Proc. of the International Symposium on Advanced Vehicle Control*, 2014.
- [82] S. Lefevre, C. Laugier, and J. Ibanez-Guzman. Exploiting map information for driver intention estimation at road intersections. In *Proc. of the IEEE Intelligent Vehicles Symposium*, pages 583–588, 2011.
- [83] S. Lefevre, C. Laugier, and J. Ibanez-Guzman. Risk assessment at road intersections: Comparing intention and expectation. In *Proc. of the IEEE Intelligent Vehicles Symposium*, pages 165–171, 2012.
- [84] S. Lefevre, D. Vasquez, and C. Laugier. A survey on motion prediction and risk assessment for intelligent vehicles. *ROBOMECH Journal*, 1(1):1–14, 2014.
- [85] J. Leonard, J. How, S. Teller, M. Berger, S. Campbell, G. Fiore, L. Fletcher, E. Frazzoli, A. Huang, S. Karaman, O. Koch, Y. Kuwata, D. Moore, E. Olson, S. Peters, J. Teo, R. Truax, M. Walter, D. Barrett, A. Epstein, K. Maheloni, K. Moyer, T. Jones, R. Buckley, M. Antone, R. Galejs, S. Krishnamurthy, and J. Williams. A perception-driven autonomous urban vehicle. *Journal of Field Robotics*, 25(10):727–774, 2008.
- [86] X. Li, Z. Sun, D. Cao, Z. He, and Q. Zhu. Real-time trajectory planning for autonomous urban driving: Framework, algorithms, and verifications. *IEEE/ASME Transactions on Mechatronics*, 21(2):740–753, 2016.
- [87] M. Liebner, M. Baumann, F. Klanner, and C. Stiller. Driver intent inference at urban intersections using the intelligent driver model. In

- Proc. of the IEEE Intelligent Vehicles Symposium*, pages 1162–1167, 2012.
- [88] M. Likhachev and D. Ferguson. Planning Long Dynamically Feasible Maneuvers for Autonomous Vehicles. *The International Journal of Robotics Research*, 28(8):933–945, 2009.
- [89] S. N. Luko. Risk management - Principles and Guidelines. *Quality Engineering*, 25(4):451–454, 2009.
- [90] P. Lytrivis, G. Thomaidis, and A. Amditis. Cooperative Path Prediction in Vehicular Environments. In *Proc. of the IEEE Intelligent Transportation Systems Conference*, pages 803–808, 2008.
- [91] R. Madhavan and C. Schlenoff. The effect of process models on short-term prediction of moving objects for unmanned ground vehicles. In *Proc. of the IEEE Intelligent Transportation Systems Conference*, pages 471–476, 2004.
- [92] M. McNaughton, C. Urmson, J. M. Dolan, and J.-W. Lee. Motion planning for autonomous driving with a conformal spatiotemporal lattice. In *Proc. of the IEEE International Conference on Robotics and Automation*, pages 4889–4895, 2011.
- [93] D. Meyer-Delius, C. Plagemann, and W. Burgard. Probabilistic situation recognition for vehicular traffic scenarios. In *Proc. of the IEEE International Conference on Robotics and Automation*, pages 459–464, 2009.
- [94] R. Miller and Q. Huang. An adaptive peer-to-peer collision warning system. In *Proc. of the IEEE Vehicular Technology Conference*, volume 1, pages 317–321, 2002.
- [95] M. Montemerlo, J. Becker, S. Bhat, and H. Dahlkamp. The stanford entry in the urban challenge. *Journal of Field Robotics*, 7(9):468–492, 2008.
- [96] B. Morris, A. Doshi, and M. Trivedi. Lane change intent prediction for driver assistance: On-road design and evaluation. In *Proc. of the IEEE Intelligent Vehicles Symposium*, pages 895–901, 2011.
- [97] J. Morton and T. A. Wheeler. Deep Learning of Spatial and Temporal Features for Automotive Prediction. Technical report.

- [98] J.-M. Nigro, S. Loriette-Rougegrez, and M. Rombaut. Driving situation recognition with uncertainty management and rule-based systems. *Engineering Applications of Artificial Intelligence*, 15(3):217–228, 2002.
- [99] M. Nikolaou. Model predictive controllers: A critical synthesis of theory and industrial needs. *Advances in Chemical Engineering*, 26:131–204, 2001.
- [100] M. Peden, R. Scurfield, D. Sleet, D. Mohan, and A. Hyder. World report on road traffic injury prevention. Technical report, World Health Organization Geneva, 2004.
- [101] D. Petrich, T. Dang, G. Breuel, and C. Stiller. Assessing Map-Based Maneuver Hypotheses using Probabilistic Methods and Evidence Theory. In *Proc. of the IEEE Intelligent Transportation Systems Conference*, pages 995–1002, 2014.
- [102] D. Petrich, T. Dang, D. Kasper, G. Breuel, and C. Stiller. Map-based long term motion prediction for vehicles in traffic environments. In *Proc. of the IEEE Intelligent Transportation Systems Conference*, pages 2166–2172, 2013.
- [103] M. Pivtoraiko, R. A. Knepper, and A. Kelly. Differentially constrained mobile robot motion planning in state lattices. *Journal of Field Robotics*, 26(3):308–333, 2009.
- [104] M. Platho, H.-M. Gros, and J. Eggert. Predicting Velocity Profiles of Road Users at Intersections Using Configurations. In *Proc. of the IEEE Intelligent Vehicles Symposium*, pages 945–951, 2013.
- [105] M. Platho, H.-M. Gross, and J. Eggert. Learning driving situations and behavior models from data. In *Proc. of the IEEE Intelligent Transportation Systems Conference*, pages 276–281, 2013.
- [106] M. Platho, H.-M. Groß, J. Eggert, H.-M. Gross, and J. Eggert. Traffic situation assessment by recognizing interrelated road users. In *Proc. of the IEEE Intelligent Transportation Systems Conference*, pages 1339–1344, 2012.
- [107] A. Polychronopoulos, M. Tsogas, A. Amditis, and L. Andreone. Sensor Fusion for Predicting Vehicles’ Path for Collision Avoidance Systems. *IEEE Transactions on Intelligent Transportation Systems*, 8(3):549–562, 2007.

- [108] A. Polychronopoulos, M. Tsogas, A. Amditis, U. Scheunert, L. Andreone, and F. Tango. Dynamic situation and threat assessment for collision warning systems: the euclide approach. In *Proc. of the IEEE Intelligent Vehicles Symposium*, pages 636–641, 2004.
- [109] C. Rodemerk, S. Habenicht, A. Weitzel, H. Winner, and T. Schmitt. Development of a general criticality criterion for the risk estimation of driving situations and its application to a maneuver-based lane change assistance system. In *Proc. of the IEEE Intelligent Vehicles Symposium*, pages 264–269, 2012.
- [110] SAE On-Road Automated Vehicle Standards Committee and others. Taxonomy and Definitions for Terms Related International. Technical report, 2014.
- [111] T. Schamm and J. M. Zollner. A model-based approach to probabilistic situation assessment for driver assistance systems. In *Proc. of the IEEE Intelligent Transportation Systems Conference*, pages 1404–1409, 2011.
- [112] C. Schlenoff, R. Madhavan, and Z. Kootbally. PRIDE: a hierarchical, integrated prediction framework for autonomous on-road driving. In *Proc. of the IEEE International Conference on Robotics and Automation*, pages 2348–2353, 2006.
- [113] K. Schmitt, R. Mannale, and R. Isermann. Situation Analysis, Warnings and Emergency Braking for Collision Avoidance in Overtaking Situations - PRORETA 2. *IFAC Proceedings Volumes*, 43(7):744–749, 2010.
- [114] J. Schneider, A. Wilde, and K. Naab. Probabilistic approach for modeling and identifying driving situations. In *Proc. of the IEEE Intelligent Vehicles Symposium*, pages 343–348, 2008.
- [115] D. Schramm, M. Hiller, and R. Bardini. Single Track Models. In *Vehicle Dynamics: Modeling and Simulation*, pages 223–253. Springer Berlin Heidelberg, Berlin, Heidelberg, 2014.
- [116] M. Schreier. *Bayesian Environment Representation, Prediction, and Criticality Assessment for Driver Assistance Systems*. PhD thesis, Technical University of Darmstadt, 2016.
- [117] M. Schreier, V. Willert, and J. Adamy. Bayesian, maneuver-based, long-term trajectory prediction and criticality assessment for driver

- assistance systems. In *Proc. of the IEEE Intelligent Transportation Systems Conference*, pages 334–341, 2014.
- [118] R. Schubert, E. Richter, and G. Wanielik. Comparison and evaluation of advanced motion models for vehicle tracking. In *Proc. of the IEEE Information Fusion Conference*, pages 1–6, 2008.
- [119] R. Schubert, K. Schulze, and G. Wanielik. Situation Assessment for Automatic Lane-Change Maneuvers. *IEEE Transactions on Intelligent Transportation Systems*, 11(3):607–616, 2010.
- [120] G. Shafer. Dempster-shafer theory. *Encyclopedia of artificial intelligence*, pages 330–331, 1992.
- [121] V. Shvetsov and D. Helbing. Macroscopic dynamics of multilane traffic. *Physical Review E*, 59(6):6328–6339, 1999.
- [122] R. Simmons, R. Goodwin, K. Z. Haigh, S. Koenig, and J. O’Sullivan. A layered architecture for office delivery robots. In *Proc. of the International Conference on Autonomous Agents*, pages 245–252, New York, New York, USA, 1997. ACM Press.
- [123] J. Sorstedt, L. Svensson, F. Sandblom, and L. Hammarstrand. A New Vehicle Motion Model for Improved Predictions and Situation Assessment. *IEEE Transactions on Intelligent Transportation Systems*, 12(4):1209–1219, 2011.
- [124] U. Stählin. Eingriffsentscheidung für ein Fahrerassistenzsystem zur Unfallvermeidung. *Fortschritt-Berichte VDI. Reihe 12, Verkehrstechnik / Fahrzeugtechnik*, (683), 2008.
- [125] Statistisches Bundesamt. Verkehrsunfälle. Technical report, 2014.
- [126] H.-S. Tan and J. Huang. DGPS-Based Vehicle-to-Vehicle Cooperative Collision Warning: Engineering Feasibility Viewpoints. *IEEE Transactions on Intelligent Transportation Systems*, 7(4):415–428, 2006.
- [127] A. Tarko, S. Kanipakapatnam, and J. Wasson. Modeling and Optimization of the Indiana Lane Merge Control System on Approaches to Freeway Work Zones, Part I. *Joint Transportation Research Program*, page 345, 1998.
- [128] Ö. S. Tas, F. Kuhnt, J. M. Zöllner, and C. Stiller. Functional System

- Architectures towards Fully Automated Driving. In *Proc. of the IEEE Intelligent Vehicles Symposium*, pages 304–309, Gothenburg, Sweden, 2016.
- [129] C. Tay. *Analysis of Dynamic Scenes: Application to Driving Assistance*. PhD thesis, Institut National Polytechnique de Grenoble - INPG, 2009.
- [130] P. Thomas, A. Morris, R. Talbot, and H. Fagerlind. Identifying the causes of road crashes in Europe. *Annals of advances in automotive medicine*, 57:13–22, 2013.
- [131] S. Thrun, M. Montemerlo, H. Dahlkamp, D. Stavens, A. Aron, J. Diebel, P. Fong, J. Gale, M. Halpenny, G. Hoffmann, K. Lau, C. Oakley, M. Palatucci, V. Pratt, P. Stang, S. Strohband, C. Dupont, L.-E. Jendrossek, C. Koelen, C. Markey, C. Rummel, J. van Niekerk, E. Jensen, P. Alessandrini, G. Bradski, B. Davies, S. Ettinger, A. Kaehler, A. Nefian, and P. Mahoney. Stanley: The robot that won the DARPA Grand Challenge. *Journal of Field Robotics*, 23(9):661–692, 2006.
- [132] T. Toledo, H. N. Koutsopoulos, and M. Ben-Akiva. Integrated driving behavior modeling. *Transportation Research Part C: Emerging Technologies*, 15(2):96–112, 2007.
- [133] M. Treiber, A. Hennecke, and D. Helbing. Congested traffic states in empirical observations and microscopic simulations. *Physical Review E*, 62(2):1805–1824, 2000.
- [134] M. Tsogas, X. Xun Dai, G. Thomaidis, P. Lytrivis, and A. Amditis. Detection of maneuvers using evidence theory. In *Proc. of the IEEE Intelligent Vehicles Symposium*, pages 126–131, 2008.
- [135] C. Urmson, J. Anhalt, D. Bagnell, C. Baker, R. Bittner, M. N. Clark, J. Dolan, D. Duggins, T. Galatali, C. Geyer, M. Gittleman, S. Harbaugh, M. Hebert, T. M. Howard, S. Kolski, A. Kelly, M. Likhachev, M. McNaughton, N. Miller, K. Peterson, B. Pilnick, R. Rajkumar, P. Rybski, B. Salesky, Y.-W. Seo, S. Singh, J. Snider, A. Stentz, W. Whittaker, Z. Wolkowicki, J. Ziglar, H. Bae, T. Brown, D. Demitrish, B. Litkouhi, J. Nickolaou, V. Sadekar, W. Zhang, J. Struble, M. Taylor, M. Darms, and D. Ferguson. Autonomous driving in urban environments: Boss and the Urban Challenge. *Journal of Field Robotics*, 25(8):425–466, 2008.

- [136] J. Wei, J. M. Snider, T. Gu, J. M. Dolan, and B. Litkouhi. A behavioral planning framework for autonomous driving. In *Proc. of the IEEE Intelligent Vehicles Symposium*, pages 458–464, 2014.
- [137] K. Weiss, N. Kaempchen, and A. Kirchner. Multiple-model tracking for the detection of lane change maneuvers. In *Proc. of the IEEE Intelligent Vehicles Symposium*, pages 937–942, 2004.
- [138] J. Weng and Meng. Q. Decision Tree - Based Model for Estimation of Work Zone Capacity. *Transportation Research Record*, (2257):40–50, 2011.
- [139] M. Werling, S. Kammel, J. Ziegler, and L. Groll. Optimal trajectories for time-critical street scenarios using discretized terminal manifolds. *The International Journal of Robotics Research*, 31(3):346–359, 2012.
- [140] R. Wiedemann. *Simulation des Strassenverkehrsflusses*. PhD thesis, Karlsruhe Inst. f. Verkehrswesen d. Univ. Karlsruhe, 1974.
- [141] World Health Organization. Global status report on road safety 2013: supporting a decade of action. Technical report, 2013.
- [142] W. Xu, J. Pan, J. Wei, and J. M. Dolan. Motion planning under uncertainty for on-road autonomous driving. In *Proc. of the IEEE International Conference on Robotics and Automation*, pages 2507–2512, 2014.
- [143] Y. Yim and S.-Y. Oh. Modeling of Vehicle Dynamics From Real Vehicle Measurements Using a Neural Network With Two-Stage Hybrid Learning for Accurate Long-Term Prediction. *IEEE Transactions on Vehicular Technology*, 53(4):1076–1084, 2004.
- [144] M. J. Zaki and W. Meira. *Data Mining and Analysis: Fundamental Concepts and Algorithms*. Cambridge University Press, 2014.
- [145] J. Zhang and B. Roessler. Situation Analysis and Adaptive Risk Assessment for Intersection Safety Systems in Advanced Assisted Driving. In *Autonome Mobile Systeme*, pages 249–258. Springer Berlin Heidelberg, 2009.
- [146] Z. Zhang, K. Huang, and T. Tan. Comparison of similarity measures for trajectory clustering in outdoor surveillance scenes. In *Proc. of*

the International Conference on Pattern Recognition, pages 1135–1138, 2006.

Curriculum Vitae

Personal Data

| | |
|----------------|-----------------------|
| Name | Florian Damerow |
| Date of Birth | 20. August 1984 |
| Place of Birth | Ludwigshafen am Rhein |

Education

| | |
|-------------|--|
| 2007 – 2012 | Main Studies , Electrical Engineering and Information Technology, majoring in Automation, Technischen Universität Darmstadt Degree: Dipl.-Ing. (very good) |
| 2008 – 2009 | Studies Abroad , Electrical Engineering / Automation, Lunds University, Sweden |
| 2005 – 2007 | Basic Studies , Electrical Engineering and Information Technology, Technischen Universität Darmstadt |
| 2004 | Gymnasium zu St. Katharinen Oppenheim Degree: Abitur (good) |

Professional Experience

| | |
|-------------|---|
| from 2017 | R&D Engineer ADAS , Continental AG - ADC Automotive Distance Control Systems GmbH, Lindau. |
| 2013 – 2016 | Research Associate , Technischen Universität Darmstadt, Control Methods and Robotics / Honda Research Institute Europe, Offenbach. |
| 2012 – 2013 | Research Associate , Bosch GmbH, Schwieberdingen. |
